Quantitative seismic intepretation in evaporite formations

LEONARDO MÁRCIO TEIXEIRA DA SILVA

Universidade Federal Fluminense

Departamento de Geologia e Geofísica

Programa de Pós-Graduação

Niterói

December 17th, 2021

QUANTITATIVE SEISMIC INTEPRETATION IN EVAPORITE FORMATIONS

LEONARDO MÁRCIO TEIXEIRA DA SILVA

Thesis submitted to the Programa de Pós-Graduação em Dinâmica dos Oceanos e da Terra of Universidade Federal Fluminense in partial fulfillment of the requirements for the degree of Doctor in Science - Geology and Geophysics.

Advisor: Prof. WAGNER MOREIRA LUPINACCI, Ph.D.

NITERÓI

DECEMBER 17TH, 2021

QUANTITATIVE SEISMIC INTEPRETATION IN EVAPORITE FORMATIONS

Thesis submitted to the Programa de Pós-Graduação em Dinâmica dos Oceanos e da Terra of Universidade Federal Fluminense in partial fulfillment of the requirements for the degree of Doctor in Science - Geology and Geophysics.

Approved by the Committee on December 17th, 2021.

Committee:

Prof. Antônio Fernando Menezes Freire, Ph.D.
(GIECAR/GGO/UFF)

Alexandre Rodrigo Maul, Ph.D.
(Petrobras)

Álvaro Favinha Martini, Ph.D.
(Petrobras)

Sávio Francis de Melo Garcia, Ph.D.
(Petrobras)

Prof. Wagner Moreira Lupinacci, Ph.D.
Advisor
(GIECAR/GGO/UFF)

Ficha catalográfica automática - SDC/BIG
Gerada com informações fornecidas pelo autor

S586q Silva, Leonardo Márcio Teixeira
Quantitative seismic intepretation in evaporite formations / Leonardo Márcio Teixeira Silva ; Wagner Moreira Lupinacci, orientador. Niterói, 2021.
147 p. : il.

Tese (doutorado)-Universidade Federal Fluminense, Niterói, 2021.

DOI: http://dx.doi.org/10.22409/PPGDOT .2021.d.10551704721

1. Geociências. 2. Geofísica. 3. Evaporitos. 4. Bacia de Santos. 5. Produção intelectual. I. Lupinacci, Wagner Moreira, orientador. II. Universidade Federal Fluminense. Instituto de Geociências. III. Título.

CDD -

Bibliotecário responsável: Debora do Nascimento - CRB7/6368

Acknowledgements (Agradecimentos)

The ones to whom I dedicate these acknowledgments speak Portuguese, therefore...

É, mãe! Seu filho, que estudou a vida toda em escola pública e saiu da periferia do interior do Rio de Janeiro, chegou até aqui. Esta tese carrega um formalismo científico, recheado de conceitos acadêmicos, alguns revisados, outros sob revisão. Nas entrelinhas estão seus sacrifícios, sua torcida, sua compreensão, sua paciência e seu amor. Isso faz com que essa tese diga mais sobre você que sobre mim mesmo. Te amo!

Meu irmão sempre é um amigo que eu posso contar em qualquer momento. Longas conversas sobre diversos assuntos, temas e aleatoriedades. Durante esta tese, ele se revelou um pai fantástico. Agradeço a Carla por vários momentos juntos, de alegria, de tristeza, de samba e cerveja. Desejo todo amor e felicidade para Isis e Théo, que me trazem alegrias em vários momentos. Apesar de todas as qualidades, infelizmente, meu irmão é estatístico frequentista e não abraçou Bayes como seu salvador. Ainda há tempo, irmão.

Tia Mariana sempre torceu por mim. Sempre me liga para saber como estou. É uma geradora estocástica de assunto. Porém, não tem uma ligação que não termina dizendo que reza por mim e quer meu bem. Estou bem e tudo deu certo. Tia Raimunda, tia Cecília, tio Jorge, tia Lúcia, tia Norma sempre se fizeram tão presentes na minha vida. Obrigado pela torcida.

Infelizmente, esse ano tive uma perda difícil, de alguém que comemoraria esse final de doutorado até mesmo mais que eu. Alguém de quem eu herdei a minha notável impaciência para algumas coisas, mas de quem espero ter herdado um coração tão grande quanto. Não vai ter uma ligação entusiasmada do meu tio Lincoln para dizer que está feliz por essa conquista, mas não tenho dúvidas que estaria muito. Essa saudade é o amor que fica.

Pergunto-me se a notável impaciência minha foi sentida pelo orientador com quem eu aprendi a ter mais paciência e calma. Wagner, você se tornou um amigo nesse doutorado. Você acreditou em algumas ideias inesperadas que, por vários momentos, a gente não sabia aonde chegaria. Você ajudou a dilapidá-las e transformá-las nesse manuscrito que está aqui, dizendo que tudo daria certo. Mesmo quando tivemos um artigo recusado por um editor, fizemos mudanças e colocamos em uma revista com fator de impacto ainda maior e aprovamos. Aprendi a ter paciência e me reconstruir com as críticas e sugestões. Estou muito feliz por tido você como orientador. É inspirador o que você tem feito na UFF.

“Por que a gente não inverte o sal?”. “Ahn?”. “É, o sal?!”. Eu pensei: *o Maul deve achar que eu estou com tempo sobrando em meio a uma campanha intensa de perfuração no campo de Tupi*, isso lá em 2015. Eu demorei um tempo porque, bem, o campo estava em uma campanha intensa de perfuração. Eu fiz. Voltou, porque não estava boa. Refiz, elevei o padrão do resultado e foi aí que tudo começou. Hoje a maioria dos campos da Petrobras tem inversão no sal. Essa história é para deixar registrado que você, Maul, enxergou mais longe ao propor isso e que, apesar de algumas resistências, continou. Sua tese pavimentou o caminho para várias outras, dentre elas, a minha. Eu conheci um amigo e um profissional que admiro muito. Obrigado pela dedicação, pelas sugestões (algumas esbarraram na minha teimosia), pelas palavras de conforto quando você percebeu que estava precisando. Foram importantes para mim.

A vida me trouxe excelentes amigos cuja influência carrego até hoje comigo onde quer que eles estejam. André, Renan, Reinaldo e Marcos são pessoas sempre presentes em grande parte da minha vida. Sou grato por tudo que aprendi com vocês, e sinto falta de cada um. Agradeço à Carol, Marcela, Luiz e Renan por terem me ajudado a manter minha saúde mental nesse processo de confinamento. Não sei como seria esse período sem vocês. Entre os altos e baixos, a presença de vocês foi fundamental para que eu tivesse cabeça para escrever esta tese. Meus amigos de infância que não vejo há um tempo: Dudu, Rodrigo, Aline, Amanda e Patrícia. Parece uma eternidade! Dudu, você me enche cada dia mais de orgulho. Ricardo, Linho, Carol, Reinado, Luciana, vocês me ensinaram a aceitar o contraditório e o antagonismo de ideias, entendendo que isso faz parte da construção de um pensamento saudável. Vocês têm noção da importância que foi isso para o desenvolvimento desta pesquisa? Aos amigos que me afastei, seja por essa batalha mundial contra um vírus, seja por precisar de tempo para desenvolver esta pesquisa, aos poucos vamos nos rever: Fazollo, Victor, Denis, Isaías, Leandro, Júlio, Alexandre. Marcela, Nanda, Gilson, Juliana, Balancin, Ramon, meus geradores estocásticos de saídas e bares, que nossa aleatoriedade possa voltar. Sinto saudades! Amigos, eu sei que algumas coisas também aleatórias da vida nos guiaram por caminhos diferentes, mas isso não diminui a importância de nenhum de vocês minha jornada.

Sou muito grato aos amigos que fiz na Petrobras. Álvaro Martini, por me ensinar os primeiros passos de inversão sísmica e me ajudar em vários momento dentro da empresa em que dividimos inversões, ríamos das frustrações e mais ainda das alegrias. Evângela, por me ajudar a conhecer os

benefícios da física de rochas; novos e teimosos, já falávamos em interpretação quantitativa antes de sê-la, de fato. Intepretação? Sim, é interpretação também! Mônica, Vitor Leal, Laryssa, Nathalia, João Paulo, Penna, Ana Azedias, com quem eu pude desabafar em vários momentos dessa minha trajetória, e com quem eu pude trocar pontos de vistas diferentes sobre soluções de vários problemas. Vocês ajudaram a engrandecer esta tese. Luiz Eduardo e Toríbio tem meus agradecimentos pelas incansáveis discussões filosóficas sobre probabilidade, por me ensinarem a dar aulas vendo a paixão que vocês têm ao estar ensinando. Agradeço também aos demais professores do curso de probabilidade e estatística, que ajudo a ministrar e muito valorizo, por me incentivarem a cada vez buscar soluções para a análise de incertezas: Matheus, Erick e Pedro.

Agradeço ao prof. Fernando Freire e ao geólogo Sávio Garcia por ajudarem este geofísico, graduado em Física, a lidar melhor com os conceitos de Geologia. Vocês estiveram presentes no meu *Qualify* e sempre que busquei para tirar dúvidas foram solícitos em atender.

Esta pesquisa começou como um projeto de Mestrado. Ao finalizar minha dissertação, meu orientador, prof. Wagner Lupinacci, em reconhecimento à excelência da pesquisa, me ofereceu a oportunidade de transformá-la em programa de Doutorado. Dessa forma, pulei a etapa de conclusão de Mestrado e dei continuidade ao aperfeiçoamento, visando a obtenção do grau de Doutor em Ciências. Ao ter sido aprovada pela pró-reitoria minha mudança de escopa de pós-graduação, ainda não havia tido a aprovação do segundo artigo pela conceituada *Marine and Petroleum Geology*. Essa aceitação do artigo foi posterior, e objeto de meu *Qualify*. Agradeço à Universidade Federal Fluminense por essa imensa oportunidade e ao prof. Wagner por ter acreditado que eu conseguiria manter a qualidade desta pesquisa. Há um terceiro artigo a caminho! Ter voltado à Academia e aos corredores da Faculdade depois de tanto tempo longe me restabeleceu a vontade de voltar a pesquisar, a escrever e a desenvolver ideias e, acima de tudo, a contribuir.

Agradeço também à Petrobras por me liberar parcialmente. A liberação se deu mediante aos esforços do Paulo Johann e Rui Sansonowski. Nesse último ano, em que a pressão aumenta na reta final da tese, pude contar com a compreensão da Ana Paula Martins que sempre estava disposta a ouvir sobre a cansativa vida dupla, de trabalho e doutorado. Obrigado a todos vocês.

Essa pesquisa foi desenvolvida durante uma pandemia em que todos nós lutávamos contra o que não víamos, um novo vírus, COVID-19. Escrevo no passado porque hoje, ao final desta

tese, estamos num estágio avançado de vacinação com número de mortes relativamente baixo em comparação com caos que, em desalento, presenciamos sem a certeza de cura ou imunização. Escrevo no passado porque, em dois anos, pesquisadores se debruçaram incansavelmente na busca por uma vacina que trouxesse de volta a esperança de dias melhores. Escrevo no passado porque acredito que a ciência salva e abre caminhos para futuros melhores.

À MINHA MÃE, MARCIA TEIXEIRA

À MINHA TIA, MARIANA REZENDE DA SILVA

"In solving a problem of this sort, the grand thing is to be able to reason backwards (...) Let me see if I can make it clearer. Most people, if you describe a train of events to them, will tell you what the result would be. They can put those events together in their minds, and argue from them that something will come to pass. There are few people, however, who, if you told them a result, would be able to evolve from their own inner consciousness what the steps were which led up to that result. This power is what I mean when I talk of reasoning backwards, or analytically."

(Sherlock Holmes in A Study in Scarlet - Sir Arthur Conan Doyle)

Abstract

This thesis tackles the application of quantitative seismic interpretation in evaporite formation, unprecedented in geoscience literature. It describes methodologies to identify the salt types and their elastic properties in salt sequences and puts down the subsequent relevances and application to geoscience. I demonstrate that seismic-inverted acoustic impedance reduces the uncertainties in the interpretation of salt sucessions. In a Bayesian classification, I combine rock-physic analysis and seismic inversion to deliver the spatial classification of bittern salts, halite, and anhydrite. It underpins the seismic cyclostratigraphy in the salt formation in the Santos Basin, providing a more powerful geological meaning to intrasalt events. The shift from qualitative to quantitative interpretation allows the computation of salt-type proportions maps, which infer the spatial distribution of these rocks. The seismic-based and well-based proportions converge and sustain the hypothesis that the formation is brining upwards and increasing hydrographical isolation of the basin. I also prove that the elastic properties are highly correlated and I resort to empirical equations to estimate them spatially, a remarkable contribution to the construction of velocity and geomechanical models. This thesis proceeds with the uncertainty estimation of thin-bed thickness. I devise a procedure to use Monte-Carlo-based well simulation to mirror the evaporite sequence in the Santos Basin and to capture the variability of the estimation. The joint distribution of the quantitative seismic attribute and the facies-dependent total thickness renders the estimation of expectation, variance, and percentiles of the seismic-driven thin-bed thickness appraisal. The workflow to the uncertainty estimation of thin-layer thickness is versatile and extendable to other facies and several depositional environments. Before this research, quantitative seismic interpretation was exclusively applied to reservoir rocks. Henceforth, this thesis places a significant brick in the construction of the quantification of the seismic data by amplifying its application to evaporites. Additionally, it develops new methodologies that exceed the realm of geophysics and impact substantially multidisciplinary studies in geoscience.

Key-words: Evaporites, Quantitative Seismic Interpretation, Stratigraphic Interpretation, Cyclostratigraphy, Thin-layer thickness

Resumo

Esta tese foca na aplicação dos conceitos de interpretação sísmica quantitativa em formações evaporíticas, algo inédito na literatura de geociências. São descritas metodologias para identificar os tipos de sais e suas respectivas propriedades elásticas na sequência salina, bem como as relevâncias e aplicações subsequentes para geociência. Eu demonstro que a impedância acústica obtida pela inversão sísmica reduz as incertezas na interpretação dos sais. A análise de física de rochas e inversão sísmica unificadas pela classificação bayesiana oferece a classificação espacial dos sais de baixa densidade, halita e anidrita. Esta classificação de fácies assiste a sismo-cicloestratigrafia na formação salina da Bacia de Santos, trazendo maior significado geológico para os eventos sísmicos intrasais. A mudança da interpretação qualitativa para interpretação quantitativa permite o cálculo dos mapas de proporção de tipos de sal, o que infere a distribuição espacial dessas rochas. As proporções obtidas em poços e no dado sísmico convergem e sustentam a hipótese a concentração da salmoura está aumento para o topo da formação, indicando um aumento no isolamento hidrográfico da bacia. Eu também provo que as propriedades elásticas são altamente correlacionáveis e faço uso das equações empíricas para estima-las espacialmente, uma contribuição importante para a construção do modelo de velocidade e de geomecânica. Esta tese continua sua contribuição com a estimativa de incerteza para espessuras de camadas delgadas. Para isso, eu codifico em Python simulações de poços baseada em métodos Monte Carlo para emular a sequência evaporítica da Bacia de Santos e capturar a variabilidade das estimativas. A distribuição conjunta entre o atributo sísmico quantitativo e espessura total das fácies possibilita a estimativa do valor esperado, variância e percentis das espessuras das camadas delgadas. O fluxo de trabalho é versátil e extensível a outros tipos de fácies e sistemas deposicionais. Antes dessa pesquisa, a intepretação sísmica quantitativa era exclusivamente aplicada a rochas reservatórios. Desse momento em diante, esta tese coloca uma importante contribuição para a interpretação quantitativa, ampliando suas aplicações para seção evaporítica. Adicionalmente, ela desenvolve novas metodologias que transpõem o reino da geofísica e impactam substancialmente estudos multidisciplinares em geociência.

Palavras-chaves: Evaporitos, Interpretação sísmica quantitativa, interpretação estratigráfica cicloestratigrafia, camadas delgadas

List of Figures

List of Tables

Contents

1 Preface

The History of Science is littered with nonlinear developments. Scientists left unfinished theorems, others concealed remarkable achievements because they believed that the conjectures were not fully evolved; others insisted on theories that led to the misinterpretation of results. We also find stories of great minds that used their influence to halt the evolution of science when they sensed a threat from their eminent colleges. Some of them disregarded the paramount importance of their deeds and, as part of this chronological disorder, it was left to the posteriority to utterly blossom their ideas. Others devised new fields that appeared to be brought up from nowhere. Science has a cause, mostly defined by its period of development, nevertheless, it follows twisted paths.

Among many examples that can fill the lines of this thesis, I carefully chose the history of the Normal curve (Equation 1.1).

$$f(x) = \frac{1}{\sigma\sqrt{2\pi}}\ \mathrm{e}^{-\frac{1}{2}\left(\frac{x-\mu}{\sigma}\right)^2}. \tag{1.1}$$

x is the variable; μ, the mean; σ, the standard deviation.

This curve, as we know, was established by De Moivre in 1733. However, Stephen Stigler, whose book *The history of Statistics: the measurement of uncertainty before 1900* is the basis of this introductory text, traces down the outset of this grail in the work Jacob Bernoulli (1655 – 1705). Bernoulli was a prominent family of Swiss mathematicians that contributed to the development of then recently differential calculus created by Gottfried Leibniz (1646 - 1716). Bernoulli proved what is known as the weak law of large numbers and developed the Bernoulli distribution which relates to the probability of success or failure of a one-trial experiment. Bernoulli died of a “slow fever” in 1705 and his work was eventually published in 1713 by his nephew, Nicholas Bernoulli (1623 – 1708).

Jacob Bernoulli sought to expand the one-trial experiment of his distribution to the *n*-trial occurrences. This expansion waited for 15 years to pave its grounds by Abraham De Moivre (1657 – 1754). Abraham De Moivre was a French expatriate mathematician who was persecuted by the court of

King Louis XIV for being Protestant and escaped to London where he became a close friend of Isaac Newton (1647 – 1727) and Edmond Halley (1656 - 1742). In London, he published his *Miscellanea Analytica* in 1730 whereby he engaged in the expansion of the Binomial distribution. By then, the outright proof of the expansion was not properly set up, which causes De Moivre to send a posterior note in 1733 to complete his Binomial approximation to the Normal curve. The most famous curve in the history of Statistics was printed separately from the main body of De Moivre's book as an additional note in Latin and added to the subsequent editions of the *Doctrine of Chances*.

Pierre-Simon Laplace (1749 – 1827) enjoyed a very different recognition in France in comparison to his compatriot De Moivre. While De Moivre went into exile in England after King Louis XIV revoked the Edict of Nantes which grants substantial rights to French Protestants, Laplace found the doors of the Palace of Versaille wide open where the court of France esteemed him as a renowned scientist. Between 1772 and 1781, Laplace took on the deduction of a curve of errors that could explain the differences between the Newtonian predictions and the astronomical measurements. Laplace's struggles can be summarized in the sentence in his 1774 memoir: "But of an infinite number of possible functions, which choice is to be preferred?". His first choice dates from 1774 when he hypothesized that the curve was proportional to e^{-ax}. In his 1777 and 1781 memoirs, Laplace derived the curve of errors in the form of:

$$y = \frac{1}{2a} log\left(\frac{a}{x}\right).$$

x is the variable and a is a constant.

In 1809, Carl Friedrich Gauss (1777 – 1855) published his concept of the curve of errors as it is generally conceived, widely accepted nowadays. Gauss proposed that the curve of errors is proportional to e^{-ax^2}. Along with the formulation of the curve of errors, Gauss invoked that he developed the least-squares methods. One century early, a controversy struck the academic world when Leibniz and Newton claimed to be the founder of Calculus. Gauss' statement requesting the discovery of the least-squares methods emerged another controversy because Adrien-Marie Legendre (1752 – 1833) released the foundations of this methodology in his work of 1805 *Nouvelles Méthodes*

Pour La Détermination Des Orbites Des Comètes.

Unlike the circumstances around the debate about the discovery of Calculus, the discussion on the starting point of the least-squares method hit on another level. Gauss declared that he derived the least-squares method before 1805 and requested testimony from close friends in his favor. The posterior review of the evidence presented in this deadlock suggests that Gauss had told the truth about his former achievements in the discovery of the method (PLACKETT, 1972). However, he left it unpublished and this procedure did not outreach his personal annotations or was communicated in the academic media. Furthermore, Gauss' derivation for the Normal curve is mathematically inconsistent or, as stated by Stigler (1986), "reasoning unpalatable (...), a logical aberration – it was essentially both circular and non sequitur". Gauss started with the condition that the curve needed to be symmetric, it also should be close to zero outside the possible errors, and its observation with equal care under the same circumstances is the arithmetic mean. He used the conclusions as axioms. Gauss himself admitted this insufficiency of reasoning years after the publication of the curve (STIGLER, 1986).

By this time, 35 years later from his first strive, Laplace was still seeking the curve of errors. The curve in the form of logarithm was mathematically untreatable and, chiefly, lacked solid foundations for the justifiable usage. In 1810, Laplace presented to the French Academy the first demonstration of the Central Limit Theorem which shows that the estimates that can be described as a linear function of observable variable approximate to e^{-ax^2}, in the modern notation, to Normal distribution. The least-squares method is a particular case that leads to the smallest expectation of the errors. However, Laplace associated this discovery with the law of errors after Gauss' publication. That indicates that Gauss provided the connection between the least-squares method and probability, nevertheless, Laplace delivered the robust demonstration to the Normal curve.

Who named the Normal curve is still blurring. Gillispie (2000) stated that the term "Normal" was coined by Francis Galton, although he does not specify when. Francis Galton (1822 – 1911) studied medicine at Cambridge, however, he never fully pursued the medical career. After receiving his inheritance, Galton set off to African to explore the limits of this vast continent. He was driven by an extreme curiosity and pervaded distinguished areas of knowledge. Nevertheless, one especially drew his attention: the study of heredity. Galton tabulated vast measurements of human features,

including the vague concept of talents, which he faulty attributed to family inheritance. In this study of heritage, he fitted the e^{-ax^2} curve to describe some human features, regarding as mediocre the largely lower-bound deviations from the average. One finds here two prominent influences on Galton's work: Adolphe Quetelet (1796 – 1874), who introduced the usage of statistical tools in Social Sciences, and, Galton's cousin, Charles Darwin (1809 – 1882). His famous books *Hereditary Genius* and *Natural Inheritance* already referred e^{-ax^2} curve as Normal curve (GALTON, 1869; GALTON, 1889). Presumably, this term reveals a perception of a period when human behavior ought to fit into standard patterns.

Darwin's influences continued thriving in Statistics at the beginning of the 20th century. Karl Pearson (1857 - 1936), impacted by the disclosures of *On the Origin of Species*, wrote a series of papers called *Mathematical contributions to the theory of evolution* whereby he set the fundamentals of the mathematical developments to Statistics. In his 1894 paper, which granted him acceptance to the Royal Society, he put down "A frequency-curve, which, for practical purposes, can be represented by the error curve, will for the remainder of this paper be termed a normal curve" (PEARSON, 1894). Also, in this seminal paper, Pearson coined the term "standard-deviation", and employed it as a statistical test. In his work of 1896, he demonstrated how to calculate the correlation as we know it today, which currently is referred to as the correlation coefficient of Pearson. This variable is necessary for the establishment of the two-dimension Normal curve (PEARSON, 1896). Pearson's prestige exerted influence not only on the enhancement of statistical tools but also on the recognition of the precursors of this new field. After two centuries from the discovery of the Normal curve, he glorified its creator by writing a paper to *Biometrika*, the most influential journal of Statistics at the time, in which he attributed this accomplishment to Abraham De Moivre (PEARSON, 1924; ARCHIBALD, 1926). This appreciation passed unnoticed by Laplace and Gauss!

The history of the Normal curves provides a framework to understand what underlies the development of science. The usage of this curve was modified in favor of the prevalent thought. Despite the significant contribution to the science of the measurements, De Moivre was unable to capture the relevance of this function in the theory of errors. At the core of this oversight lies the period of history when it happened. At the end of the 17th century and the beginning of the 18th century,

annuities caused financial damage to the Crown. Annuities were a standard way to raise public money, mostly to finance The Great Navigations, in exchange for security payment. However, the clauses of the contract were causing constant deficits in the Crown treasures which led the Monarchy to contract the greatest scientists at the time to point out the possible sources of the losses. Abraham de Moivre, Edmond Halley, Christiaan Huygens (1629 – 1695), Gottfried Leibniz (1646 – 1716) list the eminent workforce which embraced this task. For this purpose, the pursuit of the law of errors was not the center of attention (HACKING, 2013).

The winds changed at the end of the 18th century. Legendre, Gauss, Laplace, Tobias Meyer (1723 – 1762) sought theoretical laws that could explain the divergence of the measurements about the same observation, mostly the astronomical measurements. This objective was very contrasting with the first half-century scientists. Presumably, if this objective had the utmost value in De Moivre's mind, he would realize the applicability. What changed? Stigler (1986) hints at the development of nautical instruments that drastically modified marine navigations. These instruments freed the dependences of weather conditions and land sightings to guide the navigators to find the locations. In 1715, England had constantly offered prices to those who discovered the longitude at sea. In 1815, this price reached the amount of £101,000 (£9 million corrected for inflation). If Stigler's suggestion is correct, and I believe it is neatly founded, the sponsorship of the Monarchy and the increasing enthusiasm on the Great Navigations guided the prevailing research.

The research of this thesis follows the shift in the prevailing interests. Of course, the Monarchy and the Great Navigations are over in Brazil. The counterpart lies in the proposal of the sponsorship instead. The oil industry provides the major funding for the groundwork on which the quantitative seismic interpretation towers its theories and experiments. As we will see, the research in this area of knowledge was chiefly devoted to carbonates and siliciclastics, where, in return, encompassed the most profitable reservoirs. In this context, the literature lacks a profound examination of quantitative seismic interpretation in evaporite formations.

Quantitative seismic interpretation (QI) has been widely applied to the quantitative characterization of reservoir rocks. The name became popular because of the homonymous book by Avseth, Mukerji and Mavko (2005). The definition of QI is quite broad. In the preface of this book,

they state that "Quantitative Seismic Interpretation demonstrates how rock physics can be applied to predict reservoir parameters, such as lithologies and pore fluids, from seismically derived attributes. It shows how the multidisciplinary combination of rock physics models with seismic data, sedimentological information, and stochastic techniques can lead to more powerful results than can be obtained from a single technique". In another definition, quantitative seismic interpretation applies the concepts of rock physics to reduce the uncertainties in seismic interpretation.

Since the publication of *Quantitative Seismic Interpretation*, many books dedicated to improving and cataloging the development of techniques focusing on seismic-derived quantitative information of reservoirs. Doyen (2007) writes about the application of geostatistical techniques to include seismic data into the reservoir modeling in *Seismic Reservoir Characterization: An Earth Modelling Perspective*. *Seismic Amplitude: An Interpreter's Handbook* by Simm and Bacon (2014) assembles many study cases Seismic Reflections of Rock Properties by Dvorkin, Gutierrez and Grana (2016) informs the advances of rock physics including digital rock, *Seismic Petrophysics in Quantitative Interpretation* by Vernik (2016) pays special attention to unconventional reservoirs. However, none of these books mentions the quantitative characterization of evaporite-bearing sequences. In this sense, this thesis extends the workflow of quantitative seismic interpretation beyond reservoir rocks and includes the evaporites.

What ignited the blazes of the scrutiny on the intrasalt formations is evident to us: the supergiant pre-salt reservoirs in Brazil. Notably, geoscientists published several papers about the salt formations since the association of oil-profitable sources with salt-bearing basins was steadily established. In Brazil, from the 1980s to 2000s, the interest in the Brazilian salt basins emerged when several studies demonstrated the strong influence of salt tectonism on the big oil accumulations of the Campos Basin. Salt flow deformed and pushed up the overlying strata forming anticline structures responsible for oil traps. Remarkably, the first wells in the Campos Basin aimed to drill such structures.

While the post-salt reservoirs led to the investigation of salt-associated structures and the inference of models for oil accumulations, the development of the pre-salt reservoirs required the internal characterization of the evaporite sequence. By the 2010s, the benefits from the knowledge and the issues from the neglect of the proper characterization of intrasalt formations were mapped by each

area of the Exploration and Production chain. Seismic processing inferred that the knowledge of intrasalt velocity can improve pre-salt imaging and decrease the uncertainty in time-depth conversion. The improvement of the elastic-property models in evaporites has significant impacts on the geomechanical models, a valuable tool to forecast the stress loading in the wellbore casing during drilling and production operation. These troubles pose significant dangers workforce and reduce the return of investment in the risky areas. Those issues oriented the focus the examination on the inner events of the evaporite formations, especially in the Santos Basin.

Being part of the change in the prevailing thoughts yields me the opportunity to write about the reasons that shift the attention to QI of evaporites. Likewise observed in the history of the Normal curve, the specification of date can not be precisely postulated since the modification of current thoughts flows slowly, albeit turbulently, towards the answer. However, I hope the readers will find the outset of intrasalt examinations in the references. Moreover, the citations are a source of the prevailing thought. For instance, the resort to the usage of empirical equations to derive the elastic properties is on the table since the 1980s. Nevertheless, as a portrait of the interest at the time, they were not determined to the evaporites. The application to shales, siliciclastic, and carbonates prevailed. We devised these statistical tools for the evaporites and offered a broad view of applications thereof. The readers will find the same elucidation about the new proposal to the usage of the seismic-derived volumes of facies probability. In this sense, this thesis is not a mere extension of reservoir-applicable tools to rock salts. It delivers new evaluation and interpretation in QI workflow that can be pertinent to reservoir rocks.

The composition of a thesis based on articles issued a challenge to the ordination of subjects. During my Master of Science program, Universidade Federal Fluminense approved my upgrade to the Ph.D. program based on the excellence of my research. Still, in the preparation of my dissertation for Master of Science program, I decided to invert the chronological order of the articles, that is, the second article took precedence over the first one. That happened because I weighed them under different views. However, now I reject the proposal of modifying the established order of the papers, mainly because it contemplates the development of the reasoning upon which I conceptualize this thesis. Furthermore, I take the advantage of this article-based thesis to formulate this introduction as

a storytelling of the events of each article. It also enables me to break through the academic rigidity upon which the scientific papers are devised and provided. Bearing this in mind, I expect to bring more clarification to this thesis with this introduction that contextualizes each article. Each one of them had a cause, nevertheless, they followed twisted paths.

1.1 Looking inside salt bodies

The 2010s represent the turning point in the investigation of salt bodies in the Santos Basin to the inner events within this formation. One of the first aspects is related to the quality of the seismic imagining in the pre-salt formations. Interbed multiples of intrasalt reflections obscure the presalt imaging with coherent noises, hampering the interpretation of the reservoir rocks (GRIFFITHS; HEMBD; PRIGENT, 2011). Illumination studies also clarify that the evaporite sequence patterns in the salt formation influence the seismic amplitude, impacting the credibility of the amplitude-based interpretation (JARDIM et al., 2015; MAUL et al., 2015). In addition to the illumination studies, a synthetic model based on reserve-time migration pointed out that feeding the salt body with near-constant velocity results in discontinuities and diffraction-like events in pre-salt images (JI et al., 2011; WANG; HUANG; WANG, 2017).

Warnings on the necessity of seeking knowledge about the rock properties within the salt body were in the minds of engineers who devised well paths and performed geomechanical models (COSTA et al., 2010). These tasks require the knowledge of Poisson's ratio and Young's modulus. Therefore, the research needed to extend the investigation of the compressional velocity, and include the elastic properties. The resolution is found in *Elastic properties of rock salt in the Santos Basin: relations and spatial predictions*, published in *Journal of Petroleum Science and Engineering*, first paper of this thesis (TEIXEIRA; LUPINACCI, 2019).

At the time when the reservoir asset team envisaged the necessity of the estimation of the elastic properties of the rock salt in three dimensions, the ones who embraced this task encountered a primary difficulty to obtain the elastic property at well location. Most logs lacked the density in the salt formation and partly had unreliable shear velocity acquisition. At first sight, a group of geophysicists

proposed to use the facies description in well logs to fill the gaps of acquisition in the compressional velocity and density (AMARAL et al., 2015). The requisite satisfied the proposal of calibrating the velocity cube for time-depth conversion with the inclusion of salt heterogeneities. Yet, it still left the estimation of the elastic properties unsolved.

In 2017, I made a presentation at the *14th International Congress of the Brazilian Geophysical Society* whereby I suggested the solution for this estimation. The resolutions overcame two vexing situations: i) it assessed the elastic properties in the rock salt beyond density and compressional velocity; ii) it unleashed the previous interpretation of the facies in evaporite formations to appraise them. They were based on the estimation of empirical equations (TEIXEIRA et al., 2017b).

The resort to the empirical equations is a regular duty in the geophysical workflow. Two famous empirical equations are widely applied, even beyond their original proposition, to estimate the density and shear velocity from compressional rocks in reservoir rocks: Gardner, Gardner and Gregory (1974) and Greenberg and Castagna (1992). Likewise remarked in the increasing interest in the elastic properties of evaporites, both equations araised from the prevailing necessity to obtain the density and shear velocity.

Greenberg and Castagna (1992) relations are an extension of the work of Castagna, Batzle and Eastwood (1985). Castagna, Batzle and Eastwood (1985) derived a series of empirical equations that related shear velocity to compressional velocity for silicate rocks. Two decades before, Pickett (1963) observed the facies-dependent behavior between these two elastic properties, however, the formulation of $v_s - v_p$ equation passed unimportant. Which forces drove the formulation of these equations in 1985 that were unaware in 1963? In 1984, one year before, Ostrander (1984) documented that Poisson's ratio strongly affects the reflection coefficient as a function of the angle of incidence and regarded this effect as an indicator of gas-bearing reservoirs. The angle vs amplitude analysis (AVO) was born as a direct hydrocarbon indicator (DHI). However, this analysis required the knowledge of shear velocity which, by the 1980s, was absent or unreliable in several well logs.

My presentation in 2017 founded the basis of the article of 2019 (TEIXEIRA et al., 2017b; TEIXEIRA; LUPINACCI, 2019). Nevertheless, as a natural journey of science development, it

underwent profound modifications due to academic improvements. My 2019 paper includes the estimation of uncertainty with the insertion of the confident interval. Also, I modified the derivation of the density from the velocity. Currently, I reject how it was proposed in 2017.

At first, the estimation of density from compressional velocity is applicable to reservoir rocks since the work of Gardner, Gardner and Gregory (1974). Thus, as a conventional statement, I assumed that the power function could correlate these two properties. However, the power function implies that if the density increase, so the velocity does. However, tachyhydrite presents lower velocity than carnallite, nevertheless, the density increases. Therefore, evaporite breaks the premise of Gardner's equation.

As occurred in the history of the Normal curve, the use of Gardner's relationship appears to be taken out of context. The authors investigated the relationship between reflection and porosity to explain how the reservoir properties affected the seismic amplitude. I believe the discovery of the bright spot at the beginning of the 1970s instigated this research. In the paper, they employed the Peterson, Fillippone and Coker (1955) approximation which states that, under low contrast of acoustic impedance, the reflection coefficient can be written as:

$$R = \frac{1}{2} \ln \frac{\rho_1 V_1}{\rho_2 V_2}. \tag{1.2}$$

Therefore, they proposed that density and velocity follows the empirical equation:

$$\rho = 0.23 V^{0.25}, \tag{1.3}$$

which led to

$$R = \frac{1}{2} 1.25 \ln \frac{V_1}{V_2}. \tag{1.4}$$

In the conclusion, they wrote: "A simple systematic relationship exists between the velocity and density of many sedimentary rocks in situ. For these rocks, the empirical relationship permits estimation of reflection coefficients from velocity information alone.". Therefore, the authors derived Equation 1.3 for a specific proposal: assess the reflection coefficient from velocity and link it to

porosity. The author did not furnish this equation as an attempt at deriving density from velocity. Even if it was the case, evaporites were not in mind. Therefore, I reject the use of power function to density and velocity in these rocks.

At this point, I disclose that empirical equations are adequately interpreted under the circumstances that ignited their appearance. In this paper, the refinement of the velocity model and the geomechanical model provoked the derivations of such equations. Thus, instead of estimating density from velocity, I argue that Young's modulus can be evaluated from compressional velocity. With shear velocity, density can be estimated.

The estimation of the elastic properties from compressional velocity fulfills the requirements to complete the well logs where these properties are absent and the compressional velocity is consistent. Where there is no information about v_p, the facies-dependent averages is the suitable solution. In addition to v_p, the paper focused on the estimations of the elastic properties from the acoustic impedance. The reason resides in the fact that the acoustic impedance is the reliable volume from the model-based seismic inversion. Thus, it is the basis of the three-dimensional property within salt formation.

In many instances, including Gardner, Gardner and Gregory (1974) and Castagna, Batzle and Eastwood (1985), the empirical tendencies that correlate elastic properties are segmented by facies. For instance, carbonate and clastic rocks follow different tendencies. That raises a question if evaporite fall into the similar situation where facies should control the trends in estimates. The reason why I did proceeded with this assumption is clearly in the graphs of the first article. The elastic-property trends of salt types are alike. Thus, splitting the empirical equations into facies introduces needless unreasable steps. Furthermore, the facies, as described by Gardner, Gardner and Gregory (1974) and Castagna, Batzle and Eastwood (1985), indicate an assembly of depositional facies. In stipulating a relation to clastic rocks, for instance, they included from fine- to coarse-grained sandstones into one tendency. I see no reason to estipulate discrete trends for tachyhydrite, carnallite, halite, and anhydrite. Additionally, I observe no evidence that this implication will rise the prediction of seismic-inverted properties. In fact, I hypothesize the opposed effect because, in this context, a misinterpretation in the salt types implies in an unaccurate estimation of the elastic properties. This is an avoidable step.

Further developments employed the empirical equations herein derived and proved their applicability in different areas of reservoir modeling. During the writing of this paper, in 2018, we tested the impact of the inclusion of the elastic property in evaporite formation in geomechanical modeling (TEIXEIRA et al., 2018). The model implemented the workflow of this article to incorporate the heterogeneities in salt formations. The results evidenced that the inclusion of elastic properties in the intrasalt formation impacts the calculation of the displacement in the ocean bottom.

In 2019, I co-authored an article for the *Brazilian Journal of Geophysics* in which we revealed that the inclusion of the intrasalt velocity in the migration process improves the pre-salt seismic imagining (MAUL et al., 2019) . In this version, we argued that regarding the salt as inhomogeneous supports the convergence of full-waveform inversion (FWI). Also, the study advised that the events in pre-salt reservoirs displayed more-consistent continuous amplitude. This was the onset of the consequence of inspecting the rock properties of the salt sequence properly.

The in-depth investigation of the influence of salt stratifications on the E&P processes was the main theme of Alexandre Maul's thesis (MAUL, 2020). During his Ph.D. program, he researched the consequence of inserting the salt heterogeneities in the pre-salt reservoirs, chiefly on two fronts: volumetric uncertainty in reservoirs and seismic migration. The addition of intrasalt velocity was evaluated under several considerations. The use of empirical equations to relate acoustic impedance and compressional velocity attained remarkable results.

Nevertheless, the procedure to include the salt velocity permeates different paths. In a paper in *Petroleum Geoscience*, which I co-authored, Maul et al (2021) discussed five methods to populate the salt velocity, three of them by a transformation of the empirical equation and the seismic-inverted acoustic impedance. Although they are not highlighted in the text with this sense, these procedures underlie historical attempts at adding adequately the rock property into evaporite formations. Each of them represented how the methodology evolved.

Out of the five methods, I focus my attention on two. One method weighted the velocity model by the seismic amplitude; the other applied the empirical equation (or rock-physics transforms) to appraise the velocity from the seismic-inverted acoustic impedance. The difference in the well markers

and the seismic horizons, after time-depth conversion, demonstrated that the second method, which employed the empirical equations, succeeded in comparison with the amplitude-weighted method. The amplitude-weighted method failed to capture the low-velocity salts.

Why does the seismic amplitude fail to identify the low-velocity salts? And why does the seismic-inverted acoustic impedance succeed? Which are the implications of these findings for the seismic interpretation? What else can the seismic inversion benefit the evaporite characterization? The answer lies in the second article of the thesis.

1.2 The salt types behind the enigmatic wiggles

When Gauss derived the Normal curve, being proportional to e^{-ax^2}, he started with the assumption that each error is independent and equally probable. Furthermore, the curve should be symmetric and the maximization of the independent errors would provide the least-squares methods (STIGLER, 1986). He devised a curve based on the observation of how errors are distributed and associated it with the theory of probability. That restrained the wide use of the curve in Gauss' application to the least-squares methods under a new interpretation.

Laplace derived the Normal curve by the approximation to distributions of linear combinations of large numbers of independent random variables. The particular derivation of the Normal curve under the law of large numbers expanded the possibility of its application which did not escape from Laplace's perception. He promptly realized what he had at his hand and that the employment of the Normal curve lengthened out the astronomical measurements, the domain of the application of the least-squares method at the beginning of the 19th century. In his *Théorie Analytique des Probabilités*, a masterpiece written in 1812, Laplace envisaged (GILLISPIE, 2000):

"It is primarily there the approximation of formulas that are functions of large numbers has its most important application (...). It is on the regularity of the mean outcomes of events taken in large numbers that various institutions depend, such as annuities, tontines, and insurance policies (...) I limit myself here resolving the most general of them".

Maul et al. (2021b) pointed out that the inclusion of the salt velocity by the use of the seismic-inverted acoustic impedances delivered more precise depth positioning of seismic events in pre-salt reservoirs. A similar conclusion is described for the improvement of seismic migration, which will be detailed later. Although this paper systematized a rigorous examination of this fact in 2021, we have observed these accomplishments a couple of years before. In 2020, a synthetic experiment, which mirrors the deposition of the salt formation in the Santos Basin, provided the answer to why outcomes of the seismic inversion furnish superior results in comparison to the seismic amplitude. Additionally, this new perception extended the application of seismic-inverted data in evaporite formations.

In *Quantitative seismic-stratigraphic interpretation of the evaporite sequence in the Santos Basin* published in *Marine and Petroleum Geology*, I simulated the noiseless seismic response of a typical evaporite sequence in the Santos Basin (TEIXEIRA; LUPINACCI; MAUL, 2020). This experiment concluded that bittern salts and anhydrite embedded in thick halite layers produce similar results and, in a highly heterogeneous salt stratification, the salt-type identification in seismic amplitude is strongly uncertain. In the same experiment, I inverted the synthetic seismogram. The result was remarkable! In this noise-controlled data, the acoustic impedance distinguished the evaporites explicitly. Therefore, it left no room for the doubt that the characterization of salt types lies in seismic-inverted outcomes.

The expansion of the application of the acoustic impedance volume started with a detailed interpretation in well log. In the 2000s, based on seismic expressions, four major cycles were interpreted in the evaporite sequence of the Santos Basin, the Ariri Formation. In the next decade, these cyclostratigraphic sequences were also defined in well logs. I followed the previous interpretations which determined four major cycles (FREITAS, 2006; JACKSON et al., 2015; RODRIGUEZ et al., 2018; PONTES, 2019). At this point, a debate urges on: why four major cycles? There may be more than four? There is no conclusive answers so far. The geological reasoning on this interpretation is underpinned solely by the seismic expression in some regions in the Santos Basin. Nevertheless, in this study, I found no solid evidence that led to the retermination of fewer or more cycles. Therefore, under these circumstances, I maintained the prevalent interpretation.

During the performance of the well correlation, the application of the sequence stratigraphy

in salt formations came to mind. The previous works overlooked the justification to prefer cyclostratigraphy. In the Zechstein Basin, stratigraphers attempted to perform sequence stratigraphy in the evaporite-bearing sequence (TUCKER, 1991; SARG, 2001; BECKER; BECHSTADT, 2006). Why not in the Santos Basin? The carbonate deposition in the evaporite-dominated formation in the Zechstein Basin evidences that the environment was under an open marine system. The evaporite sequence in the Santos Basin, at least in the São Paulo Plateau, is formed exclusively of rock salt. The explanation for these occurrences, and chiefly the presence of thick sequences of bittern salts, is based on the interpretation that our study area was tectonically and hydrographically isolated from the Atlantic Ocean by the Walvis Ridge. In this context, marine-seepage inflows through the Walvis Ridge fracture zones may be the key factor that controls the salinity in the isolated accumulations. Thus, a connection between the eustatic curve and precipitation is unsuitable. Either is the association of salt presence with an alleged lake curve, because, even isolated, the depositional environment is marine-fed. In the seminal book *Evaporite: sediments, resources, and hydrocarbon*, John Warren writes: "In reality, each of the evaporite cycles is made up of a highly complicated stack of parasequences that sequence stratigraphers argue represent higher-order sea-level fluctuations. In my opinion, climate-related intrabasinal autocyclicity is a more likely driving mechanism at the scale of the parasequences." (WARREN, 2006). He also disagreed and pointed out the errors inherent to the sequence stratigraphic analysis in the evaporite-bearing sequence of the Zechstein Basin[1].

The second paper of my thesis also describes a workflow to perform the seismic classification of bittern salts, halite, and anhydrite. The process combines statistical rock physics and seismic-inverted acoustic impedance. The choice of this attribute is a direct consequence of the synthetic experiment. The outcome is a reliable three-dimensional salt-type volume consistent with the well interpretation.

The facies classification expanded the employment of the acoustic impedance, previously restricted to the estimation of elastic properties. The first application consisted of the interpretation of the salt cyclostratigraphy spatially. The well interpretation associated the onset of a cycle with the precipitation of the gypsum which is recorded in the rock sequence as a presence of anhydrite. The anhydrite in facies volume guided the interpretation of the seismic horizons which established the

[1]The John Warren v. Maurice Tucker controversy

beginning of the salt cycle. That raises the geological meaning of these horizons: they do not represent a change in the acoustic character, they stand for a change in the salinity concentration of the brine. When I realized this new interpretation, I carefully remapped the seismic horizons, connecting the well and seismic interpretation of the cyclostratigraphy.

This workflow provided a meaningful geological seismic interpretation associated with a consistent facies volume. Therefore, I could take another step forward in the quantitative characterization unprecedented in evaporite formations. For each cycle, I computed the salt-type proportion maps based on seismic data. The comparison of well-based and seismic-based proportions is remarkably consistent. Therefore, I proved that seismic data is a quantitative tool for salt-bearing sequences! Both data demonstrated that from the bottom to the top of the Ariri Formation, the proportion of bittern salt was increasing, which indicates that this hydrologically isolated basin experienced a higher degree of desiccation.

The drastic rise of the bittern salts and anhydrite proportions at the end of the salt recording puzzled me straight away. The steady conclusion was that the upper cycle underwent an extreme change in salinity faster than the previous sedimentary cycles, which means that the marine-isolated system became even more hydrographically isolated. Nevertheless, the quantitative seismic interpretation brings an advantage, which exceeds the well interpretation. It offered a map of the salt distribution. In the upper cycle, the bittern-salts proportions were concentrated in isolated pond-like depressions. I hypothesize that the salt starts to flow mildly prior to the deposition of the Albian open-marine sediments. It favored, inside the hydrographically marine-isolated system in the Santos Basin, the creation of restricted mini-basins which were more susceptible to climate changes and salinity variations. That can explain the high-frequency alternation between bittern salts, halite, and anhydrite observed in the facies volumes.

The application of cyclostratigraphy went beyond the development of geological interpretation. In the previous section, I mentioned two out of five velocity models proposed by Maul et al (2021) to insert the velocity in intrasalt formations. We also investigated the benefits of combining the seismic-inverted acoustic impedance and the horizons of the salt cycles to improve depth positionings. Among them, it rendered the best results. Meanwhile, I was also participating in research to examine

how the combination of these procedures would affect the seismic imagining under the salt formation. Using the pre-salt reservoirs as a target, the inclusion of the intrasalt velocity by seismic-inverted acoustic impedance combined with the least-squares migration proved to be the best choice. The upshots are described in an article to *Journal of Applied Geophysics* with my co-authorship (MAUL et al., 2021a).

In the early 2000s, the enigmatic reflectors of salt stratifications in the Santos Basin were assumed to be intercalations of carbonate and siliciclastic rocks intruded by salt diapirs (MOHRIAK; SZATMARI; ANJOS, 2012)[2]. By the late 2000s, the well drillings left no doubt that the reflectors inside the Ariri Formation corresponded to alternations of bittern salts and anhydrite embedded in a thick halite layer, although the 3D interpretation still relied on seismic amplitude. The second paper of my thesis gave a step forwards in proposing a mechanism to reveal the salt types behind the enigmatic wiggles. Also, it provided procedures to set up the quantitative interpretation and the subsequent applications in evaporite formations. Yet, an issue was haunting the great navigations to pre-salt reservoirs: thin bittern-salts layers. So, I needed to tackle seismic resolution in the third article.

1.3 How uncertain is a thin bed?

Science is made upon debate. The Bayesian statisticians, who construct their assumptions based on the Bayes' Theorem, face severe critiques from the frequentist statisticians. The convergence upon this theme is far from being solved, although some attempts have been proposed (EFRON, 2013). Nevertheless, it appears that one thing unites Bayesian and frequentists. Most statisticians agree that *Théorie Analytique des Probabilités*, in which Laplace established the first foundations of the Central Limit Theorem and the applications of the Normal curve, is a masterpiece and a milestone in modern Statistics.

Laplace was one of the greatest minds in the history of science. Newton formulated the Law of Universal Gravitation, unifying the force that makes an apple fall on Earth and the force that makes the Earth move around the Sun. Laplace proved that Newton's Law of Universal Gravity grants stability

[2]Prof. Dr. Luiz Antonio Pierantoni Gamboa from Universidade Federal Fluminense also confirmed this prevailing misinterpretation in the early 2000s personally

to the Solar System, something that Newton himself attributed to a deity (SHEYNIN, 1971). Laplace applied the law to explain the movements of the tide, to calculate the motion of Jupiter and Saturn, to determine the orbits of the comets . He also reformulated the Bayes' Theorem in the analytical form as we know. In fact, his role in Bayesian statistics is much deeper and long-lasting than Bayes' (DALE, 1982). However, the Law of Errors took him about 40 years to formulate. The *Théorie Analytique des Probabilités* was written in 1812 and he worked on it until the last edition in 1825. Laplace died in 1827. This was his last major contribution to the scientific world. Why did it take him so long?

The postulation of the precise cause may be continuously contested. However, the period of the events gives us a hint. The Law of Errors was in minds of the 18th-century astronomers who extensively reviewed the previous measurement of the Solar System. One century early, Newton conceived the Law of Universal Gravitation. Only after this, the astronomers could devise the errors in astronomical measurements. You can only state what is an error if you can master the theory. Therefore, I was able to develop statistical measurements of thin-bed thickness estimation only after I learned from evaporites. In this context, I understand why the probabilistic estimation of thin-bed bittern salts is the last article of this thesis. The findings of the previous two articles, *Elastic properties of rock salt in the Santos Basin: relations and spatial predictions* and *Quantitative Seismic Sratigraphic Intepretation of the Evaporite Sequence in the Santos Basin*, evolved my knowledge of uncertainty analysis in evaporite formations.

By the early 1970s, researchers related the seismic amplitude to the quality of hydrocarbon-bearing reservoirs (GARDNER; GARDNER; GREGORY, 1974). Meanwhile, the bright spot emerged as the chief seismic indicator for gas and oil reservoirs. Hammond (1974) wrote in an article to *Science*: "Variations in the strength of the reflected signals were ignored, in fact, were systematically eliminated in the computerized processing of the data. *It turns out, however, that valuable information was being discarded.* Porous rock in which natural gas is trapped reflects a much stronger seismic echo than does rock filled with water." I italicized the text to highlight this early recorded attempts at employing the seismic amplitude to characterize reservoir properties.

The bright spot, however, presented pitfalls. Widess' criteria formulate that the theoretical threshold of seismic resolution of a thin-bed layer corresponds to one-eighth of a wavelength of this

layer thickness (WIDESS, 1973). At this point, tuning thickness, the amplitude reach its maximum value due to constructive interference. Thinly uncommercial reservoirs display similar seismic reflections.

By the 70s and 80s, the thickness estimation under the tuning point was based on the empirical evidence that the seismic amplitude and thin reservoir zones are linearly correlated (MECKEL; NATH, 1977; SCHRAMM; DEDMAN; LINDSEY, 1977; BROWN et al., 1986). At the core of the procedure resided a wedge model which assumed a wedge-shaped facies embedded in another type of thick facies. Later on, by the 1990s, studies introduced more realistic scenarios and included the effect of the layering patterns of stratigraphic sequences on the seismic amplitude response (NEFF, 1990; NEFF, 1993). By the 2000s and 2010s, the emergence of seismic-inverted elastic properties shed light on new attributes that can potentially assess the rock thickness. That favored the use of bandpass acoustic impedance to estimate thin-bed dimensions (CONNOLLY, 2007; SIMM, 2009). Essentially, these techniques plot the seismic amplitude and the seismically mapped reservoir isopach and apply a deterministic data-specific self-calibration. Widess (1973) derived, under some conditions, that below the tuning thickness, the thin-bed thickness and seismic amplitude were linearly correlated. I presume that the estimation of thin-layer sequence was the first applicable quantitative seismic interpretation with the outset by the 70s and 80s. This task led me back to the origins.

The facies volume was unable to classify thin-bed bittern salts. Nevertheless, a further inspection in the bittern-salts probability volume called attention to the fact that, even under the seismic resolution, the volume displays a fairly low, continuously consistent probability. A comparison between the bittern-salts probability and the bittern-salts thickness at well data indicated that the observation in the field data is qualitatively consistent. Therefore, I plotted the sum of probability versus the thickness and found a highly linear correlation. It was consonant to the previous works reporting a linear correlation between thin layers and seismic amplitude or between thin layers and the relative acoustic impedance.

In 2017 I led a research, in which I performed the Bayesian classification in a turbite reservoir, and I "verified a good match between high reservoir probability facies and high net-to-gross (NTG) in the well-log description" (TEIXEIRA et al., 2017a). I employed the reservoir probability maps to

indicate the regions of high-porosity reservoirs. I believed that reservoir properties lurked beneath the facies probability. Therefore, it was in my mind to explore the use of facies probability quantitatively, which I did not perform in this work of 2017. Furthermore, the full development of statistical tools to mature this ideia was acquired during the Ph.D. program.

The linear relationship between the sum of probability and the facies-dependent thickness delivers a deterministic approach to the problem and does not capture the uncertainty under this estimation. However, assessing the variability of the seismic estimation is a tricky task due to the limitation of well data. As Conolly stated: "Uncertainty is too complex to be adequately captured by analysing the results from a small number of wells" (SIMM; BACON, 2014). Thus, to perform this exercise, one needs to simulate the wells.

How can I simulate something which I am not familiar with? It evidences that the evolution of this article was possible solely after the interpretation of the cyclostratigraphy. In the third article of this thesis entitled *Probabilistic estimation of seismically thin-layer thicknesses with application to evaporite formations* and submitted to *Survey in Geophysics*, I coded an algorithm that simulates evaporite sequences which mirrors the salt deposition of the Ariri Formation. Essentially, it mimics a bittern-salts sequence in a thick halite layer. After this, I attributed to each salt type typical elastic properties based on the well data and performed the Backus' average as an upscale method of the effective media. Subsequently, in each simulation, I calculated the facies probability and the sum of probability. To calibrate the simulation, I compared the results to the noiseless synthetic response of this attribute in the well data of the Santos Basin. The exploration of noiseless data as a guide succeeded in the third paper.

The first attempt failed. The algorithm did not capture the variability of the synthetic response of the salt sequence in the Ariri Formation. Reexamining the salt record, I neglected the inclusion of the anhydrite at the top and base of bittern-salts sequences that occasionally occurs. With this modification, the simulation matched the rock response. It was a mistake to model the evaporite sequence as a two-facies deposit.

The simulation was not continuous in the range of the seismic attribute. For instance, if the

sum of probability indicates 5.0, this exact value was not simulated since the process is randomly stochastic. Therefore, to cover these gaps and acquire, at least, a close approximation, I simulated 50,000 wells to obtain a near-continuous response. A time-consuming procedure! Again, it was another mistake that, unfortunately, persisted quite long in my formulation. Later on, I realized that the employment of the Kernel Density Function was the key foundation that was absent in the original algorithm. It reduced the number of simulations to 500. Also, it added the capability of calculating the uncertainty of thin layers for all values in the range of the seismic attribute because it permits the computation of joint probability density function. From this function, I derived the statistical measurements and the variability of the data.

The application to the field data revealed an unexpected outcome. The cross plot between the sum of the probability and bittern-salts thickness using the field data was more scattered than in the synthetic data. The variability was underestimated because it was calibrated in noiseless synthetic data. It appended a new brick in the construction of the algorithm: the inclusion of the noise. In section 10.3.2 of *Seismic Amplitude: An Interpreter's Handbook*, Simm and Bacon (2014) discuss the estimation of uncertainty of the seismic-derived rock property. The use of Monte-Carlo-assisted simulation of wells is a central topic. The section ends with this warning: "Ultimately, of course, other uncertainties also need to be considered, including the effect of seismic noise." And the section ends! The authors did not mention how. Also, I found no reference to this procedure in literature. The inclusion of noise in pseudowells is unprecedented. Beyond the estimation of the uncertainty of thin-bed rocks, the third article also fills this gap in geophysical publications proposing a method to incorporate the noise in pseudowells. This achievement extends beyond evaporite rocks and provides a mathematical treatment to include noise in the estimation of reservoir properties.

Interpretation is at the core of geoscientist, mostly related to the events of subsurface. My final paper allowed me to debate the interpretation of the concept of probability. The frequentist interpretation of probability dominated the 20th century. The reason why it occurred is interesting, however, I left this part of the history of Statistic out of the thesis. Nevertheless, when performing Bayesian classification to unveal reservoir-quality facies, I realized that this interpretation is unplausible to seismic-derived probability volumes. So, what is the most appropriate interpretation of

this probability? I found the answer in the Ph.D. thesis of one of the most influential economists of the 20th century, John Maynard Keynes.

In his *A Treatise on Probability*, Keynes (1921) defended that probability is a mathematical solution to order the magnitude of uncertainty, a degree of rational belief based on solid evidence. It differs from the interpretation of frequentists which relates the probability to the ratio of favorable events to the possible aleatory events. Although this interpretation is subjective, it has rational foundations. Keynes gave this example to explain the idea: "when we argue that Darwin gives valid grounds for our accepting his theory of natural selection, we do not simply mean that we are psychologically inclined to agree with him; it is certain that we also intend to convey our belief that we are acting rationally in regarding his theory as probable." In a parallel postulation: when we believe that an interval exhibits a more probable facies because foundations of rock physics attested that, under a specif elastic property or a combination of elastic properties, that facies is more likely to be found. It is not a frequentist view. Keynes' conceptualization of probability is more suitable in this case. I believe that, as textbooks lack this discussion, I needed to bring it up in the article.

Beyond the interpretation of probability, the last article contextualizes the interpretation of probability as a seismic attribute. Notwithstanding the vast applicability in reservoir rocks, the previous works that applied the Bayes' classification cast aside the facies probability regarding it as a path to determinist most-probable classification. *Once more it turns out, however, that valuable information was being discarded.* Here, I explored the usefulness of this attribute as a predictor of seismically thin-bed thickness and demonstrated the potential application of these volumes, a contribution to the workflow of quantitative seismic interpretation.

In 1973 Widess posed a question in the title of his seminal paper: "How thin is a thin bed?". In 2021 I posed another question: "How uncertain is a thin bed?"

1.4 And the human gave names to all livestock

Schreiber and Tabakh (2000) describe evaporites as chemical mineral precipitations that form at the Earth's surface or in near-surface environments from brines, concentrated by solar evaporate in

restricted basins. That definition includes carbonates in the broad world of evaporites.

Warren (2006), chapter 1, proposes a division in alkaline earth evaporites – aragonite, dolomite and calcite – and evaporite salts – gypsum, halite, anhydrite, etc. In the interpretation of evaporite textures, he describes the aspect of stromatolites and microbialites. However, in chapter 2, where he discusses the depositional chemistry and hydrology, he states that "diagenesis in evaporite is more climate dependant than in siliciclastic and carbonate sediments". At this point, carbonates appear to be excluded from evaporites.

Adding further confusion, Hardie (1984) describes aragonite ($CaCO_3$), calcite ($CaCO_3$) and dolomite ($CaCO_3.MgCO_3$) as saline minerals in marine settings. Babel and Schreiber (2014) also include of carbonate in the list of salts. The Compendium of Chemical Terminology defines salt as an assembly of cations and anions. Ca^{2+}, $Mg^{2}+$, Na^{+} are cations; and Cl^{-} and CO_3^{2-} are anions. Therefore, by this definition, carbonates are salts or saline rocks.

I do not intent to propose a solution of this so-far unsolvable debate and controversy. Commonly, aragonite, calcite and dolomite are clearly referred as carbonates. I observed the tendency of separating carbonates from evaporites. The last publications by renowned Journals - such as *Geology, Marine and Petroleum Geology, Marine Geology, Journal of Structural Geology, Basin Research* – use the word *evaporites* and *salt* interchangeably with no loss of information. Hence, for the sake of text fluidity, this thesis follows the current interpretation of interchanging salt and evaporites, excluding carbonates from this group.

1.5 Structure of this thesis

In this thesis, chapter two discusses the empirical estimation of the elastic properties in the rock salt in one and three dimensions applying the methodology to the evaporite of the Ariri Formation in the Santos Basin. Chapter two offers a method to estimate the seismic-based facies distribution of salt types. In addition, it debates how the quantitative interpretation of seismic data provides new insights into the deposition environment of the Ariri Formation. Chapter four examines the estimation of the thin-bed bittern-salts thicknesses by introducing an unprecedented formulation to assess the

uncertainties of this procedure.

2 Elastic property estimation

Article published in

Journal of Petroleum Science and Engineering, volume 180, 2019

<https://doi.org/10.1016/j.petrol.2019.05.024>

Impact factor: 4.346

Authors: Leonardo Teixeira and Wagner Lupinacci

Evaporites precipitate in restricted environments dominated by a high rate of evaporation of brine-saturated fluid (WARREN, 2010) . They flow in a short period under high deviatoric stress, when compared to carbonate and clastic rocks. Salt fluidity imposes tectonic deformations, which contribute to create a suitable environment for oil migration and for trap formation. Even though evaporites constitute 2% of the world's sedimentary rocks, they represent the seal of more than 50% of the world's oil reserves (WARREN, 2006). Not surprisingly, most of prolific oil and gas provinces take place in salt-rich basins (MOHRIAK; SZATMARI; ANJOS, 2012).

Irregular and complex structures formed by halokinesis impose challenges to the seismic imaging of reservoirs below and around salt bodies (JONES; DAVISON, 2014). The refinement of the velocity model within salt bodies can improve the seismic imaging in these reservoirs. Ji et al. (2011) evaluated the reverse time migration (RTM) in synthetic and real data using two seismic velocity models: clean and dirty/stratified salt. When compared to the dirty salt model, the sub-salt images of the clean salt model display lateral weaknesses, discontinuities in the reflectors and the diffractions-like events, which could be misinterpreted as faults or fractures. Gobatto et al. (2016) proposed a workflow to assess the intrasalt information and to refine the velocity model, thereby including heterogeneities in the salt bodies. These inclusions increased the reliability of the illumination studies and boosted the seismic reprocessing of legacy data in the sub-salt reservoirs (JARDIM et al., 2015; MAUL et al., 2015; FONSECA et al., 2017). Also, a good starting velocity model, preserving the geological features, can improve the seismic imaging by prevent local minima in full-waveform inversion (VIRIEUX;

OPERTO, 2009). In addition to the P-wave, for advanced seismic interpretation, the use of converted S-waves requires the velocity modeling of shear-wave for the P-S processing of multicomponent acquisition (YANG et al., 2015).

Pore pressure changes during the reservoir development with the injection and production, thereby affecting the stress state of the reservoir and its encasing rocks. Geomechanical modeling is a powerful tool to assess the pore pressure limits to prevent those hazardous events from happening. Admittedly, the individualization of elastic properties in evaporites increases the robustness of geomechanical analyses, improving the forecast of state stress of encasing rocks. In the Aptian sub-salt reservoirs of the Santos and Campos Basins, the estimation of elastic properties and thickness of the anhydrite in the salt base is critical to predicting the production and injection limits to ensure the caprock integrity.

Drilling through salt sections is challenging. The high-viscosity and high-density contrasts between the several salt types result in movements of the multilayered evaporites, which depend on the mechanical properties, the layer geometry, stress and temperature (LI et al., 2012). The creep behavior of the rock salt causes operation problems such as washout, closing pipes, fluid loss damage and borehole collapse (DUSSEAULT; MAURY; SANFILIPPO, 2004; STROZYK, 2017). Analytical and numerical models require the knowledge of density, Poisson's ratio and Young's modulus to understand the mechanical behavior of salt bodies, to calculate subsidence caused by underlain reservoirs and to estimate the optimum fluid weight to avoid drilling problems (INFANTE; CHENEVERT, 1989; CARCIONE; HELLE; GANGI, 2006; WEIJERMARS; JACKSON, 2014; MARKETOS; GOVERS; SPIERS, 2015; WANG; SAMUEL, 2016). The identification of the low-density potash and magnesium salts before drilling is a key factor for operational safety (COSTA et al., 2010).

Many authors have demonstrated, for a wide variety of sedimentary rocks, that the elastic properties are related to each other (CASTAGNA; BATZLE; KAN, 1993; SIMM; BACON, 2014).Castagna, Batzle and Eastwood (1985) proposed empirical equations, based on statistical regressions, to estimate the shear velocity (v_s) from the compressional velocity (v_p) for brine-bearing rocks. Han (1986) demonstrated that the relationship of $v_p - v_s$ depends on clay content. Greenberg and Castagna (1992) presented an extension for mixed lithologies and fluid contents by applying an

interactive algorithm using Biot-Gassmann's fluid substitution (GASSMANN, 1951). Others studies indicated that the relationship between the velocities may yield non-linear transforms (KRIEF et al., 1990; VERNIK; FISHER; BAHRET, 2002). Gardner, Gardner and Gregory (1974) advocated that density and velocity can be related by an exponential function. Banik, Koesoemadinata and ElKaseeh (2010) proposed a quadratic equation to estimate the Young's modulus (E) from the acoustic impedance (I_p) of shale.

Information on the relationships between the elastic properties for evaporites is scarce. Most of published studies describe these relationships for sandstone, limestone, dolomite and shale (CASTAGNA; BATZLE; KAN, 1993; SIMM; BACON, 2014) and, for rock salt, the laboratory measurements are mostly restricted to the halite-rich samples (JUSTEN; JR.; SOUZA, 2013; YAN et al., 2016; ZONG et al., 2017). Although the presence of salt is associated with oil-prolific basins, they are the encasing rocks of reservoirs and, as punctuated by Warren (2006), "very few oil companies wish to characterize what is an undeniable seal facies". Thus, the characterization of ancient evaporite basins may represent a complex task.

This study comprises log measurements of evaporites such as tachyhydrite, sylvite, carnallite, halite and anhydrite. Therefore, we formulate the empirical equations encompassing different salt types. We estimate shear velocity, Young's modulus from compressional velocity and derive density and Poisson's ration from these properties. We compare the estimated and the measured properties using well logs to evaluate the empirical equations as property estimators. Due to the unavailability of core samples of rock salt for this study, we apply the log-calibrated $v_p - v_s$ and $v_p - E$ equations to Justen's data (JUSTEN, 2014) of Taquari-Vassouras salt mine, Brazil, to inspect the accuracy of the estimations of the shear velocity and Young's modulus from compressional velocity through laboratory measurements.

Seismic data have extensively supported the structural and stratigraphic interpretation, focusing on describing the geometry, stratification and kinematics of salt bodies (GAMBOA et al., 2009; FIDUK; ROWAN, 2012; JACKSON et al., 2015; ALVES et al., 2017; RODRIGUEZ et al., 2018). These interpretations are a qualitative analysis of the seismic data and do not evaluate how the rock properties affect the seismic signal. In this work, we propose a step further to combine rock

physics and seismic inversion to carry out the quantitative interpretation from the variation of seismic amplitude for evaporites.

While laboratory analyses are confined to sparse samples and well logs are a locally restricted information, the seismic data provide the estimation of elastic properties over large areas. Seismic inversion is a procedure to transform the seismic amplitude into acoustic impedance. It integrates seismic data, stratigraphic interpretation and well information. We performed seismic inversion and applied the empirical equations to the acoustic impedance volume in order to assess the elastic volumes of salt formation. The outcomes are seismic-driven volumes of compressional and shear velocities, density, Young's modulus and Poisson's ratio that preserve the stratifications and heterogeneities of the evaporite sequence.

2.1 Study area and data set

The Santos Basin is a rift basin formed during the South Atlantic opening. In the late Aptian, the restrictive marine environment and shallow water favored the deposition of a thick (from 200 m to 3000 m) evaporite sequence (Ariri Formation) (KARNER; GAMBÔA, 2007; DAVISON, 2007; KUKLA; STROZYK; MOHRIAK, 2018). This evaporite sequence encompasses a multilayer alternation of halite, anhydrite and Mg-k salts. The absence of clastic and carbonate rocks within the Ariri Formation hints a very fast deposition in an estimated period of 400-600 ka (FREITAS, 2006). The depositional age is still controversial. Ar-Ar dating from subevaporite volcanic sequence suggests an age range 116-111 Ma, whereas high-resolution carbon isotope interpretation indicates an age range between 125 and 130 Ma (TEDESCHI et al., 2017). These evaporites play an important role in the new discoveries of the giant fields of the pre-salt province because they are the effective seals of these reservoirs (CARMINATTI; WOLFF; GAMBOA, 2008).

The seismic data set is a part of a huge high-density acquisition that started in 2009 in the Santos Basin and aimed at characterizing the presalt reservoirs (Figure 1). The ship dragged 14 cables with 8 km length with shot and receiver intervals of 100 m. The tilted transverse isotropy Kirchhoff prestack depth migration (TTI PSDM) was performed to obtain the seismic response of the local

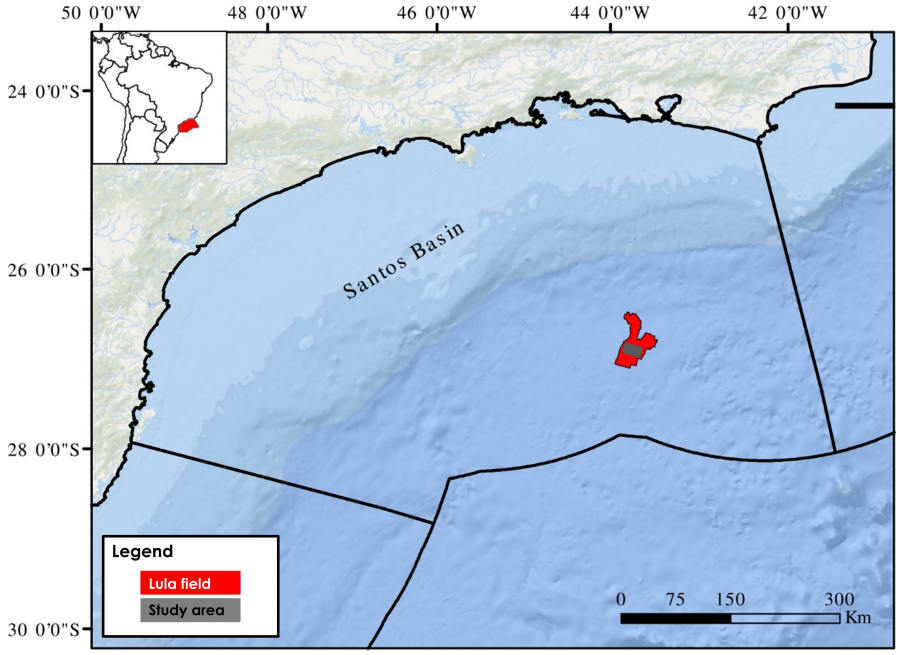

Figure 1: Location of the study area

geology. From this seismic campaign, we were allowed to investigate 98 km^2 of full-stack data. The seismic amplitude follows the Society Exploration of Geophysicists (SEG) convention, which regards the increase of acoustic impedance on the seabed as a positive amplitude or a peak. The data set comprise nine wells. The wells have gamma ray, neutron porosity and resistivity logs. However, since the target is the reservoir rocks, the data acquisition of the elastic properties in the encasing salt may be incomplete. Five wells (3-BRSA-865A, 3-BRSA-883, 3-BRSA-891A, 3-BRSA-944A, 3-BRSA-821) have the density, shear and compressional velocity logs, while four wells (BRSA-639A, 9BRSA-808, LL09, LL10) have the compressional and shear velocity logs in the salt formation.

2.2 Methodology

The methodology encompasses three major steps: well-log analysis, seismic inversion and elastic volume estimation.

Well-log analysis investigates in-situ elastic behavior of evaporate. The quality control of well logs is crucial. Caliper and coherent-wave logs assisted the identification of trustworthy parts of elastic logs. Inaccurate values with unreasonable physical meaning were removed and the well-log analysis was performed on reliable measurements. The compressional-wave and shear-wave sonic logs

provided the calculation of compressional and shear-wave velocities. We studied the relationships between the elastic properties to establish empirical equations.

The next step consists of performing sparse-spike seismic inversion, which provided the acoustic impedance volume of salt layers. Finally, we explored the empirical equations as property predictors and applied the rock-physics transforms to seismically derive volumes of compressional and shear velocities, density, Poisson's ratio and Young's modulus.

To verify the seismic predictability, we repeated the aforementioned procedure withdrawing the well BRSA-865A that were used as a blind well.

2.3 Well-log analysis

We evaluated the elastic behavior of rock salt using five wells of the Santos Basin (3-BRSA-865A, 3-BRSA-883, 3-BRSA-891A, 3-BRSA-944A, 3-BRSA-821) with the compressional velocity (P-velocity), shear velocity (S-velocity) and density logs. Figure 2 displays these properties for the well 3-BRSA-821 in the evaporitic formation to illustrate the available information. This well penetrated more than 1000 m of evaporites, described as tachyhydrite, sylvite, carnallite, halite and anhydrite. The log analysis indicates that tachyhydrite, sylvite and carnallite have low density, compressional and shear velocities, whereas anhydrite has the highest values of these properties.

The salt proportions of the wells show that halite represents about 80%, followed by 10% of the high-velocity salt (anhydrite) and 10% of the low-velocity salt (tachyhydrite, sylvite, carnallite), as specified in Table 1. Maul, Santos and Silva (2018b) presented a study of the salt facies of about 200 wells in the Santos Basin and they reported similar salt proportion. Thus, we assume that the data set is a representative sample of the Santos Basin.

We evaluated the well-log data for the establishment of the relationships between the elastic properties. As the quality of well logs affects substantially the quantitative interpretation, we executed a careful analysis in caliper and wave coherence logs to remove inaccurate values. The rock-physics relationships were established only in the reliable parts of the density and sonic logs.

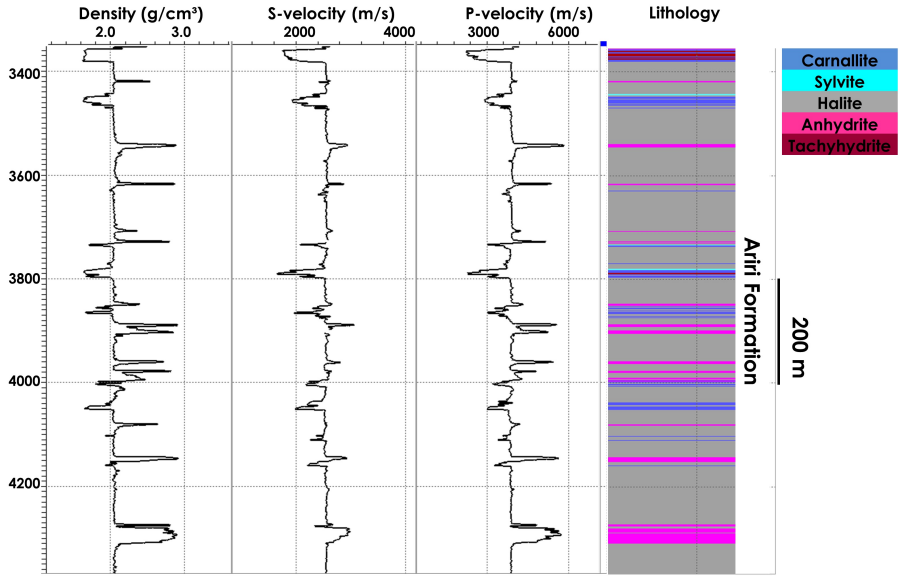

Figure 2: Density, shear velocity (S-velocity), compressional velocity (P-velocity) and lithologic logs of the well 3-BRSA-821.

Table 1: Salt proportion in the well log facies of this study (3-BRSA-865A-RJS, 3-BRSA-883-RJS, 3-BRSA-891A-RJS, 3-BRSA-944A, 3-BRSA-821-RJS).

	Salt Proportion (%)
Halite	80.5
Anhydrite	9.9
Carnallite	6.4
Tachyhydrite	3.0
Sylvite	0.2

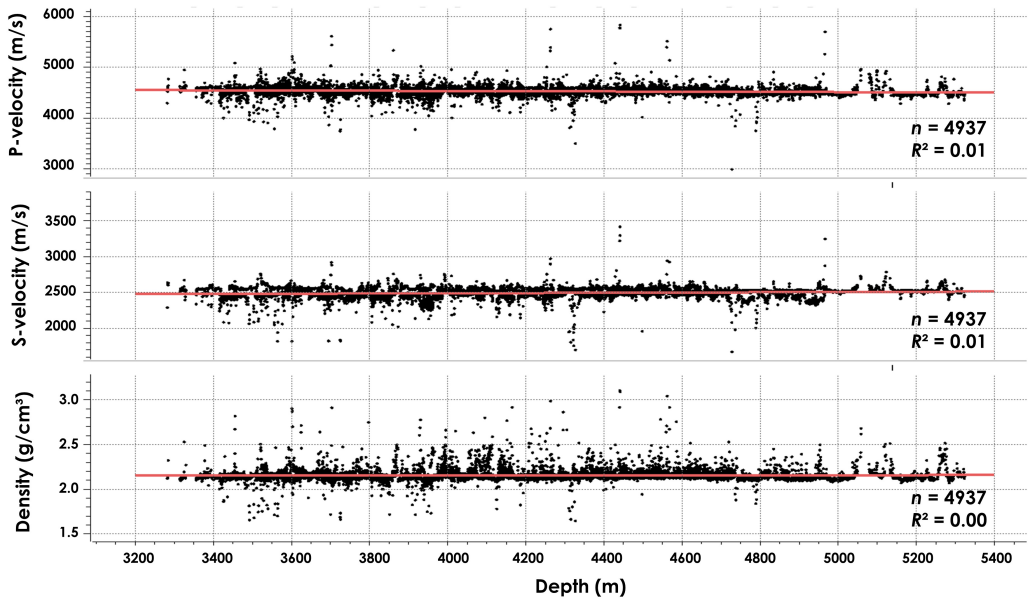

Figure 3: P-velocity (v_p), S-velocity (v_s) and density (ρ) versus depth (D) for halite (3-BRSA-865A, 3-BRSA-883, 3-BRSA-891A, 3-BRSA-944A, 3-BRSA-821). We adjusted a linear equation based on least-squares regression and found $v_p = 4602 - 0.018D$ ($R^2 = 0.01$), $v_s = 2424 - 0.016D$ ($R^2 = 0.01$) and $\rho = 2.143 - 2.814 \times 10^{-6}D$ ($R^2 = 0.00$) with velocities in m/s, depth in m and density in g/cm^3.

2.3.1 Elastic properties vs depth

Sedimentary rocks may express velocities- and density-depth trends due to compaction, diagenesis and porosity reduction. The plot in Figure 3 diagnoses the effect of compaction on the compressional velocitity, shear velocity and density for the evaporites. Inasmuch as the rock-physics depth trends depend on lithology (AVSETH; MUKERJI; MAVKO, 2005), the samples in Figure 3 are restricted to halite. Despite the fact that the wells drilled more than 2000 m through the salt formation, the elastic properties of halite are very similar. We observe that the velocities and density are unrelated to depth, therefore the compaction has small influence on these properties. Cornelius and Castagna (2018) identified a similar behavior in the rock salt of the Gulf of Mexico, reporting no influence of burial depth on the variation of compressional velocity. Here, we extend the analysis for shear velocity and density. Accordingly, we postulate that the salt composition is a key factor for the variation of elastic properties.

Laboratory measurements of halite samples reveal that the effect of pressure on velocity changes is very small (YAN et al., 2016), therefore the compaction influence on velocity is insignificant. Furthermore, the porosity of rock salt is virtually null; hence, the effect of porosity reduction due to the

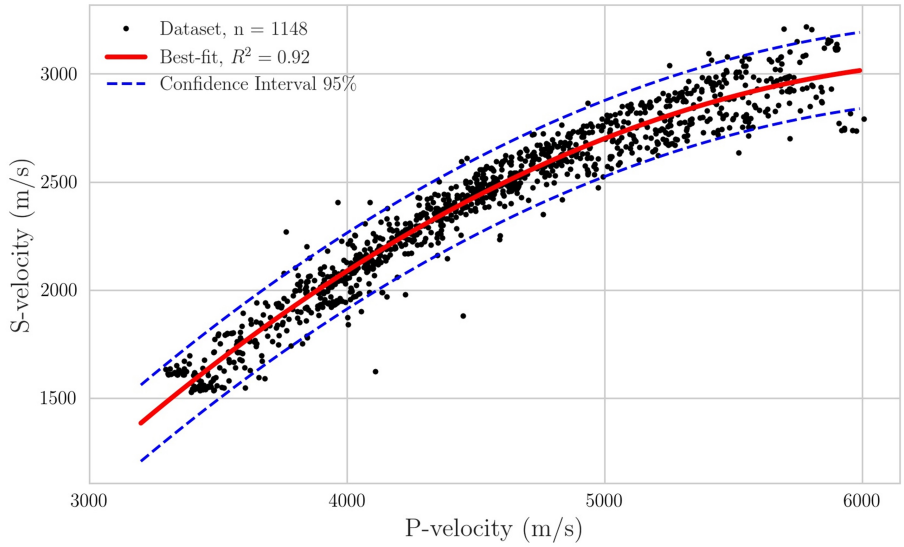

Figure 4: The cross-plot of the shear and compressional velocities. The black line represents the quadratic function relating both properties ($R^2 = 0.92$).

increase of burial depth may be negligible. Zong et al. (2017) reported a significant positive variation of compressional velocity with the increase of pressure in salt samples using ultrasonic measurements, however they associated this effect with the presence of cracks.

2.3.2 Estimation of shear velocity

We investigated the relationship between the compressional and shear velocities for the rock salt of the Santos Basin (Figure 4). We found that the shear velocity increases with the increase of the compressional velocity. Published laboratory measurements confirm this behavior for evaporites (MAVKO; MUKERJI; DVORKIN, 2009). We adjusted a quadratic function (Equation 2.1) using least-squares regression to correlate the velocities:

$$v_s = -1.944 \times 10^{-4} v_p^2 + 2.366 v_p - 4236. \tag{2.1}$$

where v_p is the compressional velocity and v_s is the shear velocity. The velocities are measured in m/s.

Equations 2.2 and 2.3 define the upper and lower bounds with 95% confidence level for $v_s(v_p)$:

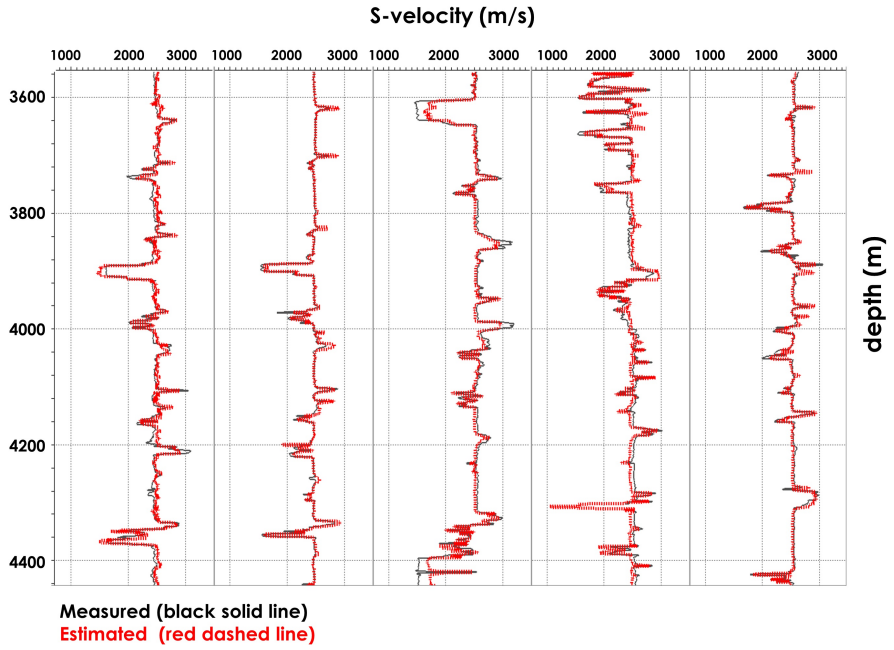

Figure 5: The comparison between the measured (black) and the estimated (red) shear velocity by applying Equation 2.1 to the compressional velocity for five wells in the salt formation (from left to right: 3-BRSA-865A, 3-BRSA-883, 3-BRSA-891A, 3-BRSA-944A, 3-BRSA-821). The curves are very similar.

$$v_{su} = -1.940 \times 10^{-4} v_p^2 + 2.362 v_p - 4052. \tag{2.2}$$

and:

$$v_{sl} = -1.947 \times 10^{-4} v_p^2 + 2.369 v_p - 4419. \tag{2.3}$$

where v_{su} and v_{sl} are the upper and lower regressions of shear velocity.

We tested the efficacy of the $v_p - v_s$ relationship by applying Equation 2.1 to the compressional velocity logs to estimate the shear velocity logs. Henceforth, we regard the least-squares regression (best-fit) as the reference for the property estimation. The comparison between the estimated and the measured curves evidences that the empirical equation can accurately estimate the shear velocity (Figure 5).

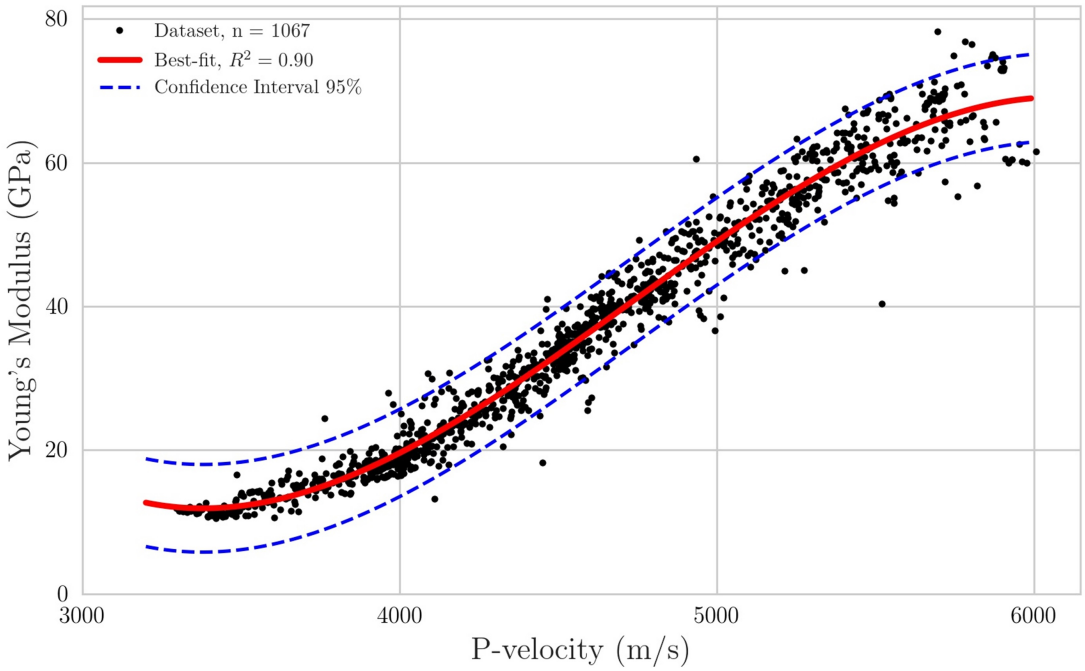

Figure 6: Cross-plot of Young's modulus and compressional velocity. The black line represents the cubic function correlating both properties ($R^2 = 0.90$).

2.3.3 Estimation of the Young's modulus

In homogeneous isotropic material, the Young's modulus (E) can be calculated from density (ρ) and compressional (v_p) and shear velocities (v_s) by the following equation:

$$E = v_s^2 \rho \frac{3v_p^2 - 4v_s^2}{v_p^2 - v_s^2}. \tag{2.4}$$

Figure 6 illustrates the cross-plot of compressional velocity and Young's modulus for the salt formation in the Santos Basin. We fitted a cubic function (Equation 2.5) using least-squares regression in $E - v_p$ domain to relate these properties ($R^2 = 0.90$):

$$E = -5.512 \times 10^{-9} v_p^3 + 7.837 \times 10^{-5} v_p^2 - 3.397 \times 10^{-1} v_p + 477.262. \tag{2.5}$$

where the Young's modulus is measured in GPa and the compressional velocity is measured in m/s.

Equations 2.6 and 2.7 define the upper and lower bounds for $E(v_p)$ with 95% confidence

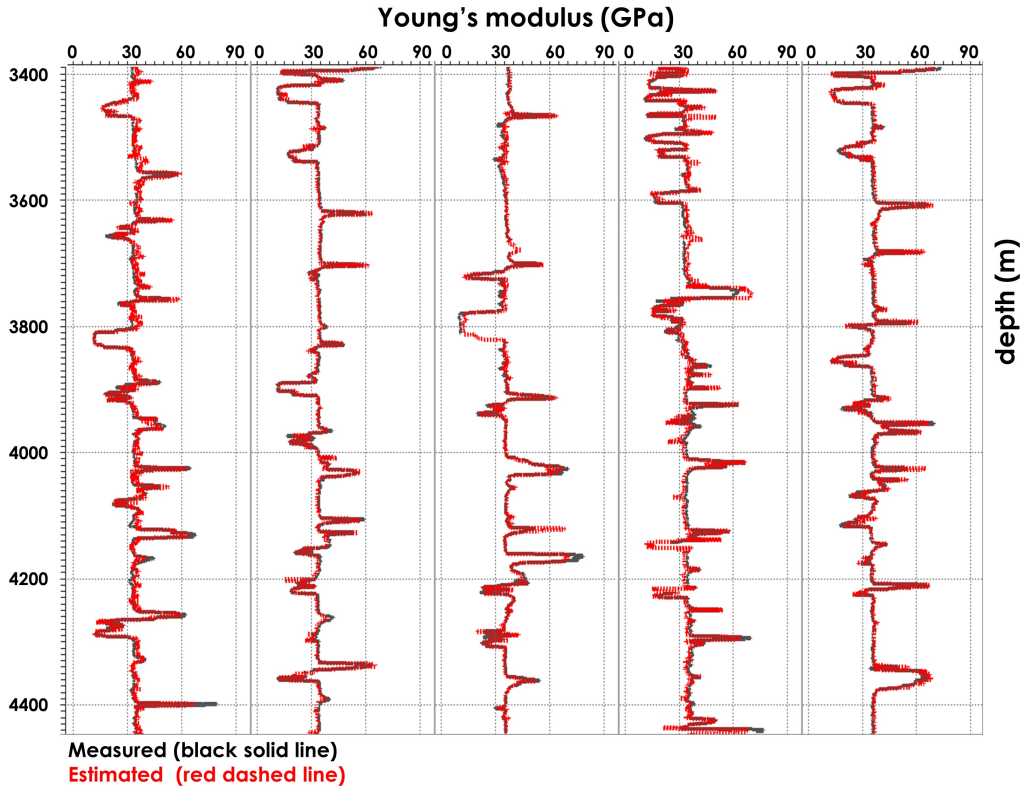

Figure 7: The comparison between the measured (black) and the estimated (red) Young's modulus. The curves are very alike.

level:

$$E_u = -5.510 \times 10^{-9} v_p^3 + 7.836 \times 10^{-5} v_p^2 - 3.397 \times 10^{-1} v_p + 483.566, \tag{2.6}$$

$$E_l = -5.513 \times 10^{-9} v_p^3 + 7.837 \times 10^{-5} v_p^2 - 3.396 \times 10^{-1} v_p + 470.957, \tag{2.7}$$

where E_u and E_l are the upper and lower bounds of the Young's modulus, respectively.

Figure 7 juxtaposes the measured and the estimated Young's modulus from compressional velocity. Likewise observed for shear velocity, the estimated and measured curves are very alike.

2.3.4 Estimation of density

Gardner's relationship (GARDNER; GARDNER; GREGORY, 1974) correlates the density and compressional velocity of a formation by an exponential function in the form of $\rho_b = a v_p^b$, where a and b are lithology-dependent constants usually calibrated in a brine-saturated samples. Gardner's relationship states a positive correlation between compressional velocity and density. The log tool response, summarized in Table 2, indicates that density decreases with the decrease of compressional

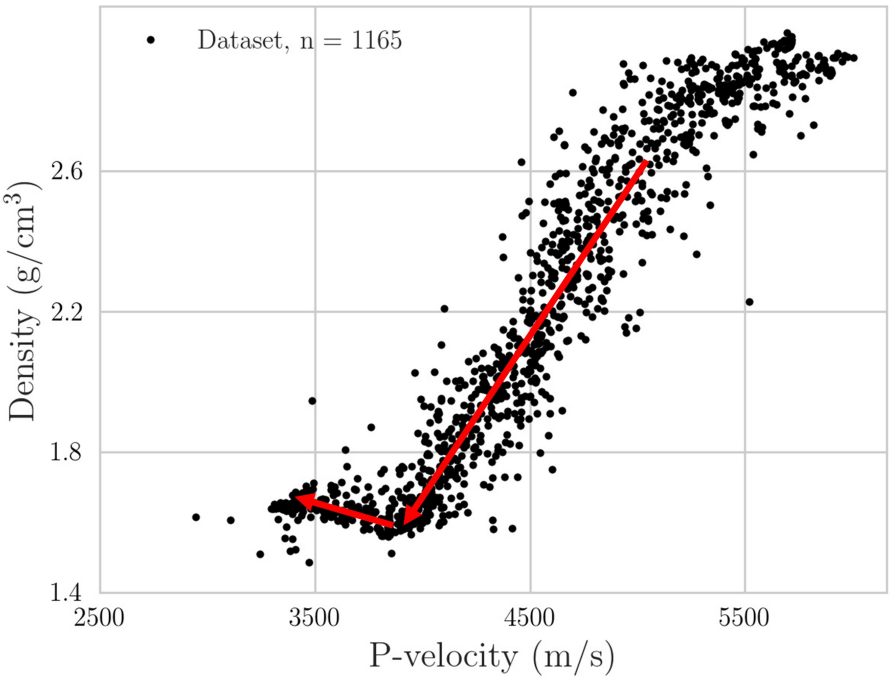

Figure 8: The in-situ condition of the $\rho - v_p$ relationship

velocity except for tachyhydrite. Tachyhydrite has lower velocity than carnallite, however it is denser, thereby indicating an inflection behavior in the $\rho - v_p$ relationship. The in-situ condition of evaporites in the Santos Basin exhibits similar response in compressional velocity at about 3900 m/s (Figure 8).

Table 2: Log response tool for evaporites (SERRA, 1990)

	Compressional Velocity (m/s)	Density (g/cm^3)
Tachyhydrite	3313	1.66
Carnallite	3908	1.56
Sylvite	4130	1.86
Halite	4570	2.03
Anhydrite	6096	2.95

The inflection behavior in the $\rho - v_p$ relationship for bittern salts implies that the Gardner's relationship is not appropriate to describe the relationship between velocity and density for evaporites. Therefore, we propose the following steps to estimate the density from the compressional velocity:

1. Estimate the shear velocity by Equation 2.1.
2. Estimate the Young's modulus by Equation 2.5.
3. Apply Equation 2.4 to compute the density from Young's modulus, shear and compressional velocities.

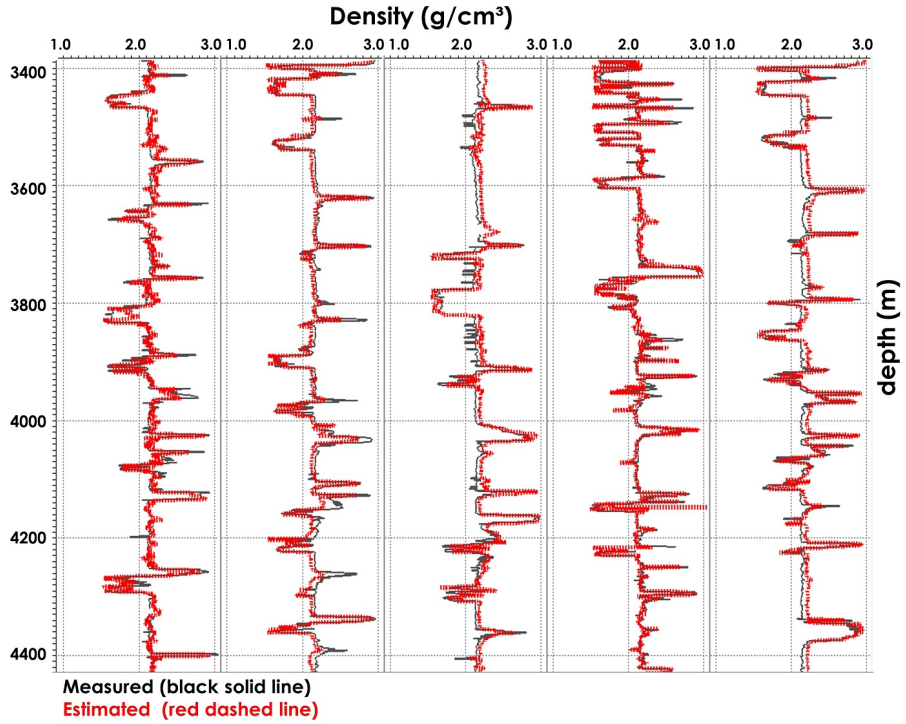

Figure 9: The comparison between the measured (black) and the estimated (red) density for five wells (from left to right: 3-BRSA-865A, 3-BRSA-883, 3-BRSA-891A, 3-BRSA-944A, 3-BRSA-821). The curves are very close to each other.

The measured and the estimated density logs are displayed in Figure 9. The measured and the estimated curves are very close to each other.

2.3.5 Estimation of Poisson's ratio

For homogeneous isotropic material, the Poisson's ratio (ν) is calculated by the following equation:

$$\nu = \frac{1}{2}\frac{v_p^2 - 2v_s^2}{v_p^2 - v_s^2}. \tag{2.8}$$

We found no evidence of correlation between Poisson's ratio and compressional velocity, therefore we discarded the calibration of an empirical equation relating these two properties. Nevertheless, the estimation of Poisson's ratio from compressional velocity can be performed by combining Equations 2.1 and 2.8. Figure 10 shows the comparison between the measured and the estimated curves.

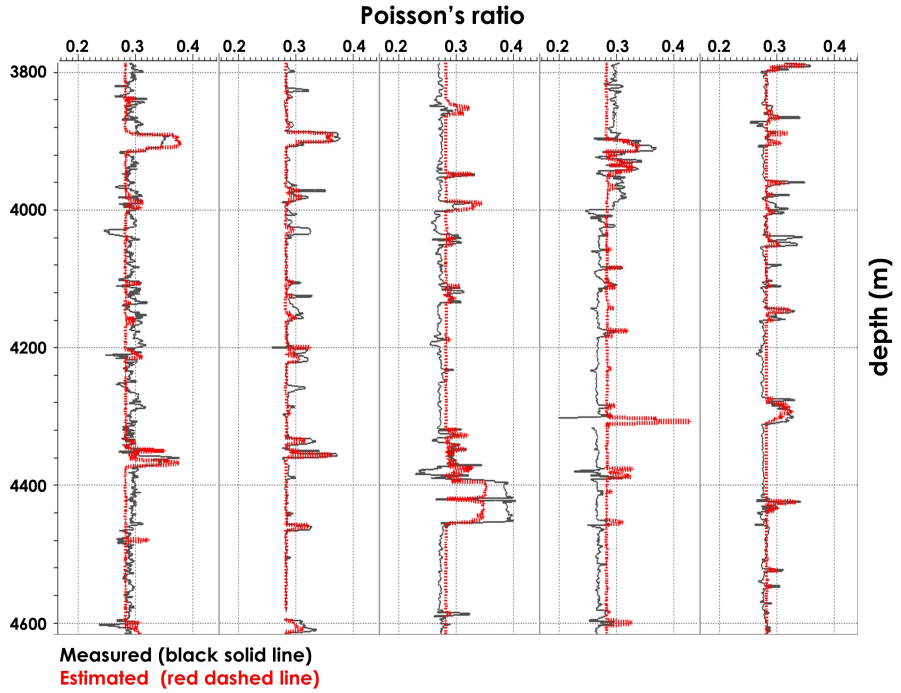

Figure 10: The comparison between the measured (black) and the estimated (red) Poisson ratio for five different wells (from left to right: 3-BRSA-865A, 3-BRSA-883, 3-BRSA-891A, 3-BRSA-944A, 3-BRSA-821).

2.3.6 Quantitative error

Figure 5, 7, 9, 10 show the comparison between the measured and the estimated elastic property logs and, visually, they evidence that the curves are very close to each other. Additionally, we calculated the mean absolute percentage error (MAPE) for each estimated elastic property to provide a quantitative appraisal between the measured and the estimated logs, as follows:

$$MAPE = \frac{1}{N}\sum_{i=1}^{N}\frac{|X_i - Y_i|}{|X_i|}. \tag{2.9}$$

where X_i is the measured property, Y_i is the estimated property and N is the number of samples.

Among the estimated elastic properties, shear velocity has the lowest MAPE, followed by density, Poisson ratio and Young modulus (Table 3). The low mean absolute percentage error (MAPE) of the elastic properties indicates that the proposed empirical equations are good estimators.

Laboratory measurements ensure robustness to rock-physics analysis. However, the data

Table 3: The mean absolute percentage error of the estimated elastic properties from compressional velocity.

	MAPE (%)
Shear velocity	2.0
Density	3.3
Poisson ratio	3.4
Young modulus	4.3

set of this study lacks core samples of rock salt to evaluate the elastic properties using laboratory measurements. We resort to the ultrasonic measurements of compressional and shear velocities from Vassoura-Taquiri mine performed by Justen (2014) to circumvent the unavailability of core samples. We applied Equations 2.1 and 2.5 to the compressional velocity of Justen's data to estimate shear velocity and Young modulus. The MAPE between the measured and the estimated values of shear velocity and Young modulus are 4.2 % e 5.1 %, respectively. Despite the empirical equations 2.1 and 2.5 are site-specific and they were calibrated using the well logs of the Santos Basin, they yield good predictions for the salt samples of Taquari-Vassouras mine. It suggests that the variation of elastic properties of evaporites exhibits similar behavior, regardless the depositional environments.

2.4 Seismic estimation of elastic properties

The halokinesis creates domes and folds with dipping layers varying from 0 to 60 degrees. Strong and complex reflections in steep interfaces of the top of salt and the layered sequence thereof originate high-amplitude interbed multiples (GRIFFITHS; HEMBD; PRIGENT, 2011). These interbed internal multiples may cause constructive and destructive interferences in seismic amplitude thereby hampering seismic imaging within the salt and the sub-salt rocks.

Figure 11 presents the seismic and the synthetic data in the salt formation for the wells 3-BRSA-865A and 7-LL-10. The well 3-BRSA-865A, Figure 11 (a), has density, P- and S-velocity logs, while the well 7-LL-10, Figure 11(b), has only the P- and S-velocity logs. We used the empirical equations as property predictors to estimate the density when it is not available to generate the acoustic impedance for the seismic welltie. We verified a good correlation in both wells when the real and the synthetic seismic are compared. The variation of the acoustic impedance in the evaporite sequence is

compatible with the reflections observed in the seismic data. The correlation coefficients between the synthetic and the seismic data are 0.75 and 0.81, respectively, for 3-BRSA-865A and 7-LL-10. The high correlation coefficient of the seismic welltie of 7-LL-10 corroborates the density estimation from compressional velocity. The seismic welltie supports the quantitative interpretation of seismic data for the rock characterization.

2.4.1 Seismic inversion in the salt formation

Seismic amplitude can spatially assist the estimation of elastic properties. This task can be performed via seismic inversion, which combines seismic amplitude, stratigraphic interpretation and well-log data to derive elastic volumes based on seismic trace inversion (LATIMER, 2011). The procedure involves seismic welltie, wavelet estimation, low-frequency model building, parametrization and careful quality control. This technique is widely used for reservoir characterization and its application can be performed to estimate the rock properties for evaporites (TORIBIO et al., 2017; TEIXEIRA et al., 2018). We performed a sparse spike inversion, following a standard workflow in the oil industry (KEMPER, 2010; SIMM; BACON, 2014).

Seismic inversion requires an initial model to include the low-frequency bandwidth, absent in seismic data. A 3D grid was created based on seismic interpretation of the top and the base of the salt formation. Statistical techniques, mostly using the distance between the wells, interpolate the low-frequency components presented in well logs, following the stratigraphy of the grid layers. Density and compressional velocity logs are indispensable to calculate the acoustic impedance log. We adopted the empirical equations as property predictors to estimate the density from compressional velocity in the wells where the density logs were not acquired.

Figure 12 displays the seismic amplitude and the acoustic impedance. The wells BRSA-865A, BRSA-369A and LL-10 are identified with the identical color-coding of the acoustic impedance volume to evaluate the quality of the seismic inversion (Figure 12 (b)). The comparison between the seismic and the wells indicates that the acoustic impedance volume closely matches the well logs. In addition, we can observe that the seismic inversion preserves the intrasalt structures observed in the seismic amplitude. The strong seismic reflectors within the salt formation relate to the contrasts of the acoustic

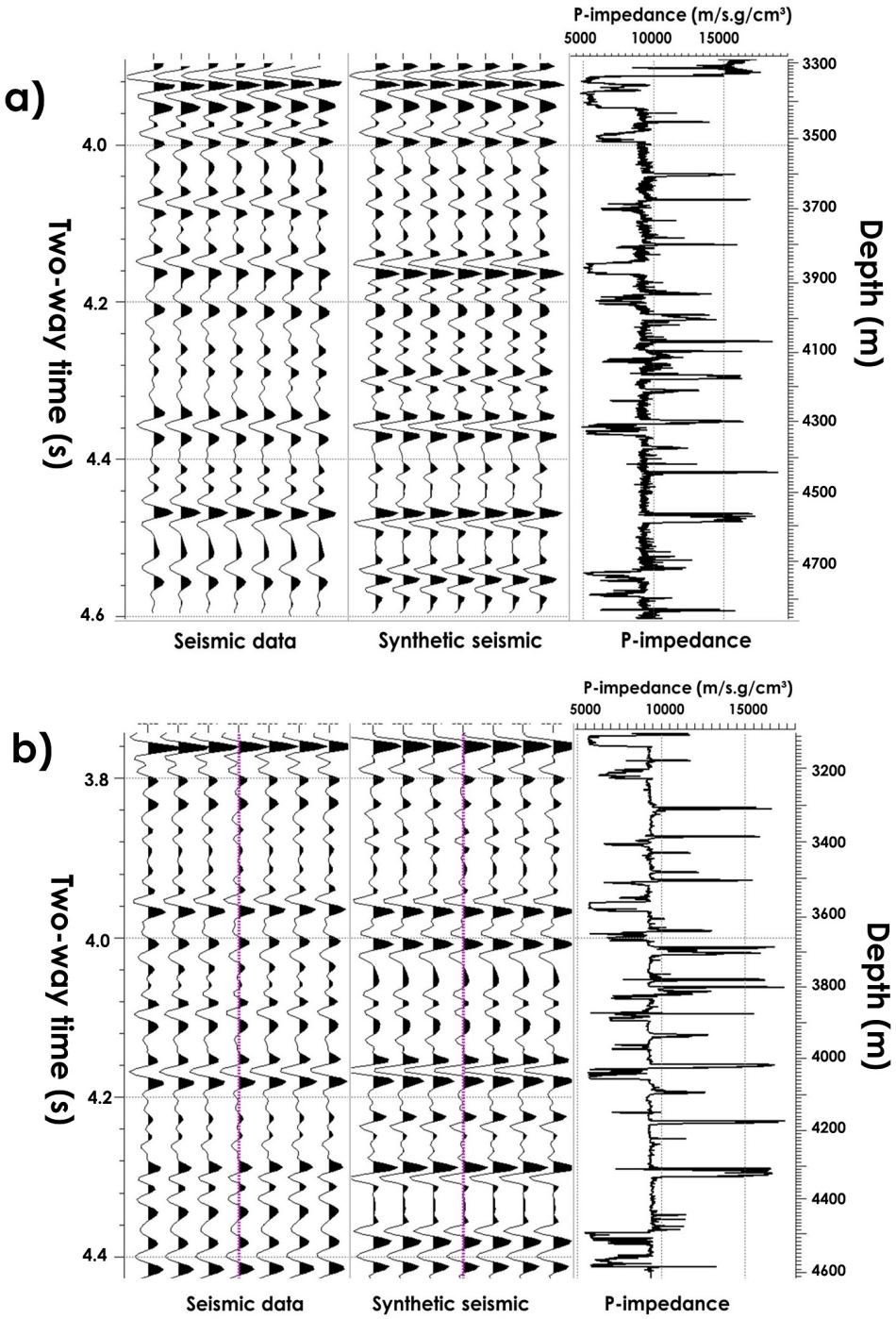

Figure 11: Seismic welltie in the evaporite formation displaying the seismic data, synthetic data and acoustic impedance log. (a) the well 3-BRSA-865A has P-velocity and density logs and (b) in the well 7-LL-10, the density log was estimated from compressional velocity.

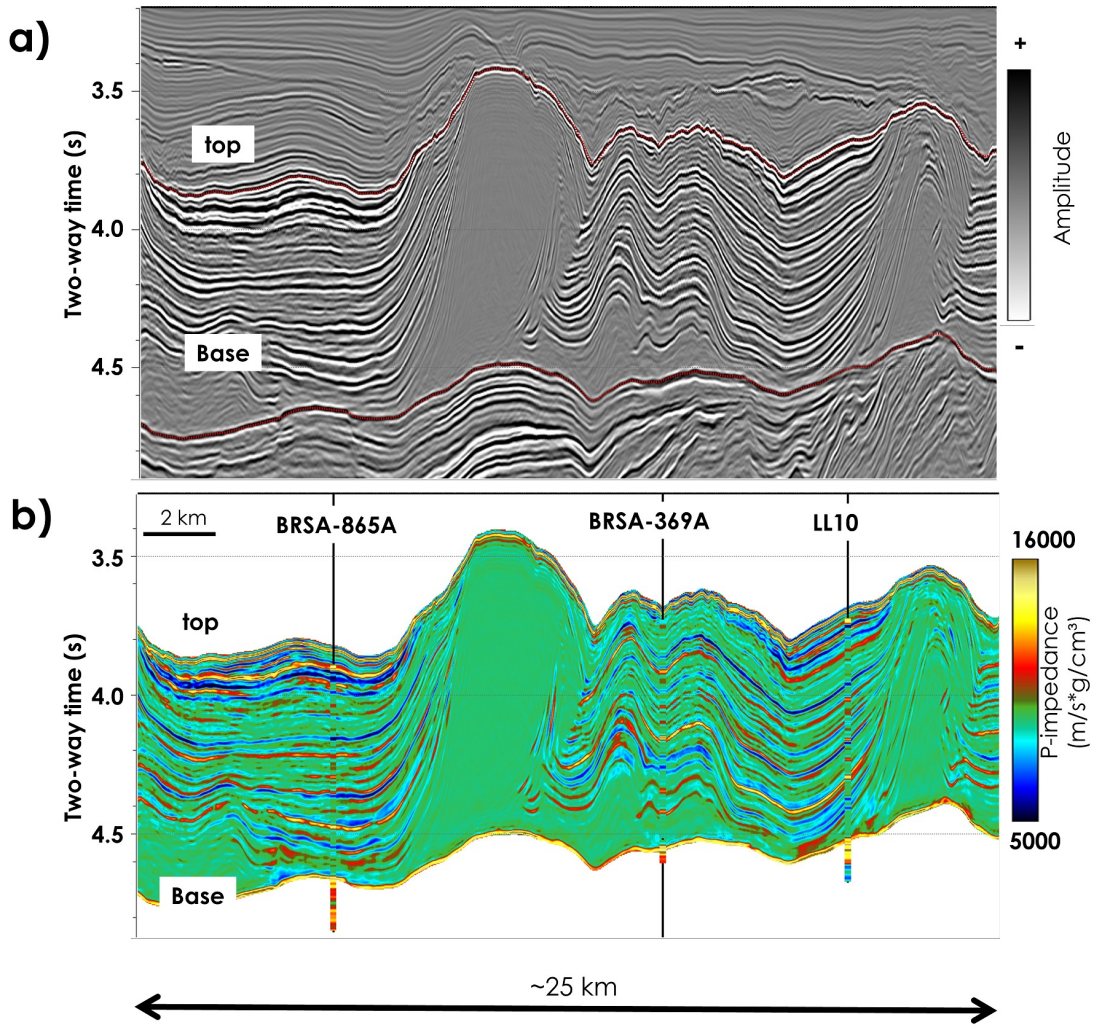

Figure 12: Seismic section in the evaporite formation displaying three wells: (a) the seismic amplitude and (b) the acoustic impedance volume. Each well path is color-coded with the same scale of the seismic section. Notice that not only the salt stratifications are preserved but also the acoustic impedance of the evaporite sequence is quantitatively assessed.

impedance of the multilayered evaporite sequence.

We cannot directly associate the low and high amplitudes with one specific rock type essentially because the seismic amplitude is a response of contrasts of elastic properties. However, the rock-physics analysis indicates that the low acoustic impedance is associated with the low-velocity (bittern) salts, such as tachyhydrite, carnallite and sylvite, whereas the high acoustic impedance is an indicative of anhydrite. The background value, approximately 9700 m/s.g/cm^3, is associated with the halite-rich salts. Notably, the acoustic impedance provides a more direct indication of the evaporite minerals, thereby assisting the seismic facies interpretation.

The occurrence of anhydrite caprock on the top of the salt, in contact with the upper layers of

the Albian carbonates, imposes a transition from low acoustic impedance to high acoustic impedance. This transition creates a strong positive reflector (red line in Figure 12(a)) on the top of salt. Mohriak, Nemčok and Enciso (2008) named this horizon as enigmatic reflector. The seismic inversion is able to recover the acoustic impedance of anhydrite (> 16000 g/cm^3.m/s) related to this enigmatic reflector. This strong positive amplitude spans over the seismic section, indicating an extensive presence of anhydrite caprock on the top of the salt formation. The dissolution of halite by meteoric water may be a plausible explanation of the anhydrite caprock formation (WARREN, 2006).

2.4.2 Spatial estimation of the elastic properties of rock salt

Following the previous approach, we also established an empirical equation correlating the acoustic impedance and the compressional velocity using well logs. We adjusted a cubic function (Equation 2.10) by least-squares regression ($R^2 = 0.92$), as displayed in Figure 13:

$$v_p = 2.897 \times 10^{-9} I_p^3 - 1.011 \times 10^{-4} I_p^2 + 1.287 I_p - 1035. \tag{2.10}$$

where I_p is the acoustic impedance measured in g/cm^3.m/s and v_p is the compressional velocity measured in m/s.

The upper and lower bounds of the 95% confidence level are given by:

$$v_{pu} = 2.889 \times 10^{-9} I_p^3 - 1.011 \times 10^{-4} I_p^2 + 1.287 I_p - 801, \tag{2.11}$$

$$v_{pl} = 2.895 \times 10^{-9} I_p^3 - 1.010 \times 10^{-4} I_p^2 + 1.287 I_p - 1269. \tag{2.12}$$

where v_{pu} and v_{pl} are the upper and lower bounds for $v_p(I_p)$, respectively.

We resorted to the empirical equations developed for evaporites to derive the seismic cubes of elastic properties from the acoustic impedance volume to cope with the limitation of the seismic inversion due to the unavailability of angle stacks. For this, the following steps are proposed:

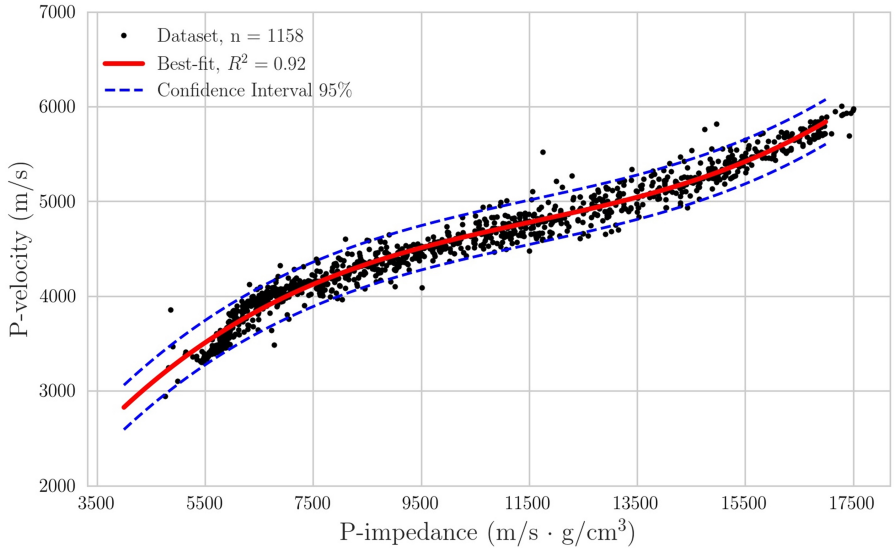

Figure 13: Compressional velocity versus acoustic impedance for the rock salt. The black line represents the cubic function relating both properties.

1. Estimate the compressional velocity from the acoustic impedance using Equation 2.10;

2. Estimate the shear velocity from the compressional velocity using Equation 2.1;

3. Estimate the density with: $\rho = I_p/v_p$;

4. Calculate the Young's modulus and the Poisson's ratio via Equations 2.4 and 2.8, respectively.

Figure 14 shows the measured and the estimated elastic properties from the acoustic impedance to verify efficiency of the empirical equations. For visual inspection, here we chose the well 3-BRSA-821 to display the curves. Additionally, for the quantitative analysis, the MAPE of each estimated elastic property is specified in Table 3, which comprises the wells (3-BRSA-865A, 3-BRSA-883, 3-BRSA-891A, 3-BRSA-944A, 3-BRSA-821) with density, compressional and shear velocities.

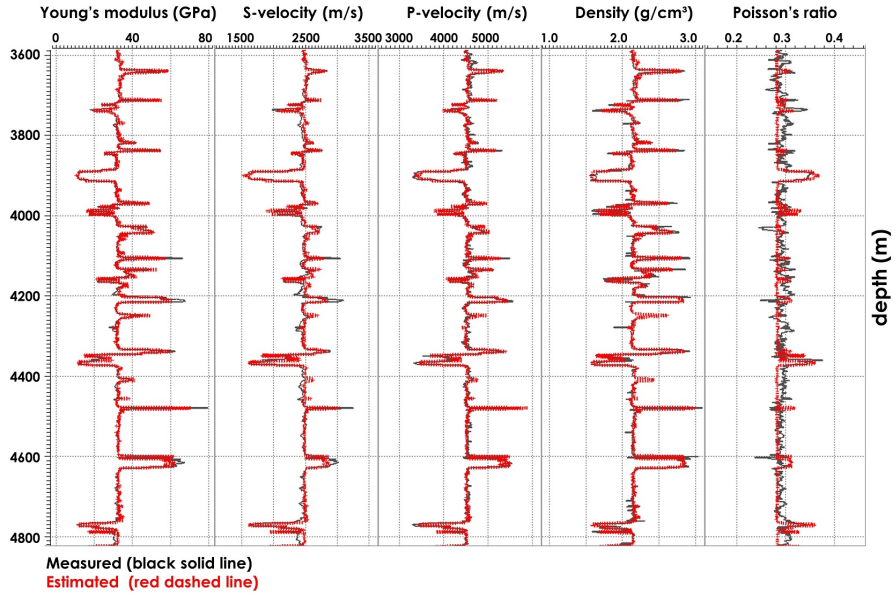

Figure 14: Comparison between the measured (red) and the estimated (black) elastic properties from acoustic impedance in the well 3-BRSA-821.

Table 4: MAPE of the estimated elastic properties from steps 1 to 4.

	MAPE (%)
Compressional velocity	1.7
Shear velocity	2.6
Density	1.5
Poisson's ratio	3.4
Young's modulus	3.7

We have developed a series of empirical equations, which enable the estimation of elastic properties of rock salt. From this, we can expand from 1D to 3D estimation thus obtaining the seismic-based volumes of the density, compressional velocity, Poisson's ratio and Young's modulus from the acoustic impedance volume. However, this procedure leads us to a usual question: are rock-physics relationships derived at log scale applicable at seismic scale?

Dvorkin and Wollner (2017) demonstrated that rock-physics transforms established in fine scale can be approximately applicable in a coarse scale (seismic scale), assuming the Backus' averaging (BACKUS, 1962) as an appropriate upscale technique. The conditions are the case of a layered geometry with null hydraulic communication at the time scale of the elastic wave propagation. The multilayered stratification and virtually null porosity of evaporites satisfy these assumptions.

Figure 15 displays the seismic section with the elastic properties estimated by applying the

empirical equations to the acoustic impedance volume. Along with the seismic section, four wells with identical color-coding compare the volumes and well logs.

We can verify in Figure 15 that compressional and shear velocities, Young's modulus and density have a good correlation with well logs. The log and the elastic volumes are very close to each other. Poisson's ratio shows a smaller correspondence between the curves and the seismic inversion outcomes for the wells BRSA-639A and LL10. The quality of the seismic-based elastic properties, as proposed here, depends on the ability of the empirical equations as property predictors and on the outcome from the seismic inversion.

The high vertical variability of the elastic properties occurs in response to the multilayered evaporite sequence of several salt types such as tachyhydrite, sylvite, carnallite, halite and anhydrite. The elastic volumes were able to adequately represent the high compressional velocity, density and Young's modulus of the anhydrite. Likewise, it was also possible to recover the low velocity, density and Young's modulus, which are attributed to the presence of bittern salts.

We performed the seismic inversion by withdrawing the well BRSA-865A to verify the efficiency of the prediction of elastic properties via seismic data, based on the methodology presented here. Figure 16 shows BRSA-865A used as blind well. The well path displays the elastic properties with identical color-coding of the seismic section. The seismic predicts that the well is located in a stratified evaporite environment with a high vertical variation of the elastic properties thus in accordance with the blind well. Therefore, we verify that the seismic inversion preserves the salt morphology observed in the seismic amplitude and, in combination with rock physics, quantitatively predicts the elastic properties of salt.

2.5 Discussion

The benefits of seismic characterization of the rock salt are not restricted to geophysical activities and, arguably, have wide interdisciplinary applications. The success of the seismic migration algorithms, the amplitude reliability and the positioning of the top of reservoirs depend on the accuracy of velocity modelling of overburden, including the evaporite sequences. During the reservoir development lifecycle, depletion may induce subsidence on the overburden rocks. Conversely, high rate

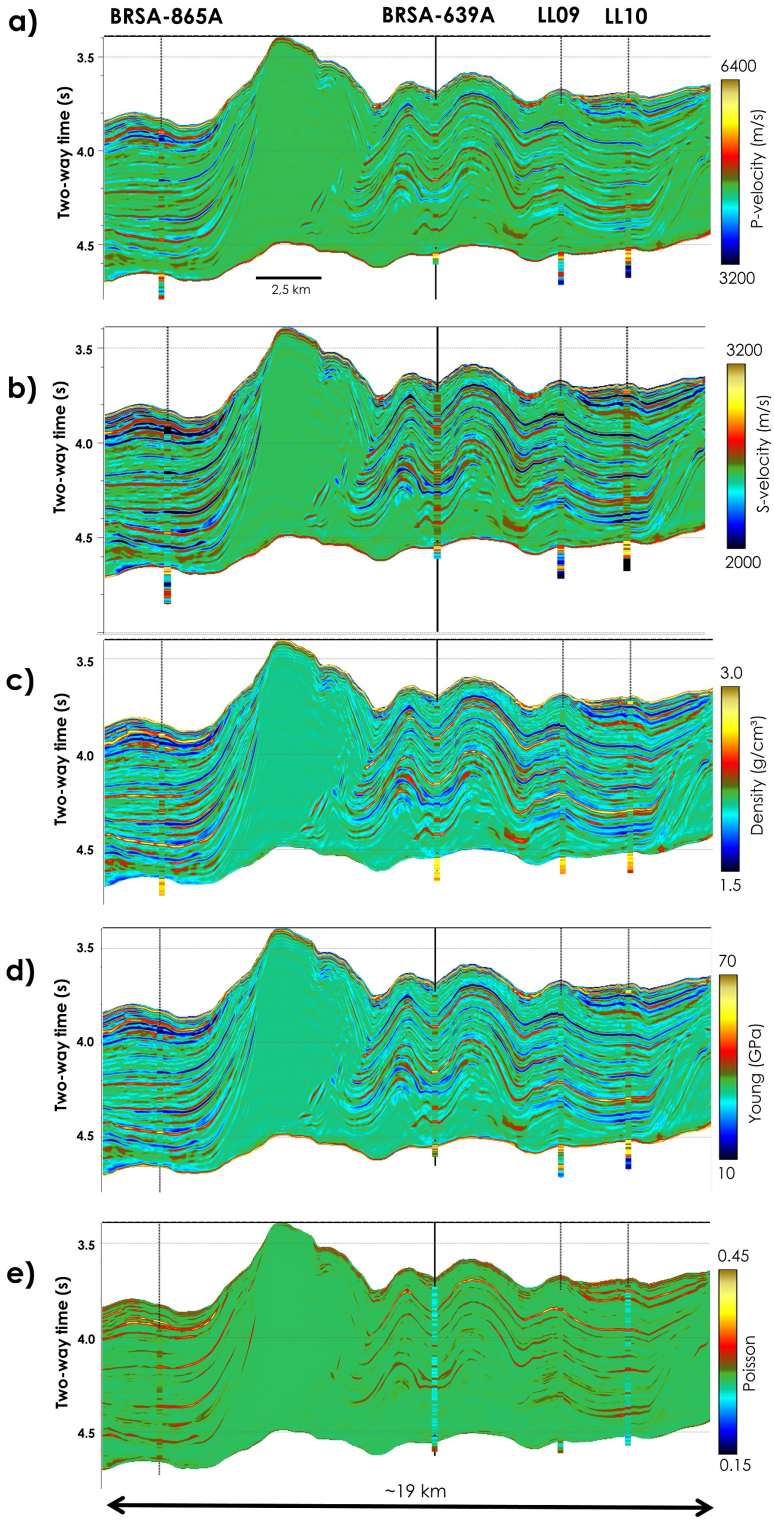

Figure 15: Elastic properties in the salt formation: (a) P-velocity, (b) S-velocity, (c) density, (d) Young's modulus and (e) Poisson's ratio. Each well path is color-coded with the respective elastic property of the seismic section.

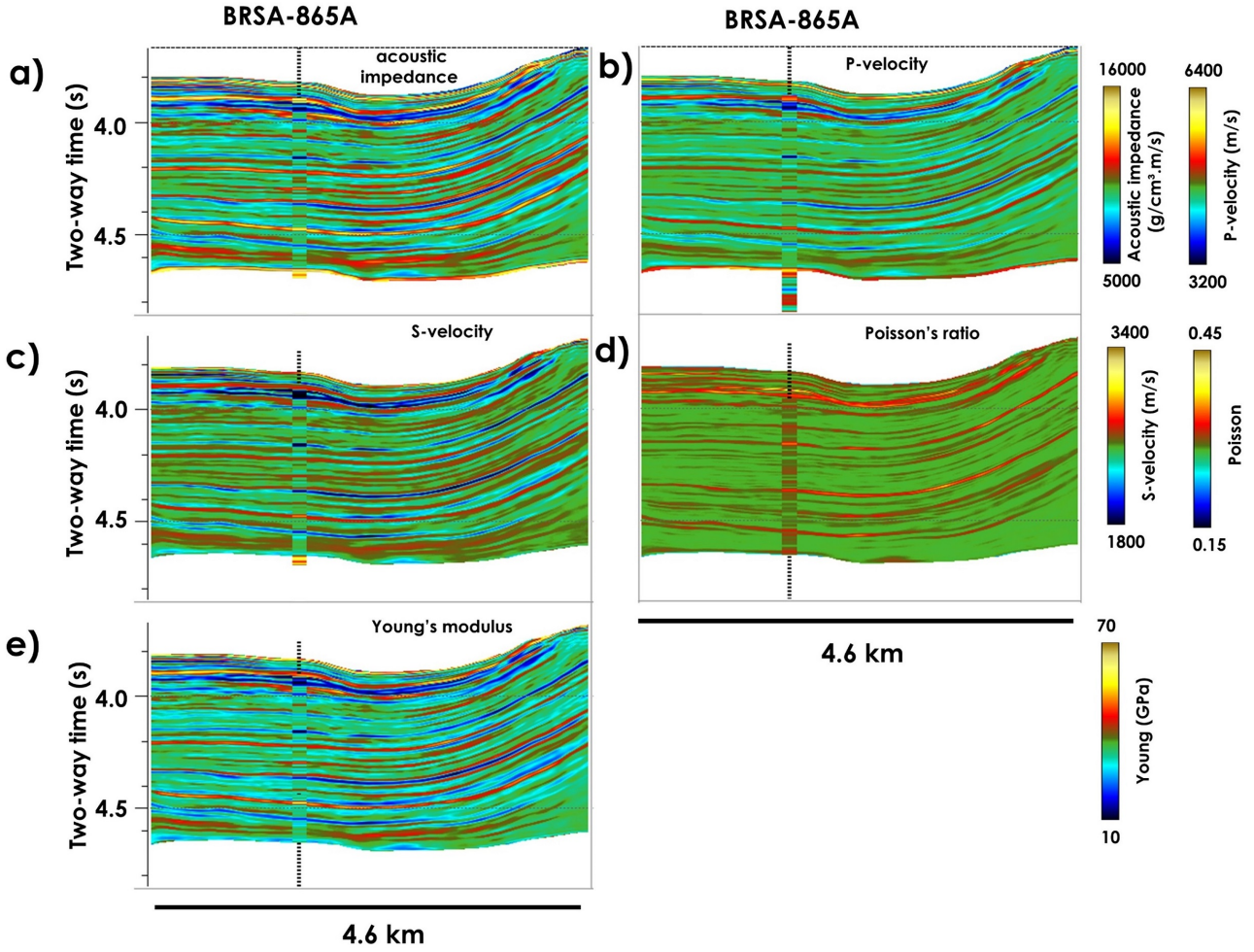

Figure 16: Elastic property prediction from the seismic data in the salt formation: (a) acoustic impedance, (b) compressional velocity, (c) shear velocity, (d) Poisson's ratio, (e) Young's modulus. The well BRSA-865A is a blind well. It is color-coded by the respective property in the seismic section.

of pressurization may induce fractures in the reservoir caprock and be responsible for fault reactivation. The knowledge of elastic properties is a critical input to forecast the stress state of overburden rocks via geomechanical analysis. Still, analytical and numerical models require density, Poisson's ratio and Young's modulus to estimate the in-situ stress conditions for well design and to optimize the fluid weight calculation to avoid drilling problems. However, most of encasing rock models represent evaporites as homogenous masses. The focus of this paper was to propose a methodology to assess the heterogeneities of the evaporite minerals, thereby refining the elastic models within the salt bodies and averting from representing them as homogeneous.

The acquisition of shear-wave velocity and density is costly and demands additional time, especially in evaporites. Due to strategic economic plans, the data acquisition (logs and sidewall samples) in the encasing rocks may be incomplete, which poses limitations to characterization of salt formation. From the available wells in this study, the sonic logs were partially acquired within the salt section. Empirical equations were established between the elastic properties using the wells with density and sonic logs. To overcome any lack of information, we explored the functionality of empirical equations as property predictors. Therefore, in wells with incomplete elastic property acquisition, the S-velocity and Young's modulus were fairly estimated from the P-velocity and, consequently, density and Poisson's ratio. The efficiency of the empirical equations was verified by comparing the measured and the estimated curves.

The empirical equations were calibrated with the well logs of the Santos Basin. These equations were able to consistently predict the elastic properties of the salt samples of the Taquari-Vassouras mine, located in the Sergipe Basin, onshore Brazil. In this case, the elastic behavior of evaporites was similar, albeit in different depositional environments.

Seismic interpretation advances in the use of converted shear waves (PS) to identify the fluid-bearing rocks. While the seismic migration of compressional wave (PP) demands the P-velocity modelling, the PS seismic migration requires a good S-velocity model to deliver outcomes that are more reliable. To this end, most initial trend models consider P-velocity and S-velocity as a function of depth. In ancient basinwide evaporites with thick salt layers, this assumption fails because well-log analysis demonstrated that velocities and depth are unrelated.

The angle versus offset (AVO) analysis has been performed as a successful workflow for hydrocarbon indicator (HILTERMAN, 2001; ROSA, 2018). It expresses the seismic response in terms of elastic property contrasts between seal and reservoir rocks. Consequently, the estimation of elastic properties in the seal rocks is as crucial as in reservoir rocks. Nevertheless, for several studies, v_s is absent or unreliable. These cases led to researches on estimating S-velocity from P-velocity of several lithologies. The quadratic equation in the form $v_s = av_p^2 + bv_p + c$ was previously proposed for sandstone, limestone, dolomite and shale (CASTAGNA; BATZLE; KAN, 1993). Each lithology has specific coefficients a, b e c. In our analysis, with the velocities in km/s, we suggest $a = -0.194$, $b = 2.366$ and $c = -4.236$ for rock salt. This equation is useful for AVO analysis in sub-salt and pre-salt reservoirs. Remarkably, we are unaware of the empirical equations which estimate S-velocity from P-velocity of evaporites with v_p range 3.2-6.0 km/s.

Why was least-squares regression preferable to the bound curves? The fact is that we can merely ensure that the property predictions fall between the upper and lower bounds with 95% confidence level. Nevertheless, the best-fit represents the curve which minimizes the sum of squared errors. The other choices imply large errors in prediction of the elastic properties. Moreover, the use of the bounds entails different and strong physical interpretations. The upper and lower limits systematically result in overestimating or underestimating the variable. For instance, the option of lower bound of the Young's modulus (Equation 2.7) leads to the interpretation of weakening of rock salt in overall formation. Likewise, the choice of bounds of compressional velocity (Equations 2.11 and 2.12) has significantly implication for time-depth conversion. Even though they produce large errors in property predictions, these situations can be useful to model exceptional cases in velocity and geomechanical analyses.

The data set is located in an area of complex halokinesis-related structures. The salt formation in central part of the Santos Basin presents large variation of tectonic deformation displaying diapirs, salt walls, anticlines, synclines, fold-and-thrust geometries, synthetic-antithetic faults, thrust faults (DAVISON, 2007; FIDUK; ROWAN, 2012; JACKSON et al., 2015; ALVES et al., 2017). This suggests that in-situ evaporites may be a mixture of diverse salt mineralogies with stress-induced fractures, different from samples in laboratory conditions. Even if these assumptions hold, the elastic

properties in both conditions shows similar response (see Table 3 and the comparison between Table 2 and Figure 8). However, this study is inconclusive whether it is a global or local behavior.

Seismic inversion plays a key role in three-dimensional quantitative rock characterization. This procedure aims to transform seismic amplitude into elastic property volumes. Angle stacks are mandatory to assess the elastic volumes via seismic inversion. There may be cases in which the amplitude relations of angle stacks are unreliable and, consequently, simultaneous elastic inversion is unfeasible. The complex shape of halokinesis-related structures severely affects the seismic imaging in and around the salt bodies, thereby reducing the confidence seismic amplitude response. The combination of rock physics and seismic inversion allowed the elastic characterization of evaporites as heterogeneous masses. A blind well confirmed the seismic predictability of elastic properties in salt formations.

The estimation of the elastic properties through property predictors imposes restrictions on the applicability of these attributes. The empirical equations are locally calibrated and depend on the geological settings where the data were acquired. The volumes of the elastic properties were generated from the acoustic impedance and, therefore, they are fully dependent. Thus, the volumes are not suitable for facies classification. For this case, the elastic volumes from simultaneous elastic inversion are appropriate.

2.6 Conclusions

Well and seismic data evidence that the salt body comprises heterogeneous rocks with a huge variation of elastic properties. The compaction does not appear to affect the elastic properties of rock salt significantly. The major influence on velocities and density may be associated with the evaporite mineralogy.

We demonstrated that the elastic properties of evaporites are correlated to each other. This aspect enables us to develop a series of empirical equations based on well log and site-specific calibration. The high correlation and low mean absolute percentage error confirm the quality and consistencies between the measured and the estimated elastic properties.

We combined rock physics and seismic inversion to estimate the compressional velocity, shear velocity, density, Young's modulus and Poisson's ratio volumes. The blind well indicates that the seismic data can successfully predict the elastic properties by applying the empirical equations as property predictors for the evaporites. The unavailability of the angle stacks prevents us from investigating if the simultaneous elastic inversion could yield better outcomes. We understand that this comparison should be appreciated in a proper opportunity.

The knowledge of the rock salt has multidisciplinary implication. We believe that this methodology can contribute to velocity modeling, seismic interpretation and geomechanical analyses for reservoir management and drilling operations.

3 Quantitative seismic-stratigraphic interpretation

Article published in

Marine and Petroleum Geology, volume 122, 2020

<https://doi.org/10.1016/j.marpetgeo.2020.104690>

Impact factor: 4.348

Authors: Leonardo Teixeira, Wagner Lupinacci & Alexandre Maul

The evaporite sequence in the Santos Basin, offshore Brazil, has attracted great attention during the last decade due to the discovery of the supergiant fields in the pre-salt province (FORMIGLI, 2007). The production of oil in the pre-salt reservoirs started in 2009 in the Lula field and, in less than one decade, reached more the 1 million barrels per day (ABELHA; PETERSOHN, 2018). The evaporites played an economic role in the discoveries of these Aptian carbonate reservoirs because they are the effective seals with thickness variation from few meters to almost 3 kilometres (CARMINATTI; WOLFF; GAMBOA, 2008).

Interest on the Brazilian salt basins emerged when several studies demonstrated the strong influence of salt tectonism on the big oil accumulations of the Campos Basin (GUARDADO; GAMBOA; LUCCHESI, 1989; MOHRIAK; HOBBS; DEWEY, 1990; DEMERCIAN; SZATMARI; COBBOLD, 1993; MOHRIAK et al., 1995; RANGEL; GUIMARÃES; SPADINI, 2003). In this basin, the timing of salt welding and halokinesis-related listric faults associated with rollover structures created perfect conditions for the oil migration from the pre-salt source rocks to post-salt reservoirs (GUARDADO; GAMBOA; LUCCHESI, 1989; BRUN; MAUDUIT, 2008). Additionally, salt flow deformed and pushed up the overlying strata forming anticline structures responsible for oil traps. Remarkably, the first wells in the Campos Basin aimed to drill such structures. In 1974, the first hydrocarbon accumulation was found in Albian limestones, followed by the discovery of commercial reservoirs in Eocene sandstones in 1975 (MOHRIAK et al., 1990). The reservoirs of the Campos Basin produce from Neocomian fractured basalts, Barremian coquinas, Early Albian limestones, and

Late Albian to Early Miocene siliciclastic turbidites (BRUHN et al., 2003).

While the post-salt reservoirs led to the investigation of salt-associated structures and the inference of models for oil accumulations, the development of the pre-salt reservoirs required the internal characterization of the evaporite sequence. By early 2000, the enigmatic reflections within the salt sequence were interpreted as intercalations of carbonate and siliciclastic rocks intruded by salt diapirs (MOHRIAK; SZATMARI; ANJOS, 2012). Intensive well drilling in the pre-salt reservoirs revealed that reflections within the salt walls are intercalations of stratified evaporites and the strong enigmatic reflector at the top of the salt sequence is the response of the abrupt contrast of acoustic impedance between the Albian post-salt sediments and the anhydrite caprock.

The internal characterization of salt bodies has multidisciplinary implications for the development of subsalt reservoirs. Recent studies demonstrated that the inclusion of the intrasalt velocity, regarding the salt stratification, improves the seismic image bellow the evaporite sequence (JI et al., 2011; FALCÃO, 2017; MAUL; SANTOS; SILVA, 2018a; FONSECA et al., 2019; DIAS et al., 2019; MAUL et al., 2019). The reliability of forward modelling of seismic amplitude and illumination studies in the pre-salt reservoirs depends on the incorporation of the heterogeneities in salt velocity models (JARDIM et al., 2015; MAUL et al., 2015). The research to increase the quality of seismic data in these giant oil and gas accumulations led to an intensive analysis of the variation of intrasalt velocity based on seismic and well data to build enhanced velocity models consistent with geological interpretations.

Drilling through salt is a challenge. Salt bodies are very heterogeneous and comprise lithologies with contrasting elastic properties, viscosities and mechanical behaviours (STROZYK, 2017). The high-viscosity and high-density contrasts of the multilayered evaporite exert strong influence on the salt movement, which depends on stress, temperature and mechanical properties (LI et al., 2012). Mg-K-rich salts have very low viscosity in comparison to the sedimentary rocks, thereby, presenting short-term creep and squeezing behaviours which can cause stuck pipe, borehole collapse, washout, fluid losses during the drilling time (DUSSEAULT; MAURY; SANFILIPPO, 2004; COSTA et al., 2011). The identification of the carnallite, sylvite and tachyhydrite prior to the well drilling is key factor for operational safety.

Seismic data have extensively underpinned the structural and stratigraphic interpretation of the Brazilian salt basins, describing their heterogeneities, distribution, morphology and kinematics (DEMERCIAN; SZATMARI; COBBOLD, 1993; COBBOLD et al., 1995; DAVISON, 2007; FIDUK; ROWAN, 2012; DAVISON; ANDERSON; NUTTALL, 2012; GUERRA; UNDERHILL, 2012; MOHRIAK; SZATMARI; ANJOS, 2012; GARCIA et al., 2012; DOOLEY et al., 2015; ALVES et al., 2017; LUPINACCI et al., 2019; PICHEL et al., 2019; RODRIGUEZ et al., 2019). The interpretations of intrasalt seismic-stratigraphic framework of the Santos Basin are based on the observation of the seismic expression of amplitude data. Freitas (2006) and Gamboa et al. (2009) interpreted four seismic facies and correlated them using wells separated by more than 200 km. Davison (2007) and Alves et al. (2017) recognized two seismic sequences: the upper layered evaporite unit and the lower poorly reflective unit. Later, Fiduk and Rowan (2012) divided the salt sequence into six zones in which strong reflective patterns correspond to three relatively competent zones and poor reflective patterns correspond to three weak detachment zones.

Inferences on seismic amplitude associated with well interpretation allowed the correspondence between the salt composition and the reflection patterns. Although the division of seismic stratigraphy sequence is still a current debate, the interpretations of the seismic expression in the evaporite sequence in the Santos Basin are very similar. Poorly reflective and chaotic-to-weakly amplitudes are indicators of halite-rich bodies. In contrast, high and strong reflective events indicate intercalation of low-dense and low-velocity salts with high-dense and high-velocity salts. Thus, high-frequency seismic expression suggests a decrease in the halite content and a high rate of intercalation of bittern salts and anhydrite.

Although the integration of well and seismic data boosted the understanding of the evaporite formation, the interpretations of seismic expressions and the analysis of reflective patterns are qualitative and do not evaluate quantitively the facies distribution in terms of seismic reflections. Teixeira and Lupinacci (2019) proposed the seismic-driven quantitative characterization of the evaporite sequence in the Santos Basin by combining rock physics and seismic inversion, however they focused on the estimation of elastic properties. Herein, we combine rock physics, seismic inversion and statistical techniques to estimate the most probable salt types that explain the seismic amplitude.

We create seismic responses of Earth models consistent with a typical evaporite deposition to demonstrate that the seismic amplitude is highly dubious to infer the salt types. Therefore, the interpretation of salt proportion based on seismic expression presents enormous ambiguity. To de-risk the seismic-based interpretation of salt types, we performed the seismic inversion in the synthetic data to demonstrate that the acoustic impedance can successfully identify the salt types. Then, the Bayesian classification applies the Bayes' theorem to combine the rock-physics analysis and acoustic impedance volume to assess the most probable facies (DOYEN, 2007). The outcome is the seismic-driven salt-type volume identifying bittern salts, halite and anhydrite.

We explore the advantages of the quantitative characterization of the evaporite sequence and propose a refinement of the intrasalt seismic-stratigraphic interpretation based on the sedimentary cycles. The procedure starts with the interpretation and correlations of salt cycles in the wells. We opted to keep the division in four major cycles to understand the influence of the variation of the sedimentary cycles on the seismic expression and correlate our results to the previous works. The integration of seismic amplitude, acoustic impedance and facies volumes played a fundamental role to extend the well-to-seismic interpretation with reliability essentially because it reduces the ambiguity in the identification of salt type. We mapped four horizons C1, C2, C3 and C4, which tie to the well-based sedimentary cycles.

The sedimentary cycle horizons may correlate the seismic events to changes in the salinity of the brine concentration. On the other hand, the interpretation of seismic expressions examines the change of reflective patterns in the seismic data, which is the response of the acoustic character variation of the stratigraphic sequence. Therefore, the seismic expression may not be intrinsically associated with the salinity change in the hydrographically-isolated marine-fed system of ancient basinwide evaporite deposits. Arguably, in the core of this analysis, rock physics is the bridge to link the salt types and seismic models.

This work delves into the benefits of transforming the qualitative analysis of seismic interpretation into quantitative characterization. The methodology enables us to derive attributes directly from the facies volume, thereby avoiding the ambiguities and uncertainties of the seismic amplitude. While the well data is a locally confined information, the seismic data provides the spatial

variability of evaporites over large areas. For each cycle, we generated maps presenting the salt type distribution to show the variabilities of the salt types within the evaporite sequence. The comparison between the seismic-based and well-based salt proportions validates the quantitative classification.

This workflow is widely recognized as quantitative seismic interpretation and have been successfully applied to quantitative characterization of the reservoir rocks (AVSETH; MUKERJI; MAVKO, 2005; VERNIK, 2016; TEIXEIRA et al., 2017a; FERREIRA; LUPINACCI, 2018). Hence, the novelty relies on the extension of this workflow to deliver seismic-based quantitative analysis of the evaporite sequence.

3.1 Geological settings

The Santos Basin is the largest salt basin offshore Brazil whose history starts with the break-up of Gondwana in the Early Cretaceous, whereby the South Atlantic Ocean began to open (KUKLA; STROZYK; MOHRIAK, 2018). The Santos Basin covers an area about 350,000 km^2 and it is bounded by the Florianopolis High to the South and the Cabo Frio High to the North (Figure 17).

The syn-rift phase formed a series of synthetic and antithetic faults, filled by volcanoclastic rocks, related to intense tectono-magmatism, and fluvial and lacustrine sediments during the Hauterivian to Late Barremian (MOREIRA et al., 2007). An unconformity separates the Barremian sequence from the subsequent Aptian sediments. The sag phase (the Barra Velha Formation) occurs during the period of thermal subsidence in the Early Aptian, filled by the deposition of carbonates from lacustrine to a restricted marine environment (MANN; RIGG, 2012; QUIRK et al., 2012) . The absence of marine fossils in the Aptian carbonate excludes the hypothesis of open-marine system during the formation of the sag carbonate platforms (WRIGHT; BARNETT, 2015). This stratigraphic sequence encompasses predominantly coquinas, stromatolites, grainstones, laminites and spherulitites, constituting the main pre-salt reservoir rocks (FARIA; REIS; SOUZA, 2017).

The eruption of the Parana-Etendeka continental basalt province in the Barremian-Aptian ages formed the Walvis Ridge Volcanic High and the Rio Grande Rise, which were presumably responsible to isolate the South Atlantic Basin from the open-marine system (DAVISON; ANDERSON; NUTTALL,

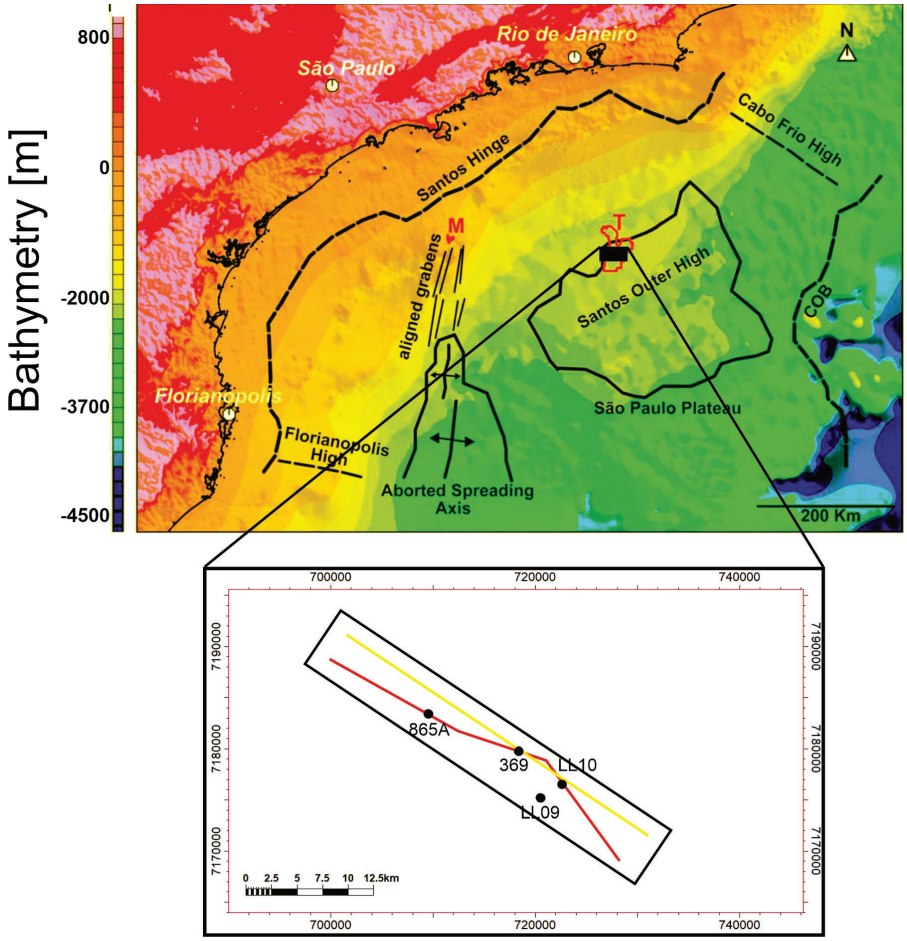

Figure 17: The Santos Basin is is bounded by the Florianopolis High to the South and the Cabo Frio High to the North (after Garcia et al. (2012) and Gamboa et al. (2019)). The map displays the ring fence of the Lula (T) and Merluza (M) fields. The black rectangle indicates the study area is located in the São Paulo Plateau. The red line relates to the seismic profile in Figure 27 and the yellow line to Figure 28.

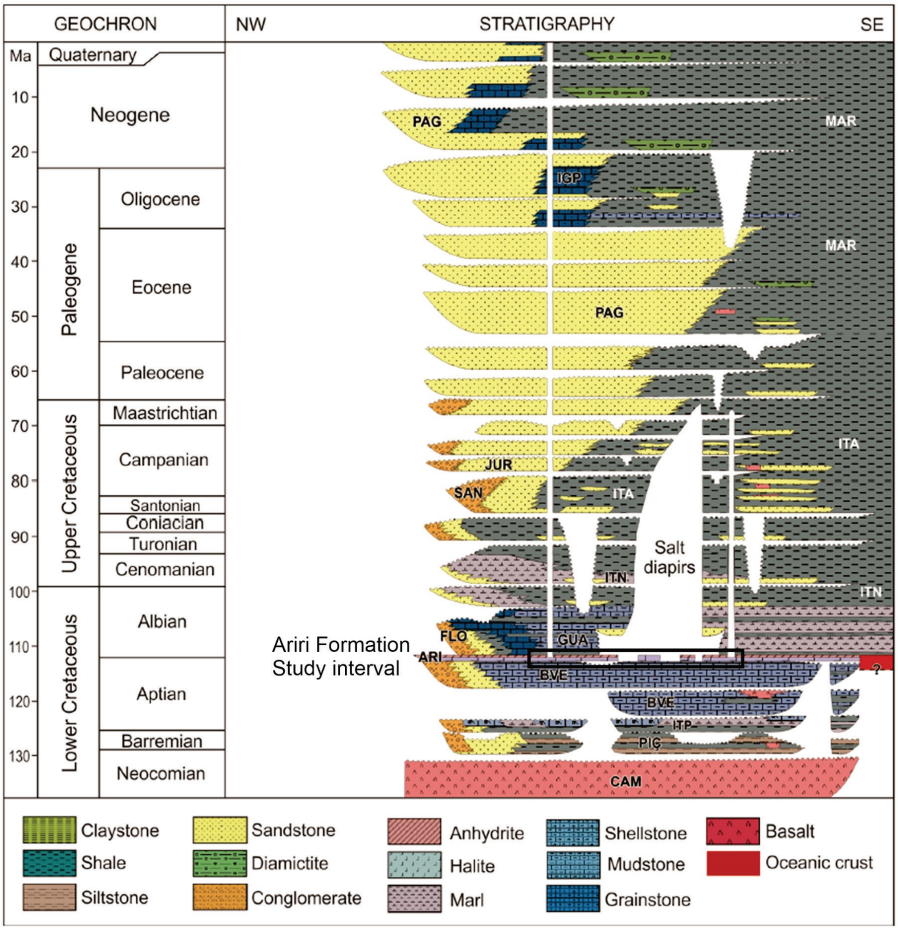

Figure 18: Schematic stratigraphic column in the Santos Basin (after Moreira et al. (2007)). The studied interval comprises the Late Aptian during the deposition of the Ariri Formation

2012; HOMRIGHAUSEN et al., 2019). The hydrographically-isolated system associated with an original tectonically-induced depression established favorable conditions to the widespread evaporite deposition in the Late Aptian, recorded by the Ariri Formation (Figure 18). Several wells from sparse locations in the Santos Basin identified thick (up to 50 m) Mg-K-rich salt layers in the evaporite successions (AMARAL et al., 2015; MAUL; SANTOS; SILVA, 2018b) . Allegedly, the percolation of seawater through fractured volcanic highs enriched the brine concentration and enabled the deposition of thick complex-salt layers (JACKSON; CRAMEZ; FONCK, 2000; DAVISON; ANDERSON; NUTTALL, 2012).

The absence of clastic and carbonate rocks in the Ariri Formation suggests a fast deposition of the evaporites compared to their encasing rocks. Freitas (2006) attempted to adjust the Milankovitch cycles to the cyclostratigraphic interpretation using well and seismic data and proposed an estimated period of 400-600 Ka for the deposition of the evaporite sequence in the Santos Basin. The depositional

age gives rise to controversy. High-resolution carbon isotope interpretation hints at an age between 125 and 130 Ma, whereas Ar-Ar dating indicates sometime between 111 and 116 Ma (TEDESCHI et al., 2017).

In the Early Albian, the marine-connected system, established by the basin subsidence and the eustatic sealevel rise, favored the deposition of carbonate sequences in the São Paulo Plateau (MODICA; BRUSH, 2004; PICHEL et al., 2018). Grainstone and oolitic shoals intercalated with fine-grained carbonate dominate the deposition sequence from the transitional to neritic environment in the middle-inner shelf (MOREIRA et al., 2007). In the study area, the Early Albian sediments are composed of deep-water fine-grained marl-dominated carbonate successions of the Guarujá Formation (CONTRERAS et al., 2010). The sediments of proximal basin margins, along the Santos hinge line, comprise alluvial-deltaic fine to coarse-grained sandstones, shales and conglomerate of the Florianopolis Formation (PEREIRA; FEIJó, 1994; CONTRERAS et al., 2010).

The Late Cretaceous to the Early Cenozoic consists of a thick succession of deep-water deposits associated with episodes of massive clastic progradation basinwards engendered by the rise of Serra do Mar (MODICA; BRUSH, 2004). These post-salt sediments experienced massive halokinesis-related tectonism which resulted in oil-prolific carbonate turtleback structures and rollover anticlines in the Albian carbonates and in the Upper Cretaceous siliciclastics (GUERRA; UNDERHILL, 2012).

3.2 Dataset and Methodology

The study integrates high-quality 3D seismic data and 4 wells located in the Lula field in the Santos Basin. A huge acquisition starts in 2009 to improve the seismic imaging of the pre-salt reservoirs. The seismic processing applied, then, an advanced workflow which included tomographic velocity and tilted transverse isotropy Kirchhoff prestack depth migration (TTI PSDM). The seismic amplitude extends to 7 s sampled in 4 ms. The seismic signal regards the positive amplitude or peak as an increase of acoustic impedance at the interface of two geological layers. The opposite is marked as a negative amplitude or a though.

The dataset contains 4 wells (BRSA865, BRSA369, LL09, LL10) with broad acquisition of logs. The log set includes neutron and nuclear resonance magnetic porosities, density, sonic and gamma ray logs. However, in the evaporite sequence, we found only gamma ray, density and sonic logs. Pointedly, only well BRSA865 has density log in the salt formation. Warren (2006) precisely punctuated the problem with dealing with the encasing rocks: "very few oil companies wish to characterize what is an undeniable seal facies". This lack of data is a constant challenge to the characterization of evaporites.

The estimation of facies relied on well log and cuttings. The description of well cuttings excluded the presence of carbonate and clastics in the Ariri Formation. Therefore, the values of gamma ray, sonic and density logs are related to the salt composition. In the Santos, the presence of anhydrite, halite, carnallite and tachyhydrite predominates. Gypsum and sylvite may occur in negligible proportions (MAUL; SANTOS; SILVA, 2018b).

The identification of the salt types was underpinned by the log responses in combination with the well-cutting descriptions. Table 5 catalogues the petrophysical characteristic of evaporites. The facies descriptions implement the following interpretation: halite has moderate velocity and low gamma ray; anhydrite has high velocity and low gamma ray; tachyhydrite has low gamma ray and velocity; carnallite has high gamma ray and low velocity. Similar well-log-based interpretations were performed in evaporites of the Santos Basin (FREITAS, 2006; JACKSON et al., 2015; RODRIGUEZ et al., 2018; MAUL; SANTOS; SILVA, 2018a) and other salt basins (JACKSON et al., 2019; BRANDÃO; VIDIGAL-SOUZA; HOLZ, 2020).

Table 5: Logging tool response in evaporite minerals (SERRA, 1990)

Salt type	Velocity [m/s]	Density [g/cm^3]	Gamma Ray [gAPI]
Carnallite	3908	1.57	220
Tachyhydrite	3313	1.66	0
Halite	4549	2.04	0
Anhydrite	6096	2.98	0

Seismic inversion is a widely applied technique which underpins the seismic-based quantitative characterization of rocks. The algorithm starts with an initial model of elastic properties created by the combination of stratigraphic-seismic interpretation and well-log interpolation. The

L1-norm sparse-spike inversion algorithm interactively changes the initial model until it reaches a satisfactory match with the seismic data. The outcomes are elastic property volumes that explain the seismic amplitude.

Rock-physics analysis consists in studying the link between elastic properties and facies. Low-density and low-velocity carnallite and tachyhydrite present similar acoustic impedance response, thereby these facies are assembled into one group for the seismic-based classification. Jackson and Hudec (2017) define three important groups for evaporites: bittern salts, halite and anhydrite. These categories are appropriate to seismic-driven facies estimation since they exhibit distinguishable acoustic response. Table 6 compares the well-based and seismic-based classifications.

Table 6: Well-based and seismic-based classifications

Facies classification	
Well data	Seismic data
Carnallite Tachyhydrite	Bittern Salts
Halite	Halite
Anhydrite	Anhydrite

Bearing in mind that the seismic inversion of full-stack data provides the acoustic impedance volume, we estimated probability density function for each facies (bittern salts, halite and anhydrite), describing the state of knowledge between evaporites and rock property. Then, we employed statistical techniques to integrate rock-physics analysis and seismic inversion in order to estimate seismic-driven facies volume. Accordingly, the algorithm employs the Bayes' theorem to compute the posteriori probability for each facies and, sample-by-sample, applies the calculation to the acoustic impedance volume in order to generate the facies volume (MUKERJI et al., 2001; DOYEN, 2007).

The methodology is summarized below:

- The modeling of seismic response of evaporites;
- Seismic well-tie to correlate the seismic reflections to the salt layer interfaces;
- Seismic inversion to transform the seismic amplitude into acoustic impedance volume;

- Rock-physics analysis to link the acoustic impedance and the salt types;
- Seismic facies classification to generate facies volume and to identify the salt types spatially;
- Seismic interpretation of sedimentary cycles.

The methodology combines data from a variety of disciplines including petrophysics, geophysics and geology to perform the quantitative characterization of evaporite sequence. The outcomes are volumes, maps and tables which infer the quantitative analysis of the salt distributions and proportions.

3.3 Cyclostratigraphy of evaporites

The salinity of brine-saturated fluid controls the stratigraphy of the basinwide evaporite deposits. When the brine reaches the concentration of four to five times the concentration of the original seawater, gypsum starts to precipitate. As the concentration increases in the superbrine fluid, at 10-12 times the original seawater, halite precipitates. As the salinity increases to anomalous concentration of 70-90 times the original seawater, the brine favors the deposition of bittern salts (WARREN, 2016). Seawater seepage in the isolated system decreases the salinity and marks the onset of new cycle with the deposition of gypsum. The dehydration of gypsum results in anhydrite. Therefore, the presence of anhydrite represents the moment of lowest salinity whereas the magnesium and potassium (Mg-K) salts indicate highest salinity in evaporite basins.

From our dataset, mudlog reports the absence of siliciclastic and carbonate deposits in the Ariri Formation. Similar documentations, collecting Santos basinwide information, confirm the absence of these rocks and report thick salt deposition (up to 3 km) in this formation (FREITAS, 2006; MAUL et al., 2019). The composition, thickness and preservation suggest that the period of salt accumulation occurred in a strong isolation of the Santos Basin from the open-marine system. Structural studies on pre-salt sag phase suggest that the salt starts to deposit on an original depression, which was tectonically and hydrographically isolated from the Atlantic Ocean by the Walvis Ridge (KARNER; GAMBÔA, 2007; FARIAS et al., 2019). In this context, marine-seepage inflows through the Walvis

Ridge fracture zones may be the key factor that controls the salinity in the isolated accumulations in the Santos Basin during the Late Aptian (DAVISON; ANDERSON; NUTTALL, 2012)

The isolation from open-ocean conditions poses challenges to the relationship between the salt deposition and sealevel changes. Thereby, the application of sequence stratigraphy may be not appropriate in basinwide evaporite accumulations, essentially because, in a marine-isolated system, the eustasy has negligible influence on the salt deposition (WARREN, 2006). Consequently, we propose the division of the evaporite formation based on the cyclicity of the evaporite sequence.

Herein, we follow the previous four-fold division of the evaporite sequence of the Santos Basin (FREITAS, 2006; GAMBOA et al., 2009; JACKSON et al., 2015; RODRIGUEZ et al., 2018; PONTES, 2019). These units reflect the seismic expression of the signal and, consequently, are related to the acoustic profile of the rock sequence. However, our interpretation is based on a presence of salt types. The onset of new cycle of evaporation starts with a negative amplitude, indicating the presence of anydrite.

Figure 19 shows the interpretation of the four cycles in the wells BRSA865, BRSA369, LL09, LL10. C1 starts with the presence of the anhydrite caprock of the pre-salt reservoirs and represents the cycle with largest proportion of halite. This cycle presents profiles of low density, low velocity and high gamma ray indicating deposition of bittern salts and, consequently, reduction of salinity. Approximately twenty-meters anhydrite marks the onset of C2. Well correlation reveals that the thickness of this layer is relatively constant. This leads us to the interpretation that the concentration of brine remained comparatively unchanged in the study area. C2 has higher proportion of bittern salts when compared to C1, which suggests high-frequency variations of salinity.

The thicknesses of anhydrite at the base of C3 vary laterally. The interpretation of velocity and gamma ray hints that the presence of tachyhydrite and carnallite differs in each well. The top of C3 suggests a drastic rise of salinity recorded by an anomalous thickness of bittern salts (BRSA865 $\approx$ 60 and LL10 $\approx$ 23 m). High gamma ray and low velocity supported the interpretation of intercalations of tachyhydrite and carnallite. Shortly below the top of C3, we observed a high-frequency nature of gamma ray which is uncorrelated to the wells BRSA369 and LL09, suggesting that the top of C3 was eroded in these wells.

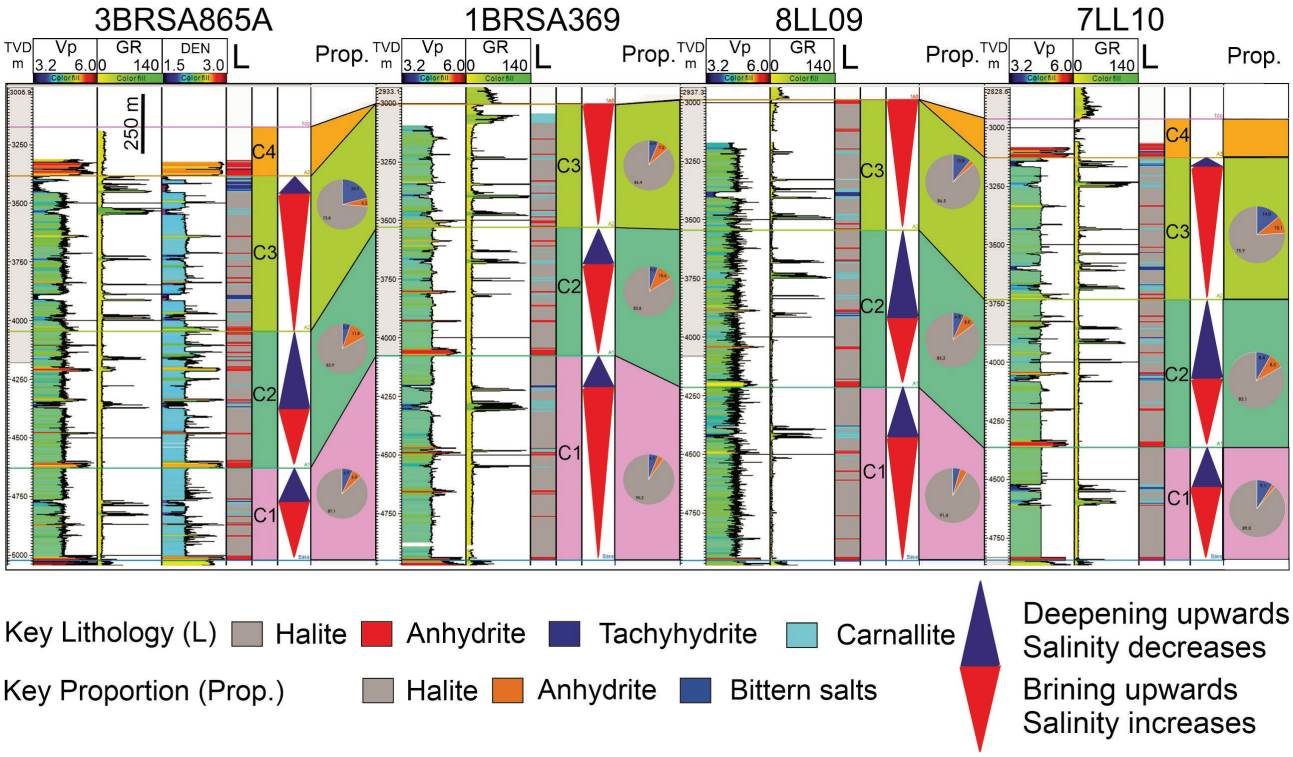

Figure 19: Sedimentary cycle in the wells BRSA865, BRSA369, LL09 and LL10. Well logs supported the interpretation of evaporite facies based on typical petrophysical properties. We opted to keep the previous four-fold division of the Ariri Formation. The presence of anhydrite marks the onset of the cycle C1, C2, C3 and C4. For each unit, we computed the well-based salt proportion, grouping carnallite and tachyhydrite into bittern salts, to compare with the seismic-based proportion. Table 7 describes the proportion. Log labels: GR - Gamma Ray [API], Vp - Velocity [km/s], DEN - Density [g/cm^3], L - lithology

Table 7: Salt proportion by cycle

	Cycle	Bittern Salt	Anhydrite	Halite
1BRSA369	C1	6.1	3.7	90.2
	C2	5.6	10.6	83.8
	C3	6.4	7.2	86.4
3BRSA865A	C1	6.9	6.0	87.1
	C2	5.3	11.8	82.9
	C3	20.9	5.3	73.8
8LL010	C1	9.1	1.9	89.0
	C2	8.4	8.5	83.1
	C3	14	10.1	75.9
7LL009	C1	4.4	4.2	91.4
	C2	6.8	8.0	85.2
	C3	10.8	2.7	86.5

The partial availability of well logs in C4 prevents us from inspecting the evaporitic succession in this cycle. Gamma ray, which provides the interpretation of carnallite, is acquired in this cycle; however, velocity log is partly absent. The absence of velocity log rises the uncertainty in the identification of anhydrite, tachyhydrite and halite. The onset of C4 is recognized in the wells BRSA865 and LL10 by high velocity and low gamma ray, which were interpreted as anhydrite whose minimum thickness is approximately 50 m. The thick anhydrite in direct contact with the underlying thick bittern salts reveals an extreme change in the salinity between C3 and C4 cycles.

3.4 Seismic response of evaporites

Evaporites present large range of density and compressional velocity and, consequently, acoustic impedance. The post-stack seismic amplitude captures the contrast of acoustic impedance of the multi-layered evaporite sequence. The study of the seismic response of plausible combinations of stratified evaporites is the basis for an accurate seismic interpretation.

The seismic response of subsurface is evaluated by creating an Earth model consisting of different rock sequences. We attribute to each layer typical values of elastic properties derived from laboratory measurement or well log. The convolution model starts with the calculation of the reflection coefficient at the interface of two different rock layers. The reflection coefficient series are convolved with a wavelet. This process generates the seismic trace of the rock sequence (SIMM; BACON, 2014).

The facies interpretation of the Ariri Formation typically describes layers of tachyhydrite, carnallite, sylvite and anhydrite embedded in thick layers of halite. These representative sequences of rock salt are seismically simulated by creating an Earth model, wherein a stratum of bittern salt or anhydrite is embedded in a halite. Table 8 specifies the log response of acoustic impedance of rock salt in the Santos Basin. Zero-phase wavelet was estimated during the seismic well-tie, which resulted in a symmetric wavelet with dominant frequency of 28 Hz.

In one scenario, the bittern salts are placed within a thick halite layer (Figure 20a). The seismic signal is a negative amplitude (trough) at the top of bittern salts followed by a positive amplitude (peak). The replacement of bittern salts by anhydrite creates a peak followed by trough at the base of

Table 8: Typical log response of mean acoustic impedance of evaporites in the Santos Basin. These values were estimated from the well logs of this dataset.

Facies	Acoustic Impedance [g/cm^3 m/s]
Bittern salts	7150
Halite	9700
Anhydrite	15200

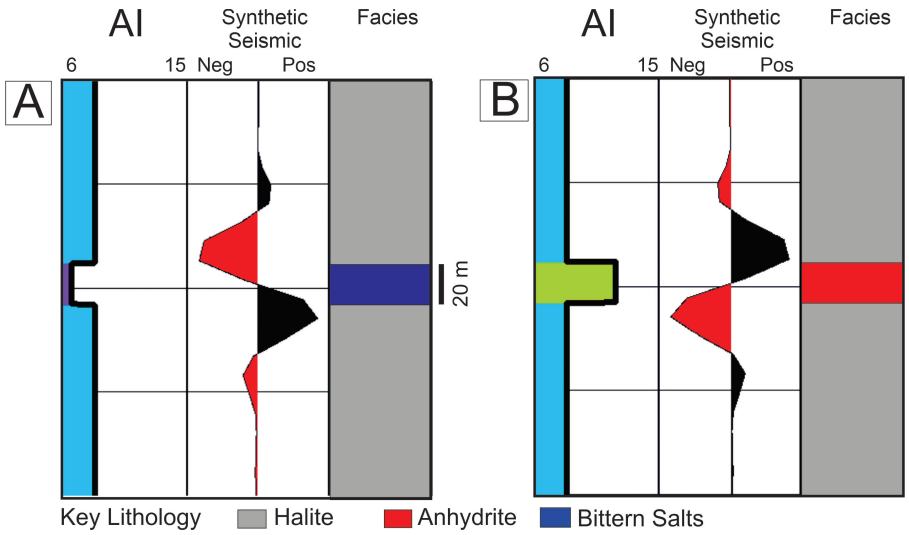

Figure 20: Seismic response of salt types embedded in thick layer of halite. The dominant frequency is estimated about 28 Hz. (a) bittern salts; (b) anhydrite. Bittern salts create a peak at the top and a trough at the base. Anhydrite exhibits an opposite signal. The seismic-amplitude-based estimation of salt type leads to misinterpretation due to the ambiguity of the seismic response. Acoustic impedance is measured in g/cm^3 km/s.

anhydrite (Figure 20b). These two scenarios demonstrate that the embedded bittern salts and anhydrite layers in a thick halite create positive and negative amplitudes. The phase of the signal is the main difference between these seismic responses.

Figure 20 clarifies that the seismic amplitude represents an ambiguous response. The increase of acoustic impedance of anhydrite generates a positive amplitude at the top as well as the increase of acoustic impedance at the base of bittern-halite interface. Therefore, the association of peak with anhydrite overestimates the interpretation of this salt. Similar explanation leads to the conclusion that the association of trough with bittern salts overestimates the interpretation of this facies.

The synthetic seismogram allows to evaluate the seismic resolution which is related to the capacity of the seismic signal to determine the top and base of geological layers. Seismic resolution depends on layer velocity, bandwidth frequency and wavelet shape (WIDESS, 1973; SIMM; BACON, 2014). Figure 21 illustrates the variation of the thickness of an anhydrite layer from 10 m to 30 m

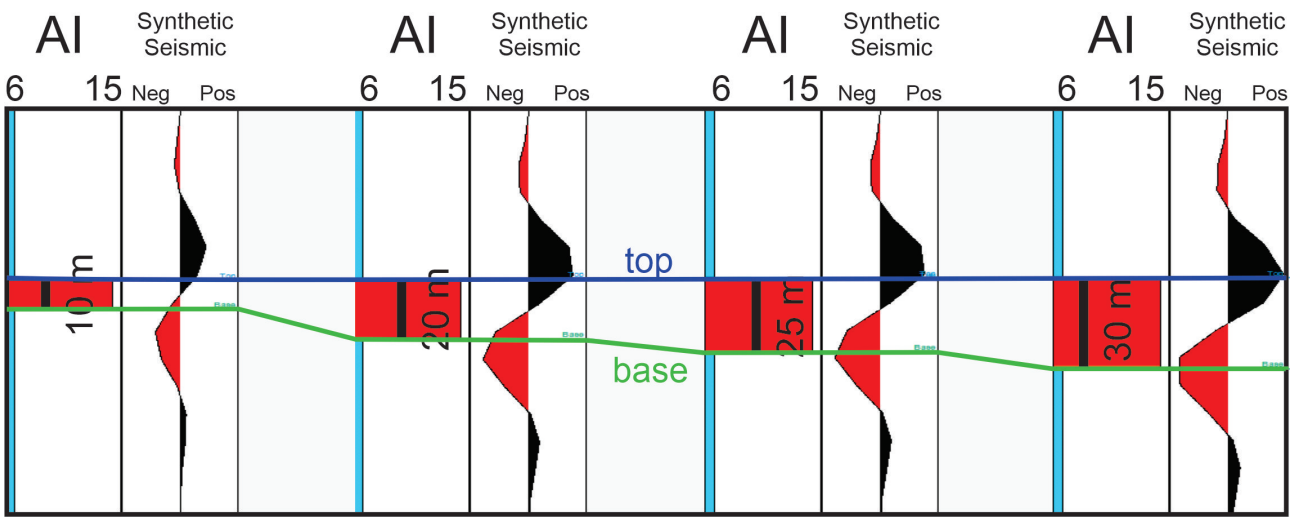

Figure 21: Seismic response of variable thicknesses of anhydrite. The analysis suggests that the seismic resolution of this dataset is between 25 and 30 m. Salt layers thinner than 25 m may have the thickness overestimated by the seismic amplitude. Label: AI - acoustic impedance [g/cm^3 km/s]

embedded in halite layer. The seismic response delimits the top and base of the 30-meter anhydrite. However, 25-meters anhydrite appears to be thicker in the synthetic data. We stipulate that the seismic resolution of this dataset is between 25 and 30 m. Salt layers thinner than 25 m may have the thickness overestimated by the seismic amplitude.

We create a multilayered sequence of bittern salts, anhydrite and halite to emulate an environment of typical deposition in thick stratified evaporite body. In this model, the bittern salts and anhydrite layers have 25 m. A seventy-meter halite layer separates them to avoid wave interference. The seismic response evidences an alternation of peak and trough which imposes ambiguity in the interpretation of the salt type (Figure 22 a). The ambiguity occurs essentially because both bittern salts and anhydrite produce positive and negative amplitudes. The synthetic seismic in Figure 20 and Figure 22 (a) indicates that positive or negative amplitude cannot be associated with the occurrence of a salt type. The reduction of ambiguity can be performed by seeking seismic attributes that de-risk the relative nature of seismic response.

The ambiguity in seismic signal occurs because of the seismic response is an interface property and depends on contrasts of rock properties. Nevertheless, evaporites have different values of acoustic impedance (Table 8). This is an indicator that this property can be a differentiator of salt types. Previous work testified that the acoustic impedance boosted the identification and the property estimation of evaporites (TORIBIO et al., 2017; TEIXEIRA; LUPINACCI, 2019). However, these works overlooked

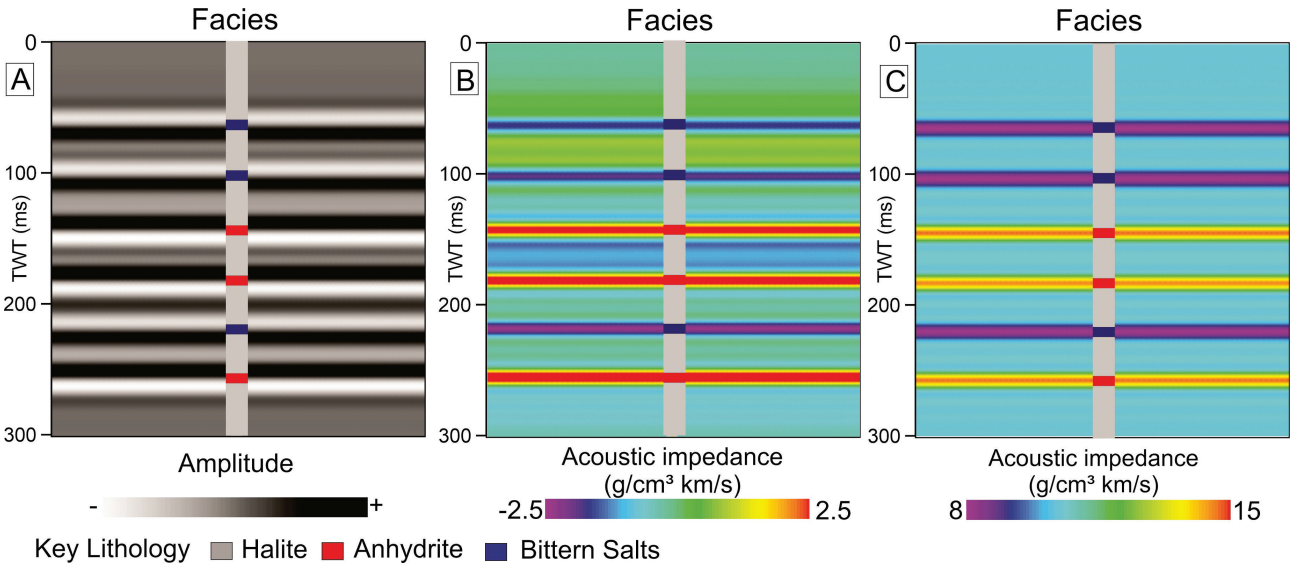

Figure 22: (a) 2D seismic profile representing the synthetic response of an alternation of bittern salts and anhydrite embedded in halite layers; (b) relative acoustic impedance from the synthetic response; (c) absolute acoustic impedance from the synthetic response. Seismic inversion de-risks the identification of salt type by estimating acoustic impedance through seismic amplitude.

the analysis of the seismic response of different salt types and the reduction of ambiguity by performing seismic inversion.

The estimation of acoustic impedance derived from seismic amplitude is performed in the oil industry by a wide-known procedure recognised as seismic inversion (LATIMER; DAVISON; RIEL, 2000; LATIMER, 2011). Further explanation about this procedure is given in the following section. To evaluate the success of the identification of the salt types using the acoustic impedance, we inverted the 2D seismic response of multi-layered evaporite sequence presented in Figure 22.

Notably, in Figure 22(b), acoustic impedance profile exhibits three different responses: light blue, related to halite; dark blue, related to bittern salts; and red, related to anhydrite. We identify three layers of high acoustic impedance and three layers of low acoustic impedance. The consistency of acoustic impedance from seismic inversion with Table 8 allows the identification of salt types and reduces the ambiguity of the amplitude response.

Seismic inversion also provides the bandpass acoustic impedance (Figure 22(c)). In this 2D profile, high positive values ($\approx$ 2.5) are associated with anhydrite and low negative values ($\approx$ - 2.5) represents bittern salts. Also, this attribute is a good differentiator of salt types, however the values for halite appear to be more unstable. Therefore, we chose the acoustic impedance to classify the salt

types.

3.5 Facies classification based on the acoustic impedance

Seismic inversion is an ordinary process for reservoir characterization (DOYEN, 2007; LATIMER, 2011). The workflow of seismic inversion for evaporite formations follows the proposal described in Teixeira and Lupinacci (2019). The construction of stratigraphic grid for the initial model relied on the interpretation of the top and base of salt body. The low-frequency bandwidth, absent in the seismic data, is created based on interpolation of well logs guided by the interpreted stratigraphy. Density and compressional velocity are indispensable for the initial model to perform the acoustic inversion. Four wells located in the seismic survey have compressional velocity from log acquisition, however, in three of them, the density is absent. Teixeira and Lupinacci (2019) describe a reliable workflow to estimate the density from compressional velocity in the evaporite formation of the Santos Basin. The authors demonstrated that the elastic properties of evaporites are highly correlated and proposed empirical equations to generate the lacking elastic properties from compressional velocity. Here, we applied their rock-physics empirical equations for the estimation of density when it is missing or unreliable. Seismic inversion algorithm employs the L1-norm sparse-spike inversion which interactively updates the low-frequency initial model until the synthetic reaches a satisfactory match with the seismic data (SIMM; BACON, 2014). The outcome is an acoustic impedance volume that explains the seismic amplitude.

Figure 23 depicts the seismic amplitude and acoustic impedance profiles intersecting the wells BRSA865A, BRSA369 and LL10 color-coded with the evaporite facies. The comparison between the well logs and seismic profile evidences the ambiguity of seismic amplitude in the identification of salt types. Real data endorses that the strongly reflective nature of the seismic expression is the response of contrast of acoustic impedance. Intercalation of bittern salts only or anhydrite only embedded in thick halite layer can reproduce high-frequency reflective patterns which, in turn, are not essentially related to alternations between these salt types.

The acoustic impedance volume captures the high-frequency reflections of seismic amplitude and the morphology of the stratified evaporite formation. The comparison of the acoustic impedance

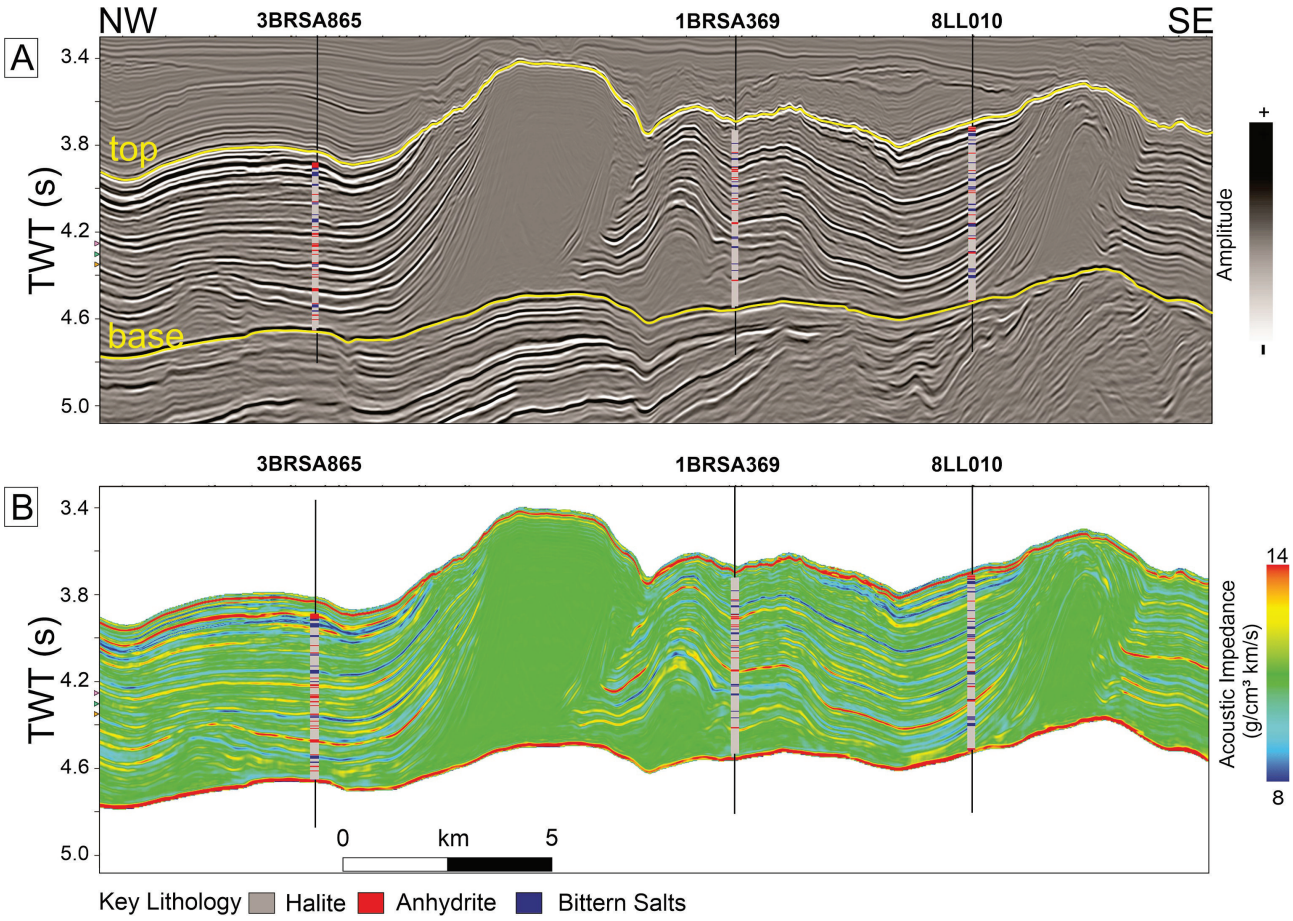

Figure 23: Seismic profile through three wells: (a) seismic amplitude; (b) acoustic impedance. Seismic inversion was performed between the top and the base of evaporite sequence in the Ariri Formation. The comparison of the acoustic impedance profile and the well logs evidences that the low-impedance layers identify the bittern salts whereas high-impedance layers allude to the presence of anhydrite. Seismic amplitude displays an ambiguous response.

profile and the well logs points out that the low-impedance layers identify the bittern salts whereas high-impedance layers allude to the presence of anhydrite (23b).

As predicted by the synthetic example (Figure 22), the association of negative amplitude with bittern salts and positive amplitude with anhydrite leads to the overestimation of these facies. In contrast, seismic inversion de-risks the interpretation of evaporite facies by transforming the interface property into layer property. Bittern salts have low density and velocity while anhydrite has high density and velocity. Since acoustic impedance is the multiplication of these properties, it becomes a good indicator of salt types. Therefore, high-frequency high-reflective seismic expression - a typical response in ancient salt basins such as in the Santos Basin - hints at a stack of evaporite facies, however, it lacks in identifying them. Comparatively, the salt domes are halite-rich bodies (> 97%). That explains the reflection-free seismic expression in domes due to the absent or negligible contrast of acoustic impedance. In these bodies, seismic inversion delivers almost constant value of acoustic impedance, which falls in a range 9.5 - 9.7 g/cm^3 km/s. This range comprises the acoustic impedance values for halite. Accordingly, we chose to use the acoustic impedance volume to perform the facies classification via seismic data.

Quantitative seismic interpretation combines geophysical and geological information by applying statistical techniques (MUKERJI et al., 2001; AVSETH; MUKERJI; MAVKO, 2005). The procedure starts with the statistical study of the elastic behaviour of facies. For each facies, we estimate probability density functions (PDF), based on well logs, which describe the state of knowledge of rock under a specific geological setting. It links the relationship between the rock and seismic attributes. Figure 24 depicts the PDFs of acoustic impedance for bittern salts, halite and anhydrite.

The seismic facies classification is supported by the Bayes' theorem which allows the calculation of the probability of each facies, given the seismic attribute. The algorithm computes sample-by-sample the posteriori probability of facies, delivering cubes of probability for each facies (DOYEN, 2007). Finally, the classifier applies the Bayes' rule and chooses the most probable facies, generating a facies volume. We applied the Bayesian facies classification to estimate the most probable facies of evaporites in the Ariri Formation. The outcome is a seismic-driven facies volume of evaporites which incorporates concepts of rock physics and seismic inversion.

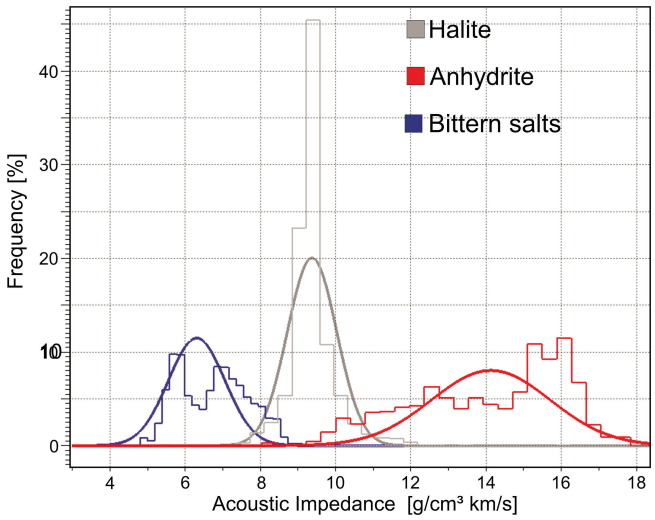

Figure 24: Histogram and probability density function for each facies: halite in grey; anhydrite in red and bittern salts in blue.

The seismic profile in Figure 25 intersects three well paths color-coded by facies. The seismic-driven facies enables a direct interpretation of evaporite, essentially because it was underpinned by acoustic impedance, which drastically reduce the uncertainty in facies identification. Presumably, seismic amplitude would fail in achieving a satisfactory classification.

The facies volume preserves seismic events of intrasalt geometry. We observe synclines and anticlines structures, near-parallel, near-isoclinal and sheet-like horizons, onlap and toplap terminations which are in agreement with seismic amplitude. High-reflective seismic expressions, manifesting the contrast of acoustic impedance, were then classified as a vertical stack of bittern salts, halite and anhydrite which is consistent with well-interpreted facies. Reflection-free and reflection-weak zones are identified as halite. That appears to be an appropriate classification inside the big domes. The well-log facies corroborates the seismic classification.

3.6 Seismic stratigraphy of evaporites

The division of the evaporite formation in the Santos Basin in four-fold unit, based on seismic expression of amplitude response of the evaporite sequences, is well conceived and established in literature (FREITAS, 2006; GAMBOA et al., 2009; JACKSON et al., 2015; RODRIGUEZ et al., 2018; PONTES, 2019). In this context, the interpretations of these authors converge into a similar seismic-based definition of these units. Jackson et al. (2015) and Rodriguez et al. (2018) named them

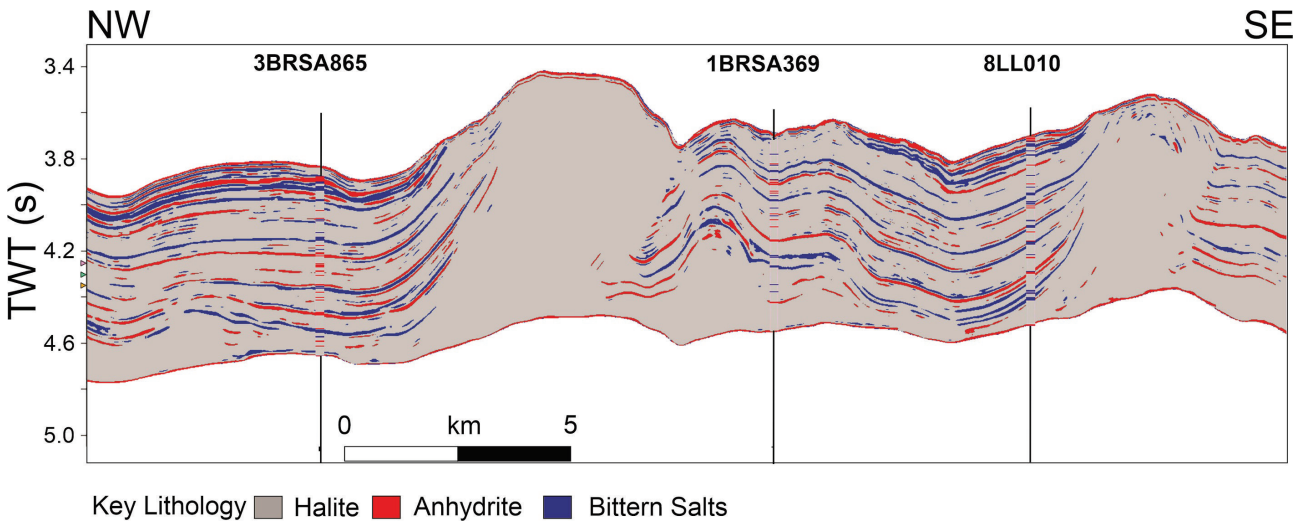

Figure 25: Bayesian facies classification applied to the evaporite sequence in the Ariri Formation. The well paths are color-coded with the same label of seismic facies classification: blue for bittern salts, red for anhydrite and grey for halite.The Bayesian classification preserves the morphology of the intrasalt events while properly identifies the evaporite facies. High-reflective seismic patterns were classified as a vertical stack of bittern salts, halite and anhydrite. The well-based and seismic-based classifications are very similar.

by A1 to A4 from the bottom to the top of the Ariri Formation. They synthesize the seismic expressions in these units as follows: A1 is poor-reflective and chaotic stratified, interpreted as halite-rich unit; A2 is strong reflective, indicating the presence of thick anhydrite layers; A3 is similar to A2 - halite-rich and poor-reflective amplitude; A4 is the strongest reflective unit, with less proportion of halite and high deposition of low-density and high-density salts.

In this work, we propose the seismic interpretation of the evaporites based on sedimentary cycles. The interpretation maintains the division into four main segments to establish a comparison with previous interpretations. Herein, we name them C1, C2, C3 and C4 from the bottom to the top of the evaporite sequence. The sedimentary cycles were interpreted in the wells BRSA865A, BRSA369, LL10, and LL09. Every cycle starts with the presence of anhydrite, which indicates a reduction of the salinity in the brine concentration.

The seismic well-tie calibrates the rock-to-amplitude response of the evaporite sequence to extend the interpretation of sedimentary cycles from well to seismic. Figure 26 compares the synthetic seismic and seismic data. The onset of the cycles is identified as a negative amplitude which corresponds to high-to-low acoustic impedance interface of the base of anhydrite layers in contact

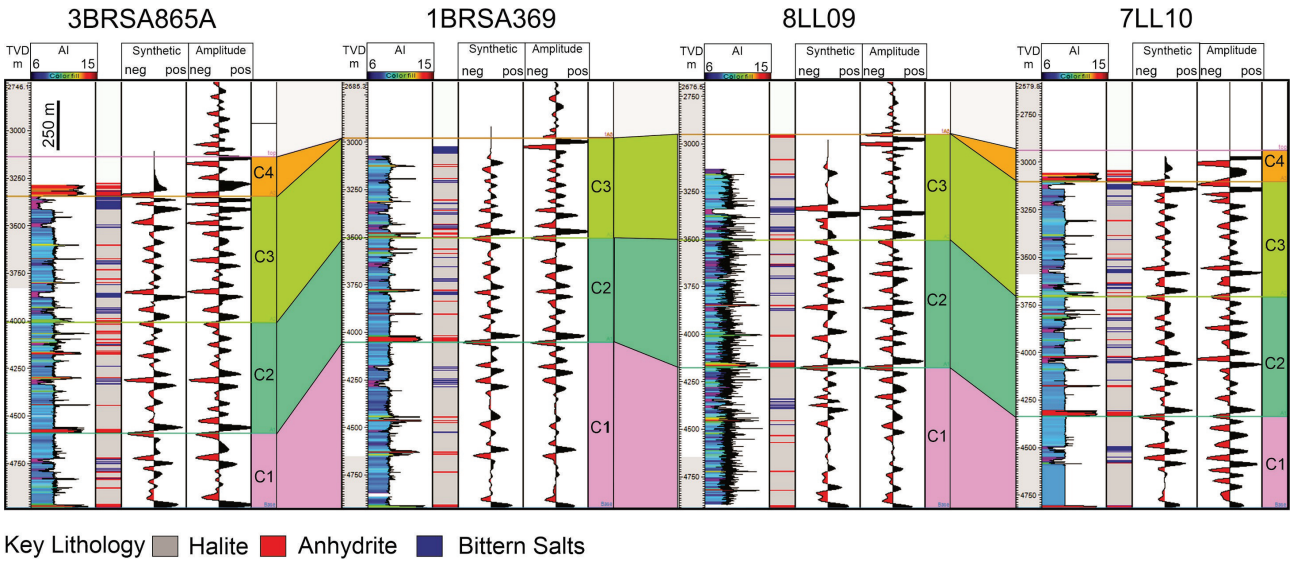

Figure 26: Comparison between the synthetic and the amplitude data. The amplitude data are an extraction of the seismic amplitude volume along the well path. The synthetic and the amplitude data are very similar, which indicates that the high quality of the seismic data. In both traces, the new cycle starts with a negative amplitude relating to the base of the anhydrite. Label: AI - acoustic impedance [g/m^3 km/s]

with, in most cases, halite layers.

The premisse of mapping the sedimentary cycles implies that an anhydrite layer marks the base of the cycle. Nevertheless, we demonstrated that the amplitude data is highly ambiguous in identifying the salt type. To reduce the uncertainty risk, mainly in the parts where wells are absent or very sparse, the acoustic impedance and seismic-driven facies volume assisted the interpretation of the anhydrite layers. Figure 27 depicts the seismic profiles and the interpretation of the cycles. This seismic profile intersects the wells BRSA865A, BRSA369, LL10. Complementarily, Figure 28 displays a crossline intersecting the well BRSA369.

The interpretation keeps the previous understanding of dividing the Ariri Formation into four main units. However, every unit in Figure 27 and Figure 28 indicates a sedimentary cycle. The seismic expressions of the cycles are very similar to those described by Jackson et al. (2015). C1 is transparent, poor-reflective cycle. This is a consequence of the low contrast of acoustic impedance of halite-rich sequence. C2 and C3 exhibit more alternation of bittern salts and anhydrite embedded in halite. Accordingly, high-frequency and high-reflective amplitudes control the seismic expression of these cycles. C4 is more restricted due to the extensive erosion. In this cycle, the strong negative and positive amplitudes are responses of strong contrast between the thick layers of bittern salts and anhydrite.

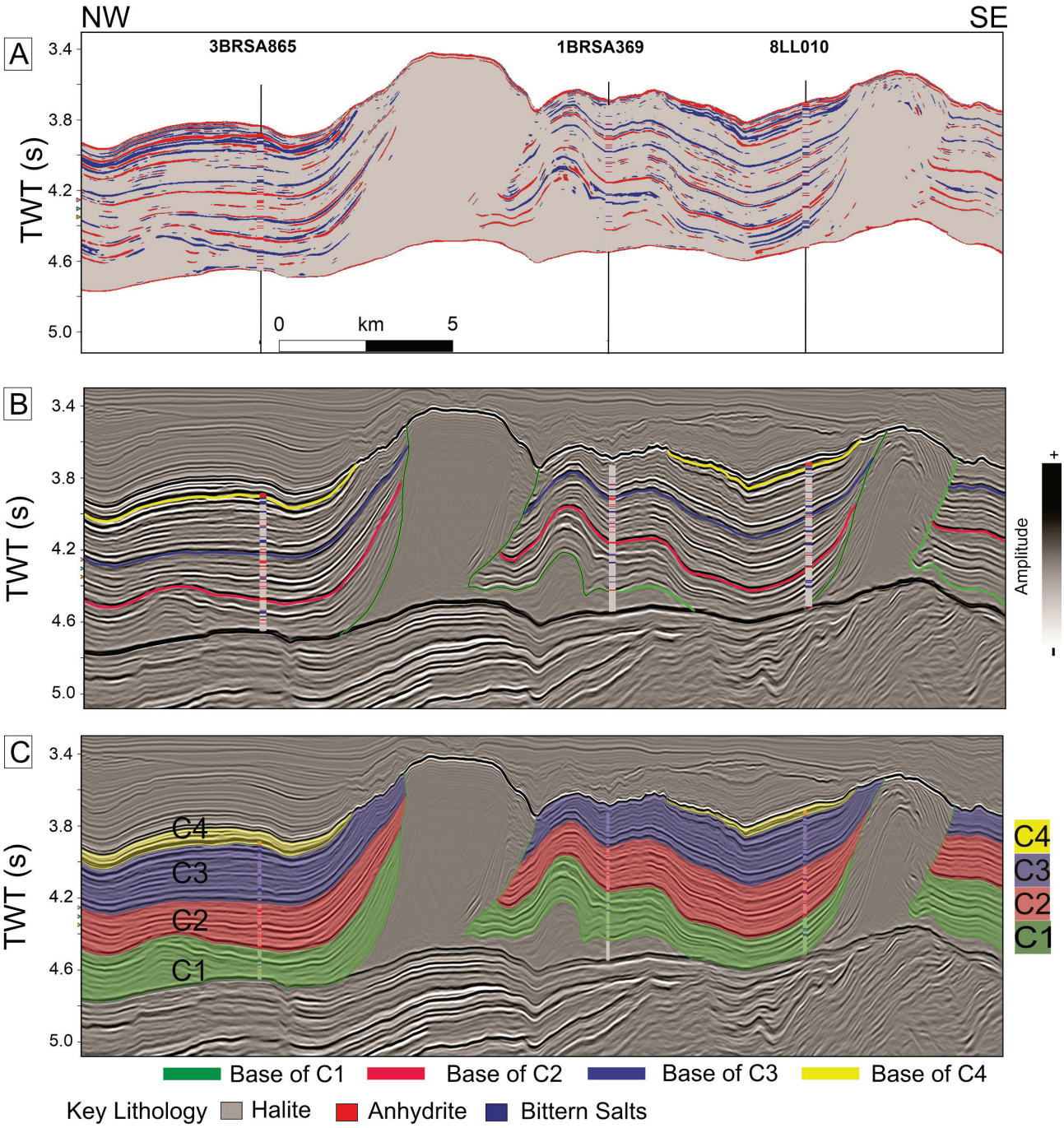

Figure 27: Seismic profile intersecting the wells BRSA865A, BRSA369, LL10. (a) Bayesian seismic classification in the evaporite formation of the Santos Basin; (b) interpretation on seismic amplitude; (c) individualization of the seismic unit. The seismic interpretation (c) is supported by the reduction of ambiguity due to Bayesian classification (a). Every cycle starts with the presence of anhydrite layers, a trough in the seismic response.

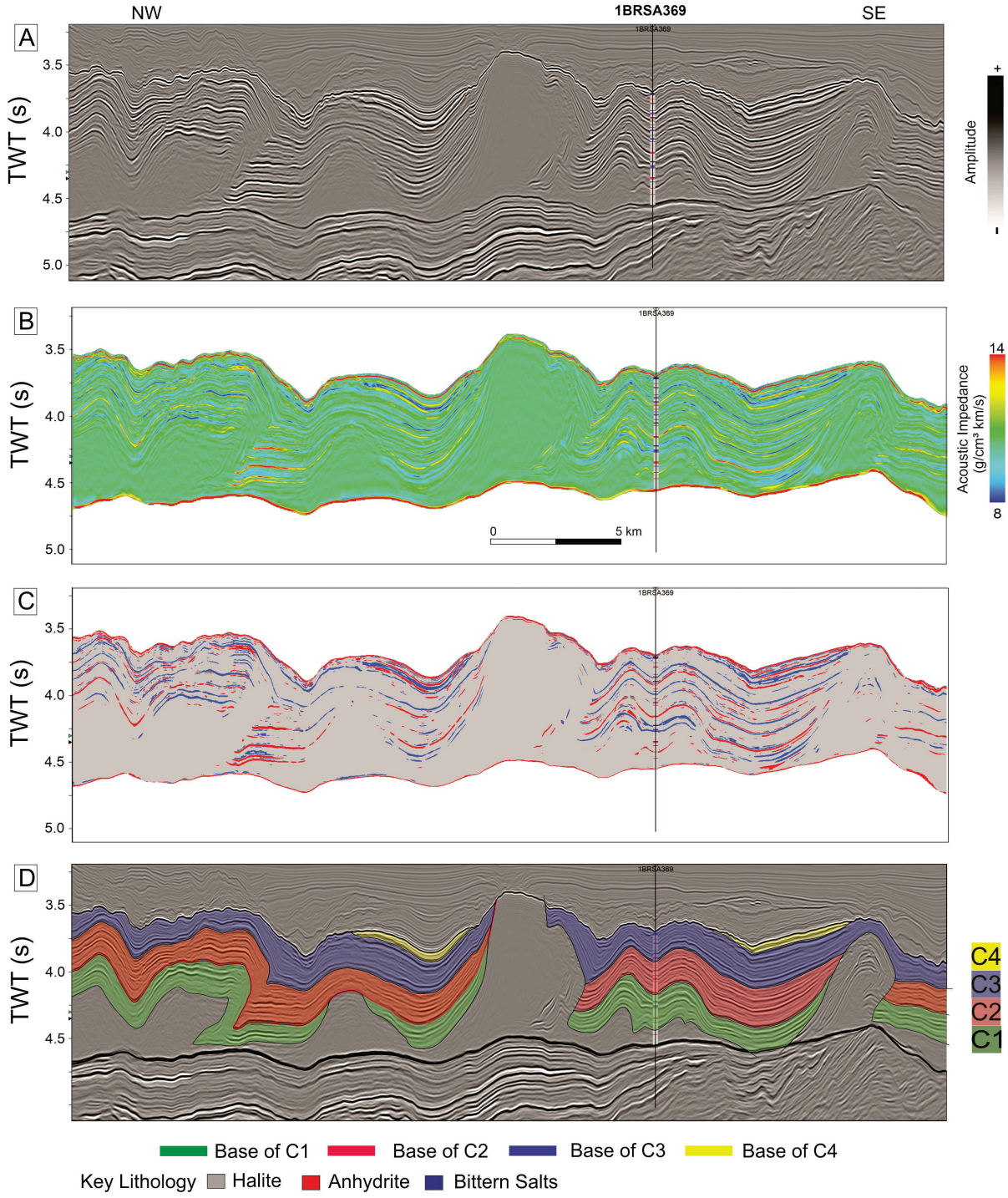

Figure 28: Seismic profile intersecting the well BRSA369. Seismic profile in the evaporite formation in the Santos Basin. (a) Seismic amplitude; (b) Bayesian seismic classification; (c) Bayesian facies classification; (d) individualization of the seismic unit. The seismic interpretation is supported by the reduction of ambiguity due to the Bayesian classification.

None of these cycles contemplates the big domes, which were mapped separately. Although the study area does not include wells that penetrated the salt domes, Maul, Santos and Silva (2018b) reported that boreholes in these structures in the Santos Basin encountered very halite-rich evaporite sequences with approximately 95% of halite. Consequently, the absence of acoustic contrasts appears in seismic data as reflection-free events. Therefore, inside these bodies, the identification of the sedimentary cycles is impaired both in well and seismic data. Moreover, the exclusion of big domes has positive implication for the quantitative analysis of seismic data. The inclusion of domes in C1 would drastically rise the halite proportion in this cycle, thereby leading to a misinterpretation of the statistical data.

3.7 Facies distributions and proportions

We computed the proportion maps of bittern salts and anhydrite for each cycle using the seismic-driven facies volume to inspect the lateral variation of salt types (Figure 29). These maps indicate that the concentration of bittern salts and anhydrite is larger in the mini-basin and it decreases towards the big domes. In addition, the maps suggest that the proportion of bittern salts and anhydrite increases from C1 to C4, that is, from the bottom to the top in the stratigraphy column.

The driven-seismic facies enables us to calculate the facies proportion by stratigraphic cycle. The algorithm counts the number of samples of a specific facies and divides by the total sample, returning the proportion of facies. Table 9 encapsulates the well-based and seismic-based proportions for bittern salts, halite and anhydrite. The comparison between them shows good agreement.

Table 9: Well-based and seismic-based salt proportions in C1, C2, C3 and C4.

	Well-based proportion (%)			Seismic-based proportion (%)		
Cycle	Bittern salts	Halite	Anhydrite	Bittern salts	Halite	Anhydrite
C1	7.5	90.3	3.2	5.1	88.5	6.4
C2	6.4	84.0	9.6	6.0	89.4	4.6
C3	15.4	78.9	5.7	13.8	75.1	11.1
C4	-	-	-	20.4	41.8	37.8

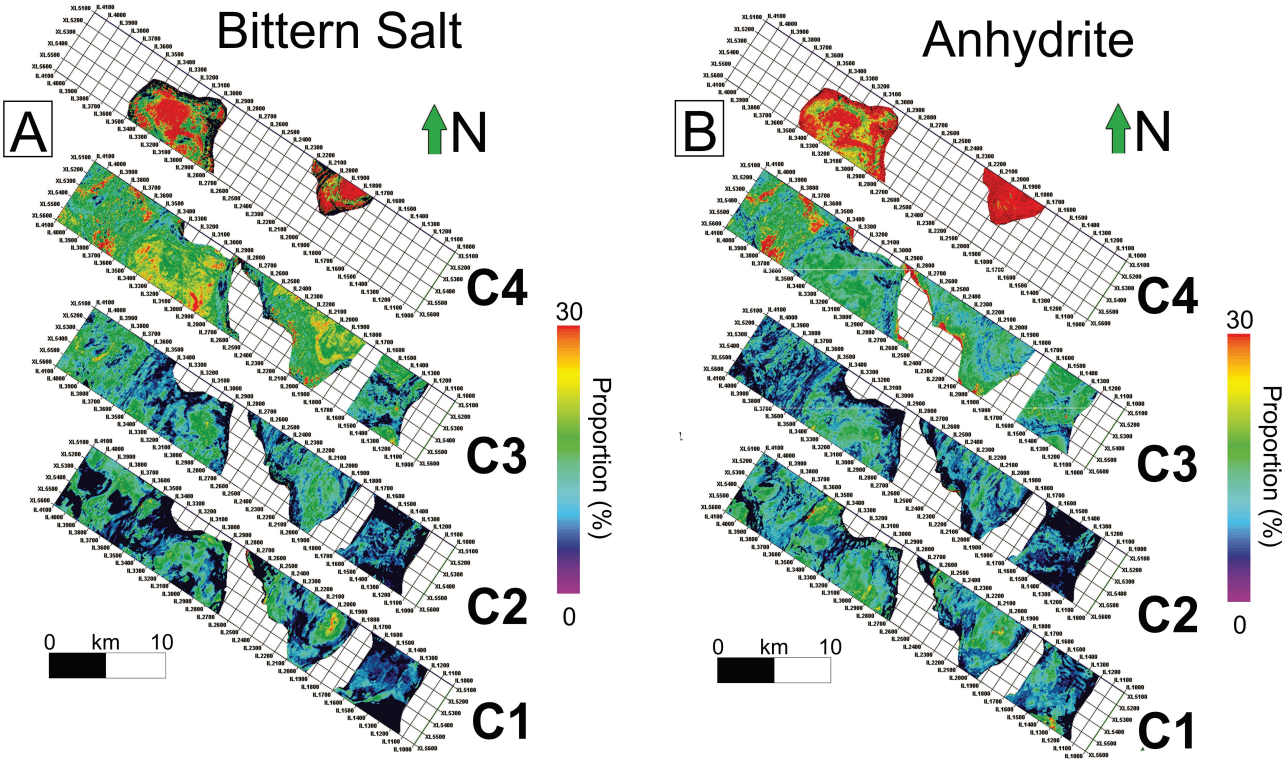

Figure 29: Distribution facies maps in the evaporite sequence of the Santos Basin: (a) bittern salts and (b) anhydrite. The proportions of these salt types increase from C1 to C4. The blank regions correspond to the big domes in C1, C2 and C3. C4 was extensively eroded.

3.8 Discussion

3.8.1 The pitfalls when interpreting salt types based on seismic amplitude

Seismic forward modeling constitutes an important step in seismic interpretation essentially because it simulates the seismic signal under a geological condition. We discussed the analysis of synthetic seismic response in which bittern salts and anhydrite are embedded in a thick halite layer to evaluate typical what-if scenarios of the evaporite sequence in salt-bearing basins. It demonstrated that seismic signal of bittern salts is a trough at the top of the layer due to the decrease of acoustic impedance in the bittern-salts-halite interface, whereas anhydrite creates a trough at the base due to the decrease of acoustic impedance in the anhydrite-halite interface. In an alternation of salt types, the association of a positive or negative amplitude with a specific salt type leads to overestimation. Oliveira et al. (2015) related high-positive amplitudes to anhydrite layers, however, they observed the misinterpretation in associating the high-negative amplitude with bittern salts. In this context, the authors chose not to classify the bittern salts (low-velocity salts). The synthetic study evidenced that misinterpretations occurred due to the dubiety of seismic amplitude. Besides, the ambiguity of seismic response alludes to the fact that amplitude-based attributes - such as root mean-square (RMS) and envelope - are inappropriate to evaluate the variation of salt lithologies.

The execution of seismic inversion in synthetic data proved that this procedure significantly improved the differentiation of bittern salts, halite and anhydrite by providing acoustic impedance volume and de-risking the evaporite interpretation based on seismic amplitude. For that reason, the acoustic impedance volume was the natural choice to underpin the seismic facies classification on real seismic data. The seismic-driven facies volume assisted the understanding of the spatial variability and assessed the heterogeneities in the salt sequence in the Santos Basin.

3.8.2 Refinement of intrasalt interpretation

The cutting samples of the evaporite-bearing sequence in the Santos Basin indicate the occurrence of halite, anhydrite, carnallite and tachyhydrite. Gypsum and sylvite are sparsely described

in insignificant amounts. We combined the interpretation of predominant facies and well-log measurement to infer the lithology in the evaporite formation based on petrophysical responses of these rocks (Table 5). The lack of sidewall cores prevented us from performing the interpretation of more complex salts.

Facies log assumes deterministic variable for each facies. We are aware of strong post-depositional salt flow creating intensive folded structures in intrasalt salt formation, altering the original sedimentary structures, which points out that the occurrence of pure salt is very unlikely. Despite the modification of the original stratigraphy, we believe that the facies logs described the predominant facies, however it still fails in indicating their proportion. Well-to-seismic correlation reveals areas more liable to intense salt-related structural deformation and helps identify those areas in which the primary sedimentation is relatively preserved.

We followed the previous studies that divided the Ariri Formation in the Santos Basin in four units based on the seismic expression of the evaporite sequence. Here, we interpreted in well logs four sedimentary cycles to correlate them to the seismic data. The onset of each cycle starts with the presence of anhydrite, determining the lowest brine concentration in the hidrographically isolated system. Accordingly, the highest brine concentration (maximum desiccation) is represented by the intracycle deposition of bittern salts.

The well-based interpretation suggests more than four cycles in the Ariri Formation ((FREITAS, 2006)). The seismic well-tie evidences that these high-order cycles can be traceable in seismic data. Nevertheless, we opted to keep the four-fold division to compare with previous works that investigated the quantitative proportion of the salt types (FREITAS, 2006; JACKSON et al., 2015; RODRIGUEZ et al., 2018). However, the cycles C1, C2, C3 and C4 may not occur in the entire salt formation of the Santos Basin. 2D lines across the basin demonstrate the absence of these cycles in the proximal/extensional domain landwards of the Cabo Frio Fault, the basinward limit of the Albian Gap (for examples, see Rodriguez et al. (2018)). The absence may still occur in regions subjected to intense halokinesis-related intrasalt deformations (for examples, see Alves et al. (2017)) or in primary salt welds or minibasins (for examples, see Jackson et al. (2014))). Therefore, this work does not advocate that the four-fold interpretation is the only possibility, however we understand that it is appropriate for

this studied area.

The hydrographically-isolated and tectonically-formed subsealevel depression is the plausible explanation for suitable large accumulations of the thick salt deposits in the Santos Basin. This context raises a fundamental problem in applying sequence stratigraphy in evaporite sequences of widespread evaporite basins, essentially because it breaks up the correlation between salt deposition in effective isolated settings and relative sealevel changes in open-marine systems (WARREN, 2006). Comparetively, Tucker (1991), Sarg (2001) and Becker and Bechstadt (2006) attempted to perform sequence stratigraphy of the evaporite-bearing sequence in the Zechstein Basin, relating the high-stand levels to carbonate depositions. However, we found no evidence of carbonate deposition in the Ariri Formation. This suggests a higher magnitude of hydrographic isolation in the Santos Basin than observed in the Zechstein Basin during the salt deposition.

We integrate information of acoustic impedance and facies volumes with seismic amplitude to perform a detailed interpretation in evaporite formations. The current interpretation of the main four-fold units is underpinned by seismic expression of amplitude data. Here, we propose the extension of the well-interpreted sedimentary cycles (C1, C2, C3 and C4) to the seismic data to evaluate the behaviour of the cycles spatially. The well-to-seismic calibration demonstrates that the seismic signal of the base of anhydrite layers is a negative amplitude which determines the onset of new cycle. In the regions away from wells, the acoustic impedance and facies volumes were the key attributes to mitigate the ambiguity of amplitude response and to carry out a trustworthy interpretation of sedimentary cycles.

The seismic expressions of the cycles C1, C2, C3 and C4 are very akin to those described in the units I, II, III and IV in Freitas (2006) and Gamboa et al. (2009), and the units A1, A2, A3 and A4 in Jackson et al. (2015) and Rodriguez et al. (2018) (Table 10, for comparison). While the interpretation based on seismic expression reflects the acoustic character of the evaporite sequence, the horizons C1, C2, C3 and C4 indicate sedimentary cycles and, consequently, changes in the salinity of the supersaturated fluid. We argue that this interpretation yields more powerful geological meaning and the new division sought other criteria to interpret the intrasalt sequence in the Santos Basin.

Table 10: Comparison between different interpretation units of the evaporite sequence in the Santos Basin.

(FREITAS, 2006)	Gamboa et al. (2009)	Jackson et al. (2015)	Sedimentary Cycle (this paper)
I	Lower halite-rich	A1	C1
II	Interbedded	A2	C2
III	Halite-rich	A3	C3
IV	Interbedded	A4	C4

3.8.3 Combination of qualitative and quantitative interpretations

We resort to the quantitative seismic interpretation to overcome the ambiguity of seismic response and identify the evaporites. The procedure is successfully applied to reservoir characterization and proved to be valuable to the characterization of the evaporites. The success resides in the combination of statistical techniques, rock physics and seismic inversion. Seismic inversion reduced the uncertainty in the evaporite interpretation; rock physics provided the link between facies and acoustic impedance; and Bayes' theorem combined both information to deliver the 3D facies estimation. This methodology proceeded with backwards modelling to reveal the most probable facies that explains the seismic response of amplitude data.

The seismic Bayesian classification is based on acoustic impedance volume which, in turn, is a product of the seismic amplitude by the application of seismic inversion. Consequently, the quality of the seismic classification is subjected to factors such as resolution, noise and illumination.

In our dataset, the seismic resolution of seismic amplitude lies between 25 m and 30 m (Figure 21). Nevertheless, seismic inversion can decrease the threshold of the seismic amplitude resolution (HILL, 2005). The comparison of well-log and seismic facies classification suggests that layers with approximately 15 m can be properly recovered. The extension of seismic resolution ensues from the fact that the facies volume is an outcome of the acoustic impedance. Still, thin layers may not be identified. Furthermore, very steep near-vertical layers around the complex-shaped salt domes are poorly illuminated and pose challenges for seismic migration to fully retrieve suitable seismic amplitudes (JONES; DAVISON, 2014). As a result, it impairs the quality of seismic classification in the vicinity of salt domes.

The similarity of the acoustic response of carnallite and tachyhydrite led us to assemble them into one class recognized as bittern salts. The individualization of these two salt types may result in misclassification between them in the facies volume. Consequently, we opted to classify the facies in bittern salts, halite and anhydrite to perform the Bayesian classification. The comparison between well log and facies volume evidences that the seismic attributes can identify the salt types (Figure 25). In addition, the comparison between well-based and seismic-based proportions in Table 9 endorses the potential of seismic data to quantitatively characterize evaporite formations.

The facies volume enables us to extract attributes directly from the seismic cube. Table 9 shows an anomalous proportion of bittern salts and anhydrite in C4 computed from seismic-derived facies. Partial acquisitions of gamma ray and sonic logs prevent us from performing the well-based interpretation of salt types accurately in this cycle. In this circumstance, we resort to the salt proportion of A4, which is fairly similar to C4, calculated by Rodriguez et al. (2018). The authors described the following proportion in the well 532A located in a thick salt domain: 20% bittern salts, 46% halite and 34% anhydrite. These well-based proportions endorse our seismic-driven proportions in the cycle C4. Remarkably, the well is approximately located 100 km far from our study area. The proportion of salt types suggests that the salinity of the brine remains quite alike over large areas in the isolated marine-fed system in the late Aptian in the Santos Basin.

The absence of clastic and carbonate rocks in the Ariri Formation hints at a fast deposition of the thick evaporite sequence with an estimation range 400-600 Ka (FREITAS, 2006). That estimation agrees with a typical rate of salt deposition of ancient basinwide evaporites (WARREN, 2006). This thick deposition within geologically-comparable short period leads us to stipulate that each cycle represents a 4th-order sequence. Presumably, the seismic-resolvable intracycle horizons represent a 5th order.

Bittern salts and anhydrite proportions rise from the C1 to C4, whereas halite proportion decreases. This quantitative analysis of salt accumulation suggests that the salt sequence was subjected to high-frequency variation of salinity from the bottom to the top of the formation. Therefore, we advocate that the overall evaporite sequence in the Ariri Formation stands for a 3th-order (Figure 30).

It is noticeable the drastic rise of the bittern salts and anhydrite proportions from C3 to

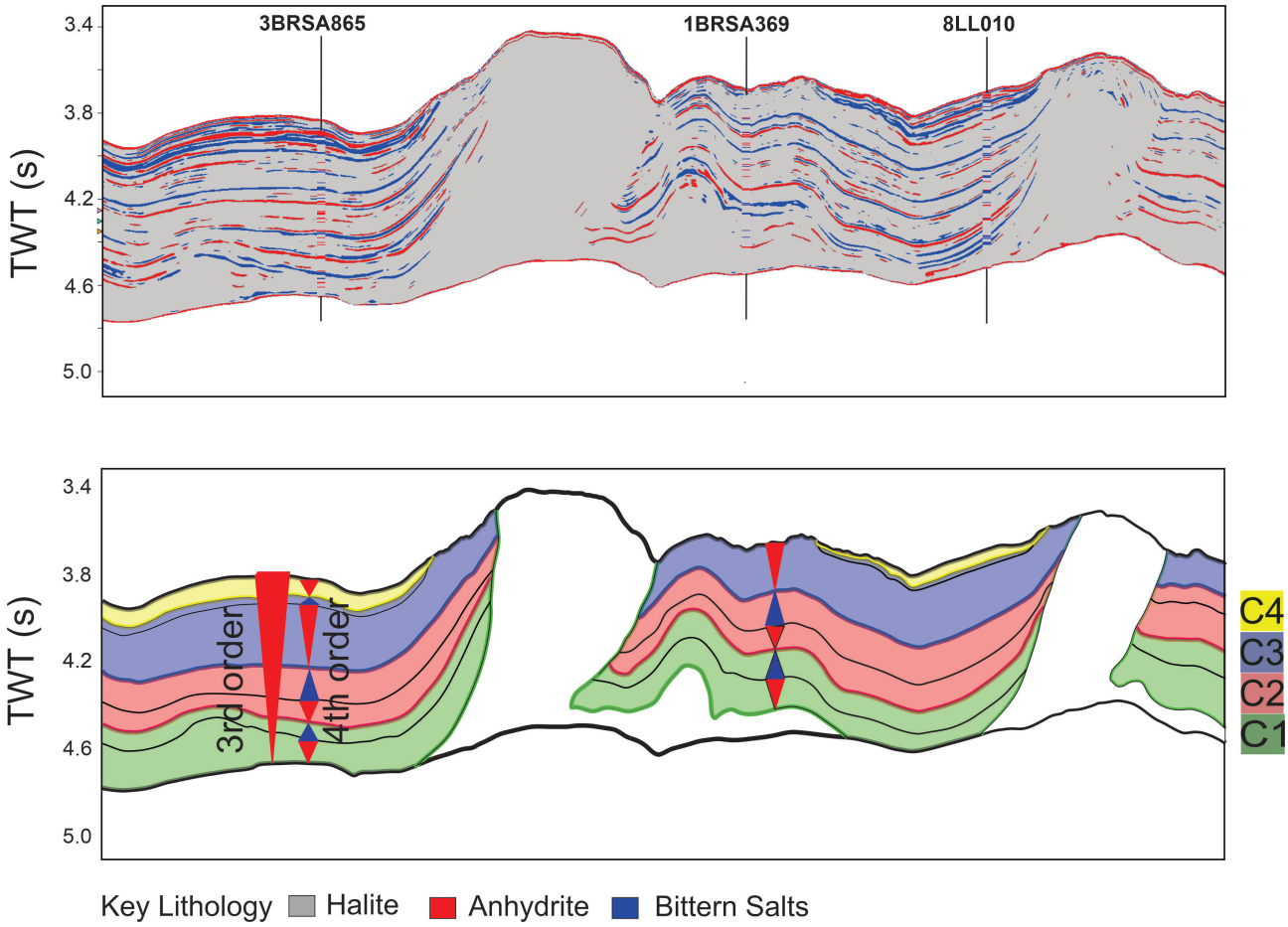

Figure 30: A schematic stratigraphy of 3th and 4th orders of the sedimentary cycles based on interpretation of well logs and seismic in the Santos Basin. The well-based and seismic-based proportions indicate that bittern salts and anhydrite proportions rise from C1 to C4, suggesting that the salt sequence was subjected to high-frequency variation of salinity from the bottom to the top of the formation

C4. This is an indication that C4 underwent an extreme change in salinity faster than the previous sedimentary cycles. Additionally, we observe that the inner reflectors thin towards the domes in C4, thereby suggesting a reduction in accommodation space and uneven relief during the salt deposition. We hypothesize that the salt starts to flow prior to the deposition of Albian open-marine sediments, plausibly in the end of C3. It favored, inside the hydrographically marine-isolated system in the Santos Basin, the creation of restricted mini-basins which were more susceptible to climate changes and salinity variations. That can explain the high-frequency alternation between bittern salts, halite and anhydrite. Alves et al. (2017) suggested the mild reactivation of pre-salt syn-rift structures prior to the deposition of the salt sequence. Presumably, the modest faulting persisted during the massive deposition of the evaporite sequence. This assumption supports the interpretation of tectonically-induced slight halokinesis prior to the complete salt deposition, creating gentle pond-like depressions.

In the North Sea, the Zechstein Salt presents lateral variation of salt types. In ZIII unit of the Zechstein Salt, smaller bischofite occurrences in isolated parts of the evaporite-dominated sequence led to the interpretation of pond-like depressions (RAITH et al., 2016). The uneven relief sustains our interpretation because the deposition of significant thickness of bittern salts demands prolonged and isolated arid conditions. In the Santos Basin, the top of C3 recorded a sixty-meters thickness of bittern salts in the well BRSA865 and twenty-three-meters thickness in the well LL10, both wells separated by a distance of approximately 15 km. Analogously, the significant difference of thicknesses in this layer suggests morphologically isolated depressions inside the basin. Here, the combined analysis of quantitative seismic characterization, well-based description of salt types and pre-salt fault reactivation converges to interpretations of the mild salt flow, thereby favoring the creation of gentle pond-like depressions, plausibly in the end of C3.

3.8.4 Application to industry: a toolkit to predict bittern salts

Reaching pre-salt reservoirs poses challenges for well drilling. Bittern salts (K-Mg-rich salts such as carnallite and tachyhydrite) are ductile, low-viscosity minerals/rocks and present short-term creep behaviour engendering borehole collapse, washout, fluid losses under the timescale of drilling operations. Costa et al. (2010) reported drilling problems in the pre-salt reservoirs related to the

presence of bittern salts in the Santos Basin. In the North Sea, kicks and losses were documented in the upper Z2 unit of the Zechstein Salt caused by the presence of Mg-K-rich salts (STROZYK, 2017). Numerical simulations of creep salt behavior to predict the evolution of well closure with time and to estimate the optimum fluid weight to avoid drilling problems demand the knowledge of the salt types (POIATE; MAIA; FALCAO, 2006). The facies-driven volume delivers a prediction of the spatial distribution of low-viscosity evaporites priori to well perforation. The identification of these rocks, mainly at large burial depths and high temperatures, provides valuable information to avoid hazardous drilling events.

3.8.5 Application to other salt-rich basins

Seismic data assisted the intrasalt characterization of saline giants in the Mediterranean Basin (BERTONI; CARTWRIGHT, 2007; LOFI et al., 2011; CARTWRIGHT et al., 2012; FENG; STEINBERG; RESHEF, 2017; GüNEŞ; AKSU; HALL, 2018), in the North Sea Basin (BECKER; BECHSTADT, 2006; GENT; URAI; KEIJZER, 2011; STROZYK et al., 2012; STROZYK et al., 2014; JACKSON et al., 2019), in the Paradox Basin (TRUDGILL, 2010). These papers documented the description of morphology, lithology variation, kinematic and structural styles of intrasalt strata by the qualitative interpretation of seismic amplitude and well data.

The transformation from qualitative into quantitative interpretation provides further information about the evaporite sequence because the core of the workflow combines petrophysical, geophysical and geological knowledges to deliver the most probable salt sequence that originated the observed seismic response. It assisted the refinement of the intrasalt seismic stratigraphy based on sedimentary cycles and the computation of quantitative attributes directly from the facies volume. Seismic inversion can be performed over large areas which indicates that regional studies can exploit the advantage of this technique.

Widespread evaporite basins lack modern analogues to shed light on tectonic, climate and eustatic conditions that originated these accumulations in the view of present days. For instance, the largest world halite deposit in the Quaternary is the Salar de Uyuni with approximately 10,000

km^2 (FORNARI; RISACHER; FÉRAUD, 2001). The extension and thickness of this evaporite deposit are insignificant in comparison to salt accumulations in ancient basinwide evaporite deposits. In the flaw of evaporite-applicable uniformitarianism, seismic and well data continue to be the primary source of ancient basinwide evaporite investigation. The step forward from qualitative to quantitative interpretation can improve the knowledge of kinematic, geometries and compositions of the evaporite-bearing intervals and the halokinesis-associated post-salt events in widespread evaporite basins. Even though the study focused on the Santos Basin, the benefits of quantitative characterization are extendable to other salt-rich basins.

3.9 Conclusions

The synthetic model demonstrates that bittern salts and anhydrite embedded in halite layers produce negative and positive amplitudes. Whereas seismic signal of bittern salts is a peak at the base of the layer due to the increase of acoustic impedance in the halite-bittern-salts sequences, anhydrite creates a peak at the top due to the increase of acoustic impedance in the halite-anhydrite sequences. Therefore, the interpretation of salt types based on seismic amplitude entails high ambiguity.

We apply the seismic inversion to transform the seismic amplitude into acoustic impedance volume. Low acoustic impedance relates to bittern salts, moderate acoustic impedance relates to halite and high acoustic impedance indicates the presence of anhydrite. The transformation of interface property into layer property reduced significantly the uncertainty in the interpretation of the evaporite sequence.

The combination of rock physics, seismic inversion and statistical technique proves to be valuable to the seismic identification of salt types. We applied Bayesian classification to deliver facies volume which classified bittern salts, anhydrite and halite. This volume indicates the most probable evaporites given the seismic amplitude and well data. It preserves the morphology, internal structures and seismic events in the salt bodies. The facies volume exhibits synclines and anticlines structures, near-parallel, near-isoclinal and sheet-like horizons, onlap and toplap terminations consistent with seismic amplitude.

We interpreted four major sedimentary cycles based on well logs. This interpretation appears to be appropriate for the studied area located in the São Paulo Plateau. However, these cycles are absent in the proximal/extensional domain or in the minibasin areas. The intense halokinesis-related intrasalt deformations pose challenges to the identification of these cycles particularly because they may be incomplete or severely folded. Therefore, the extension of four-fold cycles for the whole salt-bearing formation is still under investigation.

The analysis of synthetic response of evaporites and the seismic inversion of amplitude data are key procedures to extend the well-based sedimentary cycle interpretation to the seismic-based cyclostratigraphy. The integration of seismic amplitude, acoustic impedance and facies volumes reduced the uncertainty to map the seismic interpretation of sedimentary cycles. Previous works divided the intrasalt sequence based on the reflective patterns of seismic data. We proved that the division based on sedimentary cycles provides more geological meaning to the stratigraphic interpretation. We interpreted that each cycle may represent a 4th order. Intrasalt horizons stand for a 5th order and the overall salt deposition for a 3rd order.

The proposed workflow permits the extraction of quantitative rock attributes directly from the facies volumes. The comparison between well-based and seismic-based proportions corroborates the estimation of seismic data. Additionally, we computed proportions maps of bittern salts, anhydrite and halite to inspect the spatial variability of these facies for each cycle. Well and seismic data indicates an increase of bittern salts and anhydrite proportion from the base to the top of the Ariri Formation. It suggests that a more hydrographically isolated system in the end of the salt deposition. The salt flow prior to the deposition of the post-salt Albian sediments can be one explanation.

The workflow presents physical, petrophysical and geological foundations. It was tested in synthetic and real seismic data which represent a typical geological setting found in intrasalt sequences of widespread evaporite deposits. We argue that the combination of qualitative and quantitative interpretation can be relevant and successfully applicable to other widespread evaporite basins.

4 Probabilistic estimation of seismically thin-layer thicknesses

Article under review (R1) in

Survey in Geophysics

Impact factor: 6.673

Authors: Leonardo Teixeira, Alexandre Maul & Wagner Lupinacci

Salt body acts as a perfect seal for hydrocarbon-bearing reservoir rocks: it is virtually impermeable, and its creep behavior deforms its morphology to enclose the surrounding permeable sediments. Salt-associated oil-saturated reservoirs occur in North America, South America, West Africa, in the North Sea, in the Gulf of Suez (WESTERN; BALL, 1992; FARMER et al., 1996; MOHRIAK; SZATMARI; ANJOS, 2012; CHITALE et al., 2014). Between 2000 and 2012, 56% of the 120 giant hydrocarbon discoveries were associated with salt seals, among which was the recent discoveries of giant fields in Brazilian presalt (BAI; XU, 2014).

While the deformation of salt bodies offers a suitable environment for hydrocarbon migration and trap, its creep behavior triggers serious drilling problems. The contrasting elastic properties, viscosities, and mechanical behaviors of the multilayered evaporite successions influence the salt movement during the life of a well (LI et al., 2012). From the moment that the drilling bit penetrates the salt body, the formation experiences instability in the borehole as a result of the differential stress (WANG; SAMUEL, 2016). Documents report drilling issues such as washout, closing pipes, fluid loss damage, and borehole collapse (DUSSEAULT; MAURY; SANFILIPPO, 2004; STROZYK, 2017). These troubles pose significant dangers to workforce and reduce the return of investment in the risky areas.

Well closure rate depends on creep parameters which vary according to the salt types. For instance, tachyhydrite develops creep strain rate up to one hundred times higher than halite (COSTA et al., 2011). Still, in a typical salt sequence, carnallite, sylvite, and bischofite are more viscous rocks than halite and anhydrite (COSTA et al., 2011; RAITH et al., 2016). This group comprises potassium

and magnesium salts which are classified as bittern salts (WARREN, 2006; JACKSON; HUDEC, 2017). The prediction of the bittern salts prior to perforation is a key characterization to numerical evaluation of geomechanical models to forecast the stress loading in the wellbore casing during drilling and production operation (COSTA et al., 2010).

Seismic data provides a large-scale interpretation of intrasalt structures. The combination of well log and seismic interpretation assists the prediction of the low-viscosity salts at undrilled locations. Additionally, the seismic-based identification of bittern salts is valuable for the salt industry since these salts are high-priced sources of magnesium and potassium (RAITH; URAI; VISSER, 2017). Seismic and well data support the mapping of bischofite in the internal structure of the Zechstein Salt in the North Sea (STROZYK et al., 2012; RAITH et al., 2016; STROZYK, 2017), and the interpretation of bittern salts in the Santos Basin (FREITAS, 2006; GAMBOA et al., 2009; FIDUK; ROWAN, 2012; JACKSON et al., 2015; RODRIGUEZ et al., 2018; TEIXEIRA; LUPINACCI; MAUL, 2020; MAUL et al., 2021b; PONTES; MAUL; SILVA, 2021).

Comparisons between seismic classification and facies description in well logs indicate that the interpretation of seismic amplitude in intrasalt formations overestimates the presence of bittern salts (FALCÃO, 2017). Teixeira, Lupinacci and Maul (2020) simulate the seismic response of anhydrite-halite successions and bittern-salts-halite successions and conclude that these formations generate similar seismic amplitude responses, thereby explaining the intrinsic uncertainty. To increase the reliability of the salt type classification by seismic data, the authors make use of the acoustic impedance derived from seismic inversion, followed by the Bayesian classification. This procedure significantly improves the identification of bittern salts.

Despite the improvement in the predictions of bittern salts, the seismic classification is limited to the resolution of the seismic data. Geomechanical models evidence that thin-bed tachyhydrites with thickness around 5 m present very high closure rate during the drilling period if the mud weight is unproperly estimated (COSTA et al., 2010). This scenario suggests that unexpected thin-bed bittern salts can deform the wellbore if these layers are not predicted and included in the geomechanical models. This raises a question: how to estimate the thin-bed bittern-salts thickness from seismic data to prevent wellbore-related hazardous events?

By the 1970s, researchers related the seismic amplitude to the quality and thickness of hydrocarbon-bearing reservoirs (WIDESS, 1973; GARDNER; GARDNER; GREGORY, 1974; HAMMOND, 1974). Widess' criteria formulate that the theoretical threshold of seismic resolution of a thin-bed layer corresponds to one-eighth of a wavelength of this layer thickness. Under this threshold, the thickness is seismically unsolvable by peak-to-trough mapping in amplitude data. The thickness estimation under this point is based on the empirical evidence that the seismic amplitude and thin reservoir zones are linearly correlated (MECKEL; NATH, 1977; SCHRAMM; DEDMAN; LINDSEY, 1977; BROWN et al., 1986). Essentially, these techniques plot the seismic amplitude and the seismically mapped reservoir isopach, and apply a data-specific self-calibration. At the core of the procedure resides a wedge model which assumes a wedge-shaped facies embedded in another type of thick facies. Later on, by the 1990s, studies introduced more realistic scenarios and included the effect of the layering patterns of stratigraphic sequences on the seismic amplitude response (NEFF, 1990; NEFF, 1993).

The use of seismic amplitude to estimate thin-bed thickness lurks a potential pitfall: its dependence on the wavelet shape of field data (KALLWEIT; WOOD, 1982; BROWN et al., 1986). Therefore, the employment of seismic attributes that are, in principle, independent of wavelet shape raises the reliability of the estimation. In this sense, the emergence of the seismic-inverted elastic properties shed light on new attributes that can potentially assess the rock thickness. That favors the use of bandpass acoustic impedance to estimate thin-bed dimensions (CONNOLLY, 2007; SIMM, 2009). This strategy has the advantage of appraising the thickness directly from a layer-property seismic attribute instead of employing an interface property such as seismic amplitude.

The aforementioned procedures can potentially assist the estimation of thin-bed bittern salts. Nevertheless, they rely on deterministic approaches to achieve this end and lack an algorithm to quantitively determine the intrinsic seismic ambiguities. Here, we pose some questions: what is the uncertainty in the estimation of thin-bed thickness? How do the layering patterns affect the seismic response? How to quantify the noise content and how does it influence the thickness estimation?

The Bayesian classification is an integrative methodology that combines prior geological knowledge and statistical rock physics to carry out facies classification. The integration of consistently

geological and geophysical concepts in the Bayesian classification furnishes a versatile tool with applicability in turbidites, carbonates, and evaporites (AVSETH; MUKERJI; MAVKO, 2005; DOYEN, 2007; TEIXEIRA et al., 2017a; TEIXEIRA; LUPINACCI; MAUL, 2020; PENNA; LUPINACCI, 2021). Notwithstanding the vast applicability, the previous works cast aside the facies probability regarding it as a path to determinist classification. Here, we explore the usefulness of this attribute as a predictor of seismically thin-bed thickness. Also, we contextualize the interpretation of probability as a seismic attribute.

The Bayesian classification provides the volumes of most-probable facies and the facies probability (MUKERJI et al., 2001; AVSETH; MUKERJI; MAVKO, 2005; DOYEN, 2007). The most-probable facies is a categorical volume, while the facies probability assumes continuous values. When we apply the Bayesian classification to evaporite, we observe that the most-probable facies do not capture thin-bed bittern salts, however the facies probability of bittern salts presents non-null value, thereby indicating the presence of this salt type. In this paper we demonstrate how the facies probability and facies thickness relate to each other.

The assessment of uncertainty of rock property from seismic data is a tricky task essentially because, despite the large scale of seismic data, the well information is sparse and irregular. Therefore, the calibration of seismic attribute and rock property poorly captures the uncertainty of the data. The Monte-Carlo-assisted simulation of wells that emulate a stratigraphic sequence of site-specific deposition and the elastic property therein is a helpful tool to assess the uncertainty (DVORKIN; GUTIERREZ; GRANA, 2016). As opposed to two-facies wedge models, the simulation allows the inclusion of multiple facies. We make use of these simulations, often called pseudowells, to estimate the non-parametric joint probability density function (joint PDF) between the facies probability and layering thickness.

The joint PDF is at the core of the uncertainty appraisal of our methodology. From this function, we compute the conditional expectation, percentiles of the thin-bed thickness from the facies probability. The application of the outcomes in noiseless synthetic data confirms the efficiency of the algorithm: more than 80% of the data falls between P10 and P90 of the estimated thickness.

An issue emerges from the application to the field data. When we compute the expectation and the percentiles, the algorithm does not reproduce the uncertainty of the thickness estimation. A significant amount of thickness estimation falls outside P10 and P90 curves. The comparison of the acoustic impedance derived from synthetic and field data displays moderate differences caused by the presence of noise. In this regard, this paper discusses what is noise in the context of Bayesian classification, and provides a method to evaluate it and include it in the simulation of pseudowell. After the inclusion of the noise content, the algorithm captured the inherent uncertainties of the seismic-derived rock thickness.

4.1 Dataset

The dataset consists of high-density 3D seismic data and four wells acquired in the Santos Basin, Brazilian offshore. The seismic acquisition is part of a campaign that focused on the characterization of presalt reservoirs in this basin. The final seismic image includes the application of tomographic velocity and tilted transverse isotropy Kirchhoff prestack depth migration (TTI KPSDM). The seismic signal polarity follows the SEG (Society of Exploration Geophysical) convention which considers the positive amplitude as an increase of acoustic impedance in the interface of two layers and negative amplitude as a decrease.

The wireline logging recorded the evaporite and carbonate formations. In the carbonate formation, the set of logs comprises neutron and nuclear resonance magnetic porosities, density, sonic, and gamma ray. However, the acquisition is limited in the evaporite sequence where only gamma ray, density, and sonic logs were partially logged. The thickness of the salt sequence exceeds more than 2 km in some regions, thus providing more than 7 km of formation evaluation in four wells.

The well-logs and cutting interpretation identified the occurrence of anhydrite, halite, carnallite, and tachyhydrite and excluded the presence of carbonate in the evaporite formation. The petrophysical logs of the evaporite provided a consistent interpretation of the salt types. Halite has moderate velocity and low gamma ray; anhydrite has high velocity and low gamma ray; tachyhydrite has low gamma ray and velocity; carnallite has high gamma ray and low velocity. Tachyhydrite and

carnallite are scarcely complex salts, known as bittern salts (JACKSON; HUDEC, 2017). The facies log assisted the thickness estimation for each facies.

4.2 Methodology

The methodology delivers probabilistic thickness estimations of thin layers based on seismic data. It starts with two distinct workflows: simulation of pseudowells and seismic inversion (Figure 31). Both workflows and the steps thereof will be described in the subsequent subsections. We apply the methodology to the evaporites of the Santos Basin which comprise the seal rocks of the presalt reservoirs. However, it can be adapted to clastic and carbonate rocks to spatially estimate thin-reservoir thicknesses.

4.3 Simulation of facies

The scarcity of well data precludes the statistical analysis of seismic-driven rock property estimations. In the face of few wells, the relationship between seismic attributes and rock thickness is limited to best-fit models which chiefly put aside the uncertainty. As an alternative to overcome the scarcity of data, we make use of the generation of a large number of pseudowells to assess the intrinsic uncertainty of seismic estimation. Pseudowells are stochastic simulations of well data consistent with a particular depositional environment.

We simulate successions of bittern salts and anhydrite embedded in thick halite layers to reproduce the sedimentological sequence of the salt formation in the Santos Basin. Each pseudowell emulates a 90-m-thick salt succession, alternating presence of halite, anhydrite, and bittern salts. The simulation fixes two 25-m-thick halite layers: one at the top and one at the base. Within these pads, the algorithm includes bittern-salt layers using Monte Carlo simulation. The total thickness of these salt beds varies from 0.5 to 30 m and presents different stacking patterns. The upper limit of the total thickness represents approximately the seismic resolution of the seismic data in the study area.

The precipitation of bittern salt occurs in very arid environments when the brine concentration increases about 70-90 times the original seawater (WARREN, 2006; BABEL; SCHREIBER, 2014).

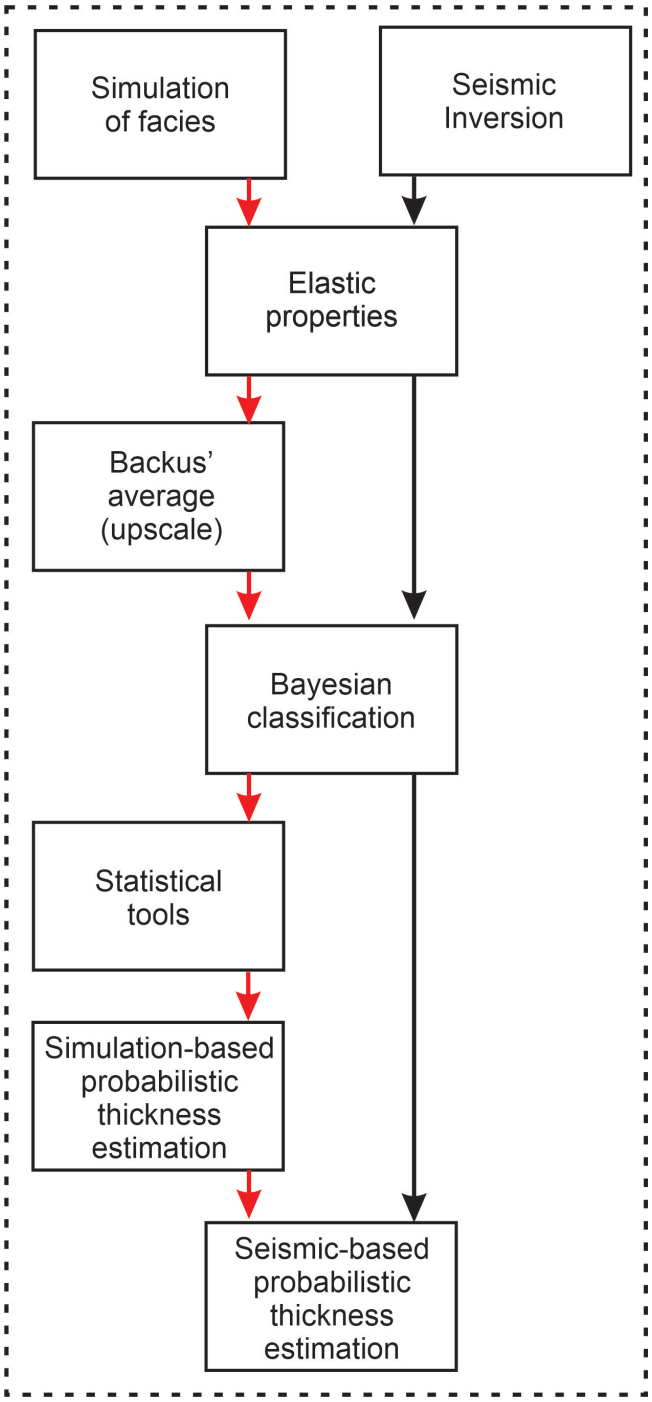

Figure 31: Workflow for the seismic-based probabilistic thickness estimation.

In this geological context, it is unexpected the presence of anhydrite between the bittern-salt layers. However, the facies description indicates that thin anhydrite layers may occur above and below bittern-salts successions. Thus, the algorithm randomly includes the possibility of anhydrite occurrence in these positions.

The method then attributes to each salt type typical values of elastic properties. To this end, we compute the average values of the compressional velocity (v_p), shear velocity (v_s), and density (ρ) for each facies based on well logs, which captures the in-situ conditions. Table 11 displays the elastic properties attributed to salt types.

Table 11: Well-log-based averages of density, compressional and shear velocities of salt types in the Santos Basin.

	Vp [m/s]	Vs [m/s]	Density [g/cm³]
Bittern salts	3950	2025	1.8
Halite	4530	2450	2.1
Anhydrite	5400	3100	2.5

The strong post-depositional salt flow creates intensive folded structures in intrasalt formations, altering the original sedimentary structures, which points out that the occurrence of pure salts is very unlikely. In this context, the description of facies in this paper refers to the dominant salt type. This description of the prevalent salt type was also applied in the core analysis of salt type in the Zechstein Basin (RAITH; URAI; VISSER, 2017). Therefore, the values present in Table 11 relates solely to the in-situ conditions of prevalent salt type in the Santos Basin. It may differ from the other laboratory and well data published in the literature (MAVKO; MUKERJI; DVORKIN, 2009; TRIPPETTA et al., 2010; TRIPPETTA et al., 2013).

At this stage, the simulation produces a representation of the elastic properties in a finely layered media compatible with a sedimentary sequence of salt type in the Santos Basin. Still, the purpose of this paper is to derive the estimation of rock thicknesses from seismic data. Therefore, we seek to synthesize the elastic-property profile of the rock sequence at seismic scale.

Backus' average is an appropriate technique to emulate v_p and v_s through a finely layered media (BACKUS, 1962; SIMM; BACON, 2014). Backus' average brings the harmonic average of the elastic moduli to bear the elastic properties of a long-wavelength effective medium in inhomogeneously

fine-laminated sequences. This technique is widely applied to calculate the effective medium of elastic constants in vertically heterogenous reservoirs (VERNIK, 2016). Here, we employ this computation to evaporites.

4.4 Bayesian Classification

This paper applies the Bayesian classification whose algorithm implements the Bayes' theorem to predict the most-probable facies and their respective probability (MUKERJI et al., 2001; AVSETH; MUKERJI; MAVKO, 2005; DOYEN, 2007). This procedure is useful because it provides a measurement of the classification uncertainty.

Let c_i be the facies and z be the seismic attributes. The process starts with the modeling of facies-conditional experimental distributions, denoted by $f_1(z|c_i)$. Additionally, one needs to provide the *a priori* probability for each facies $p(c_i)$. The *a priori* probability incorporates the subjective interpretation of facies probability before the knowledge of the seismic attribute. Bayes' theorem computes the *a posteriori* probability as follows:

$$f_2\left(c_i|z\right) = \frac{f_1\left(z|c_i\right)p\left(c_i\right)}{f\left(z\right)}. \tag{4.1}$$

where $f(z)$ is the marginal probability of the seismic attribute and $f_2(c_i|z)$ is the facies conditional probability given the seismic attribute.

We are interested in assessing the facies probability of the evaporites. Therefore, the choice of the seismic attributes should be effective in identifying the salt types. Teixeira, Lupinacci and Maul (2020) demonstrate that the seismic amplitude is highly ambiguous for this purpose and, alternatively, they propose the use of acoustic impedance to reduce the inherent ambiguity. Accordingly, we apply the Bayesian classification to the upscaled acoustic impedance to simulate the probability of facies at seismic scale (Figure 32).

The forward modeling relies on layering patterns, thereby avoiding the simplification of blocky wedge responses. However, unlike the previous works based on seismic amplitude or elastic

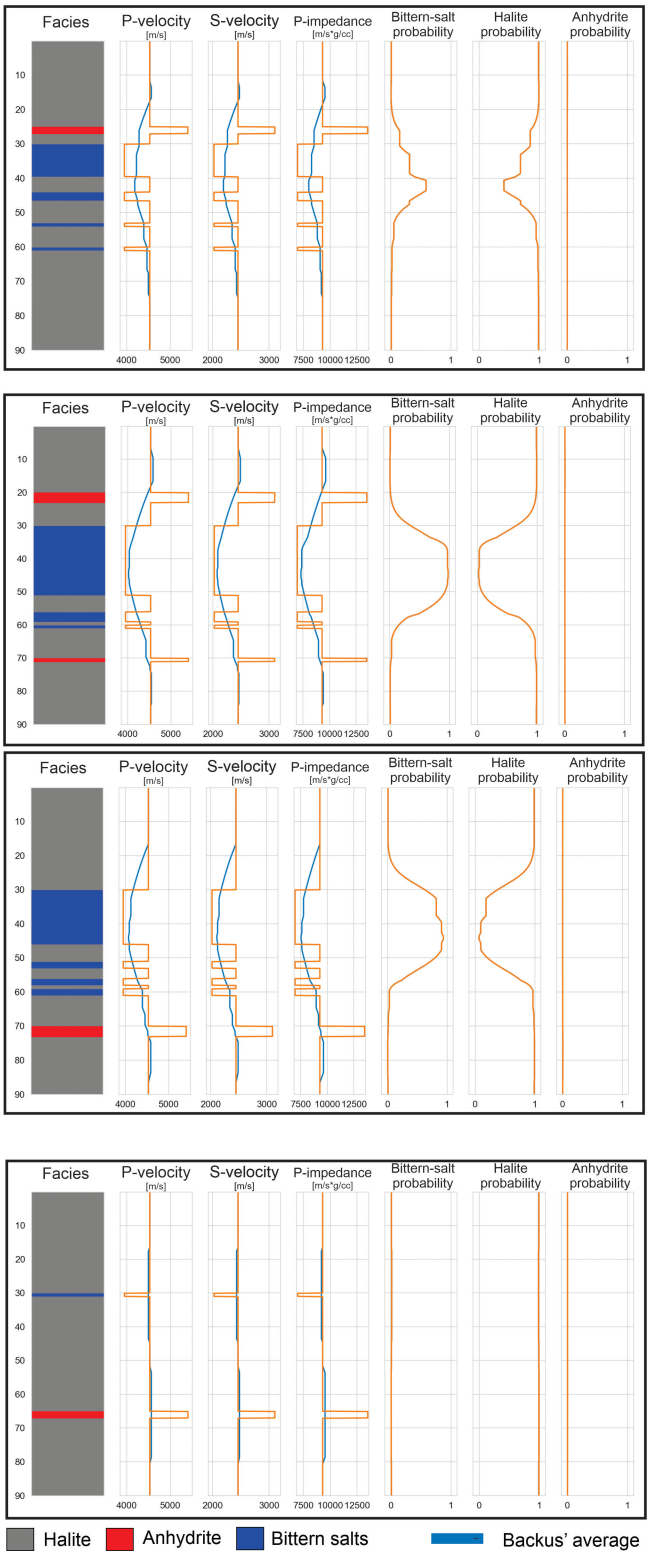

Figure 32: Four simulations based on the salt layering pattern in the Santos Basin. Bittern salts may occur in finely layering patterns or in a blocky sequence. Anhydrite may occasionally take place in the top or the bottom of the bittern-salt sequence. The orange lines in the compressional velocity (P-velocity), shear velocity (S-velocity) and acoustic impedance (P-impedance) stand for the elastic properties in a finely layering sequence, while the blue lines are the representation of the effective medium upscaled by the Backus' average. The facies probabilities are the implementation of the Bayes' theorem on the upscaled acoustic impedance.

properties, this study correlates the thin-bed thickness and sum of facies probability. To this end, the algorithm calculates the bittern-salts thickness and the integration (sum) of its respective seismic-derived probability for each simulation. Graphically, this corresponds to the area between the level zero and the curve of bittern-salts probability in the track (Figure 32).To demonstrate the effectiveness of the method, we run 20 simulations to construct a scatter plot containing 20 data points (Figure 33). Additionally, we provide the linear least-squares regression of these variables ($R_2 = 0.97$, prob (F-statistic) = 2.55×10^{15}).

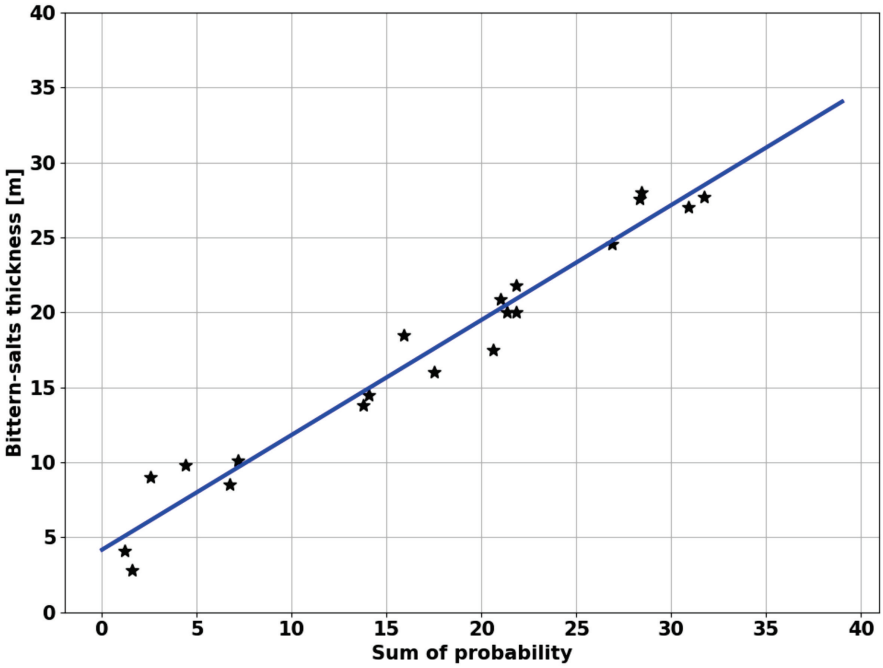

Figure 33: A scatter plot of 20 points correlating the bittern-salts thickness and the sum of probability. Each point is a pair of the rock property and seismic attribute emulated by the forward model of the salt sequence (see Figure 32) The blue line is linear least-squares regression of these variables ($R_2 = 0.97$, prob (F-statistic) = 2.55×10^{-15})

4.5 Statistical tools for uncertainty appraisal

The determinist estimation, as outlined by the linear least-squares regression in Figure 33, is the first approach to relate rock properties and seismic attributes. In addition to this inceptive procedure, simulation offers a powerful tool to generate a plethora of pseudowells that explores the intrinsic variability of seismic response. In contrast to the least-squares regression, this step deals with the assessment of the uncertainty with no assumption of gaussianity between the variables.

To explore the variability of our experiment, we generate 500 pseudowells. Subsequently, for each simulation, we extract the bittern-salt thickness and the sum of the bittern-salt probability. Therefore, our forward-modeled database counts on 500 points relating to the aforementioned variables. One can compute statistical parameters on these samples, mining valuable information about the data variability. However, if these parameters require the calculation of integrates and derivatives of the variables, the discontinuity of sampling raises vexing issues. To overcome this difficulty, we regard the reservoir property and seismic attributes in a continuous sample space represented by a probability density function (PDF) or distribution.

Parametric distributions, such as exponential, Cauchy or Gaussian distributions, can be constructed by pre-defined parameters (see Heumann, Schomaker and Shalabh (2016)). If these distributions are not appropriate, the kernel density estimation (KDE) is a useful alternative to derive non-parametric PDFs (PARZEN, 1962). Let $x_1, x_2, \cdots, x_i, \cdots, x_n$ be independent and identically distributed variables (iid). The density estimator $f(xf)$ can be defined as (SILVERMAN, 1986; BISHOP, 2006):

$$f(x) = \frac{1}{nh^D} \sum K\left(\frac{x - x_i}{h}\right). \tag{4.2}$$

where h is the window width, also called smoothing parameters or bandwidth. The higher h, the smoother $f(x)$ is. K is a non-negative function or the kernel and D is the dimension. When one chooses K to be a Gaussian distribution, the assessment of $f(x)$ is called Gaussian KDE.

This study employs the Gaussian KDE to estimate the joint distribution of rock properties and seismic attributes, for instance, facies-specific total thickness and sum of probability generated by the simulation of the salt-rich formation in the Santos Basin. The result of the KDE is the joint distribution represented by a non-parametric surface (Figure 34).

This methodology relies on the knowledge of the seismic attribute prior to estimating the facies-specific total thickness. Hence, the properly addressed question is: given the seismic attributes, which are the expected values of the rock properties and their inherent uncertainties? More specifically, given the sum of probability, which are the expected value of thin-bed thickness and its uncertainty?

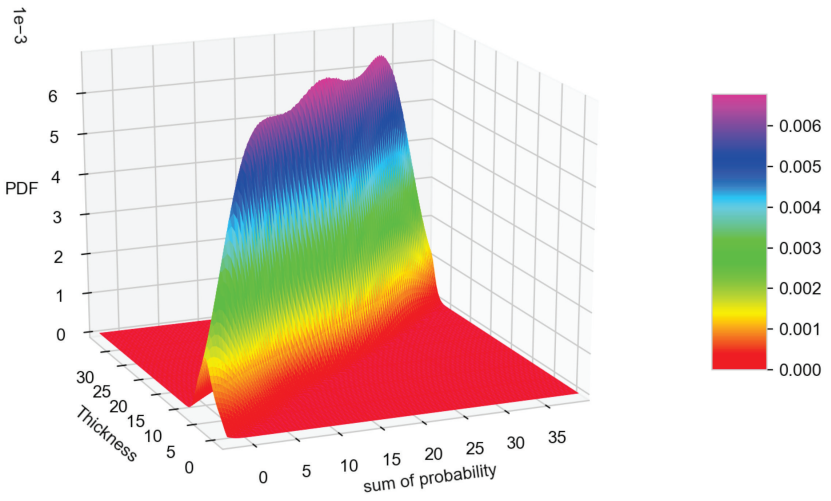

Figure 34: Joint distribution of the bittern-salt thickness and the sum of the bittern-salt probability. We employ the Gaussian kernel density estimation to derive a non-parametric surface which is the representation of the three-dimension joint PDF of the rock thickness and the sum of seismic-derived probability. The PDF enables us to describe the variable as a continuous space.

To answer this question, it is necessary to formulate the conditional probability.

Let t be the total thickness and s be the sum of the probability. The conditional distribution p of t given s is:

$$p(t|s) = \frac{f(t,s)}{f_s(s)}. \tag{4.3}$$

where $f(t,s)$ is the joint distribution of t and s and f_s is the marginal distribution of s.

$$f_s(s) = \int f\,(t,s)\ dt. \tag{4.4}$$

Equation 4.3 corresponds to the modern formulation of the Bayes' theorem (BAYES, 1763; DUDA; HART; STORK, 2000) . The outcome of Equation 4.3 is illustrated in Figure 35, which shows the conditional distribution of the layer thickness for two different values of the sum of probability.

The conditional probability is the outset of the appraisal of uncertainty evaluation. For this intent, we propose the calculation of the expectation and percentiles of the total thickness given the

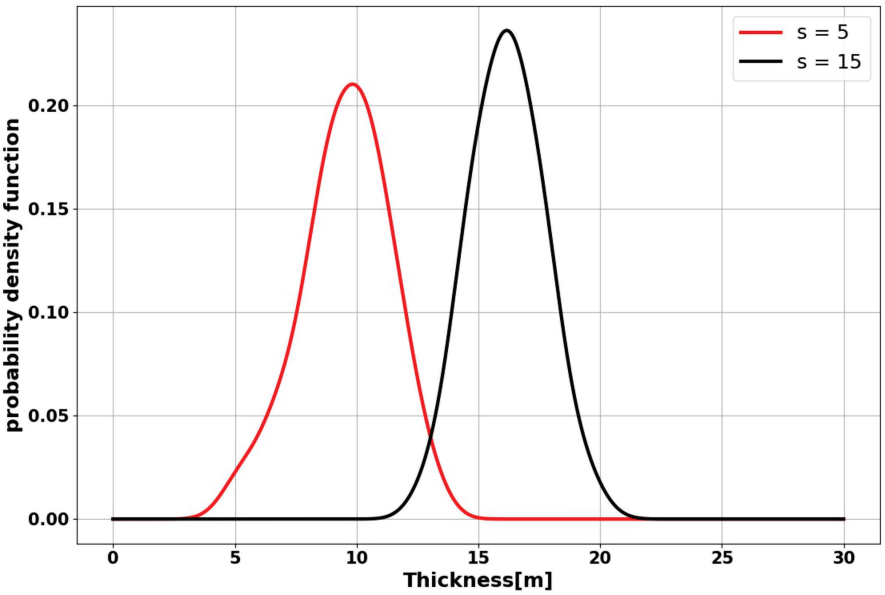

Figure 35: Conditional probability of thickness given the sum of probability. For instance, $s = 5$ and $s = 15$. An increase in the sum of probability shifts the conditional probability rightward. This indicates that the higher the sum of probability, the thicker the gross of bittern salts is.

sum of probability. By definition, the expectation is:

$$\mathrm{E}[t|s] = \int_{-\infty}^{t_q} t\, p(t|s)\, dt. \tag{4.5}$$

where $\mathrm{E}[t|s]$ is the conditional expectation of t given s. The conditional cumulative distribution of t given s is defined as:

$$F(t_q|s) \;=\; \int_{-\infty}^{t_q} p(t|s)\;\; dt \;\;=\;\; q. \tag{4.6}$$

The value t_q is called the q-percentile (DEKKING et al., 2005). Therefore, to find out the values of percentiles 10, 50, and 90, one needs to solve Equation 4.6 for $q = 0.1$, $q = 0.5$, and $q = 0.9$, respectively. Comparatively, Table 12 summarizes the expectations and percentiles for $s = 5$ and $s = 15$.

The advantage of transforming a discrete distribution into a continuous distribution is that the distribution exists for the entire range of the seismic attribute. Thus, for instance, the algorithm can

Table 12: Expectation and percentiles of seismically thin-bed thickness based on the sum-of-probability attribute, specifically for s = 5 and s = 15. Figure 35 indicates that the higher the sum of probability, the thicker the gross of bittern salts is. This table is in accordance with this statement.

	s = 5	s = 15
Expectation	9.6	16.2
P10	7.2	14.0
P50	9.8	16.1
P90	11.9	18.3

assess the uncertainty for $0 < s < 35$ which encompasses the modeling interval. The outcomes are non-parametric functions that relate sum-of-probability attribute to the expectation and, percentiles of the seismically thin-layer thickness. Figure 36 depicts these functions along with the forward-modeled points in Figure 33.

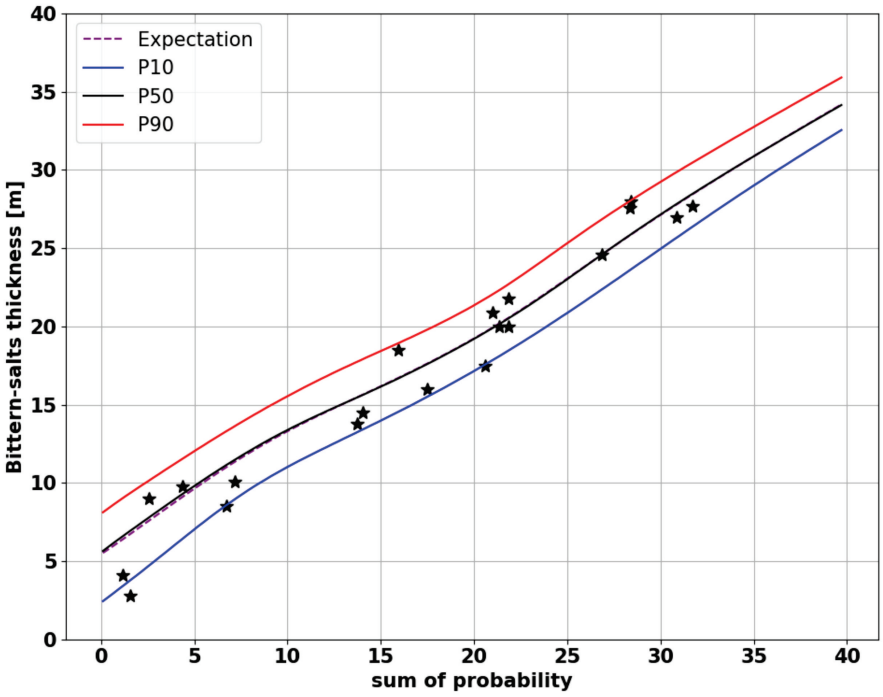

Figure 36: Expectation, P10, P50 and P90 of the seismic-based thin-bed thickness estimation. The point reflects the determinist estimation in Figure 33. While best fit provides one determinist correlation, the formulation of the joint distribution of rock properties and seismic attributes incorporates the uncertainty of the seismic estimation.

4.6 Synthetic seismic

Before appraising thin-bed thicknesses based on field seismic data, we test the methodology on synthetic seismic. The main idea in the generation of synthetic data is to provide a noise-free seismic

that emulates the deposition system of the study area. Therefore, this step enables us to distinguish which is intrinsic uncertainty due to seismic estimation of thin beds and which is noise.

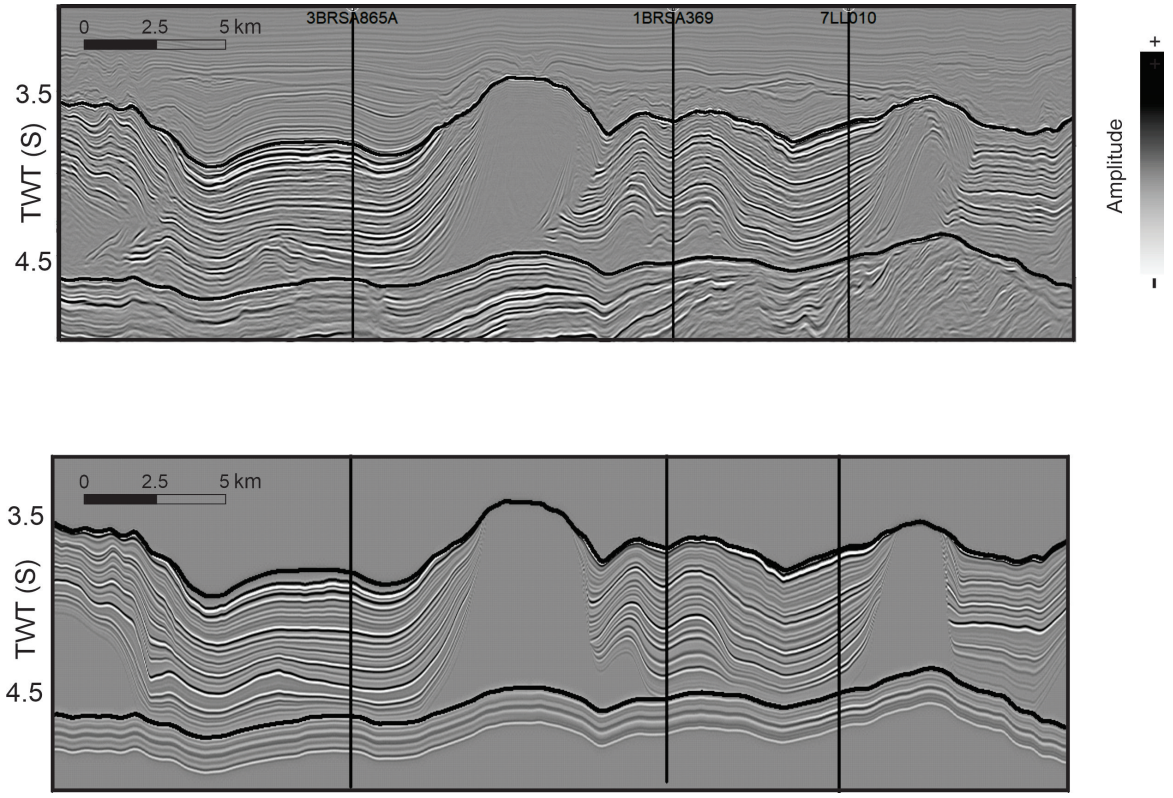

Figure 37: Field seismic (above) and synthetic seismic (below). The process uses a stratigraphic grid to generate the reflectivity model and, appropriately, to preserve the cyclicity of ancient salt record. High-reflective amplitude patterns correlate with vertical stacks of anhydrite, halite and bittern salts, whereas weak reflectivity indicates halite-rich sequences. Big domes are represented by reflection-free patterns.

As the thickness estimations are underpinned by facies probability, the process requires the derivation of acoustic impedance from seismic amplitude. To this end, seismic inversion is a functional technique to transform the seismic amplitude into rock properties of the subsurface by minimizing the difference between modeled and real seismic. This paper employs a technique that uses full-stack seismic data to derive acoustic impedance.

The inversion process starts with an initial model to fill the low-frequency bandwidth absent in seismic data. The low-frequency model is generated by well-log interpolation following the stratigraphic grid of the interpreted salt cycles (C1, C2, C3, and C4). The method solves an inversion problem based on the L-1 and L-2 norm, which minimizes the cost function. It assumes that the seismic reflectivity (parameter model) is sparse and spiky using the L-1 norm, and the residue (difference between modeled and real data) is normally distributed using the L-2 norm (DEBEYE; RIEL, 1990;

WANG; HUANG; WANG, 2017). The algorithm modifies the initial low-frequency model to minimize the difference between the synthetic and observed seismic data until it reaches a satisfactory error (LATIMER, 2011). The outcome is a volume of acoustic impedance that describes the seismic amplitude response of the subsurface (Figure 38).

Seismic inversion is known as a routinely time-consuming process in reservoir characterization. The process relies on sequential steps that include wavelet estimation, seismic welltie, construction of the low-frequency model, and quality control of results (KEMPER, 2010). The details of each step are out of the scope of this paper. Nevertheless, it is necessary to record that the same seismic pulse (wavelet), which furnishes the synthetic seismic, is applied to the inverse problem. We commit the inverse crime to ensure that inherent uncertainties of thin-bed thickness estimation are related solely to seismic resolution.

The workflow proceeds with the computation of bittern-salts probability. The Bayesian classification, as previously described, is a versatile tool whose application is not limited to well data. It is extendable to other types of data such as seismic cubes. In this case, the algorithm calculates the conditional probability of bittern salts given the acoustic impedance, sample by sample, throughout the seismic attribute. The result is a 3D bittern-salts probability (Figure 38).

We extract the seismic-driven probability along the borehole for each well location. That creates a well-log probability that contains the values of the seismic attribute. Figure 39 illustrates the log extraction in well 1BRSA369. On the basis of the forward modeling, the sum of probability correlates with layer thickness. Therefore, the subsequent steps exploit this attribute to estimate layer thickness.

First, the analysis of the bittern-salts probability log renders the occurrence and total thickness of this salt type. Additionally, to calculate the sum of probability, a depth interval must be defined. As the aim of the study is the assessment of thickness based on seismic attributes, seismic data is the appropriate instrument to bear the definition of the interval. Bittern salts embedded in a halite-rich formation produce a negative amplitude at the top of the bittern-salts sequence due to the relative decrease of the acoustic impedance, whereas the increase of the relative acoustic impedance produces a positive amplitude at the base (TEIXEIRA; LUPINACCI; MAUL, 2020). Thus, we define the interval

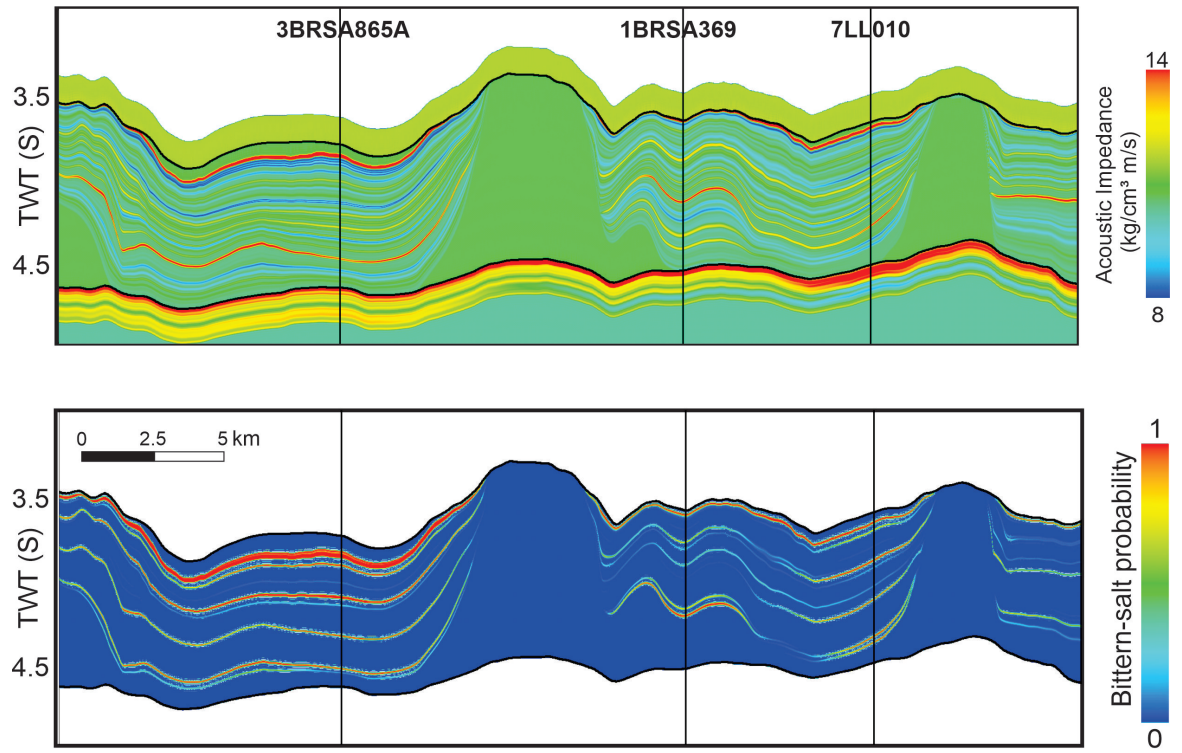

Figure 38: Impedance acoustic model (above) and bittern-salts probability (below) of the salt succession in the Santos Basin. We construct the acoustic impedance model in a stratigraphic grid by well-log interpolation. Bayesian classification provides bittern-salts probability by the application of the Bayes' theorem. Vertical variations of acoustic impedance indicate successions of different salt types. Salt domes correlate with the acoustic impedance of halite due to the high proportion of this mineral. Bittern-salts probability in these geological bodies is virtually null.

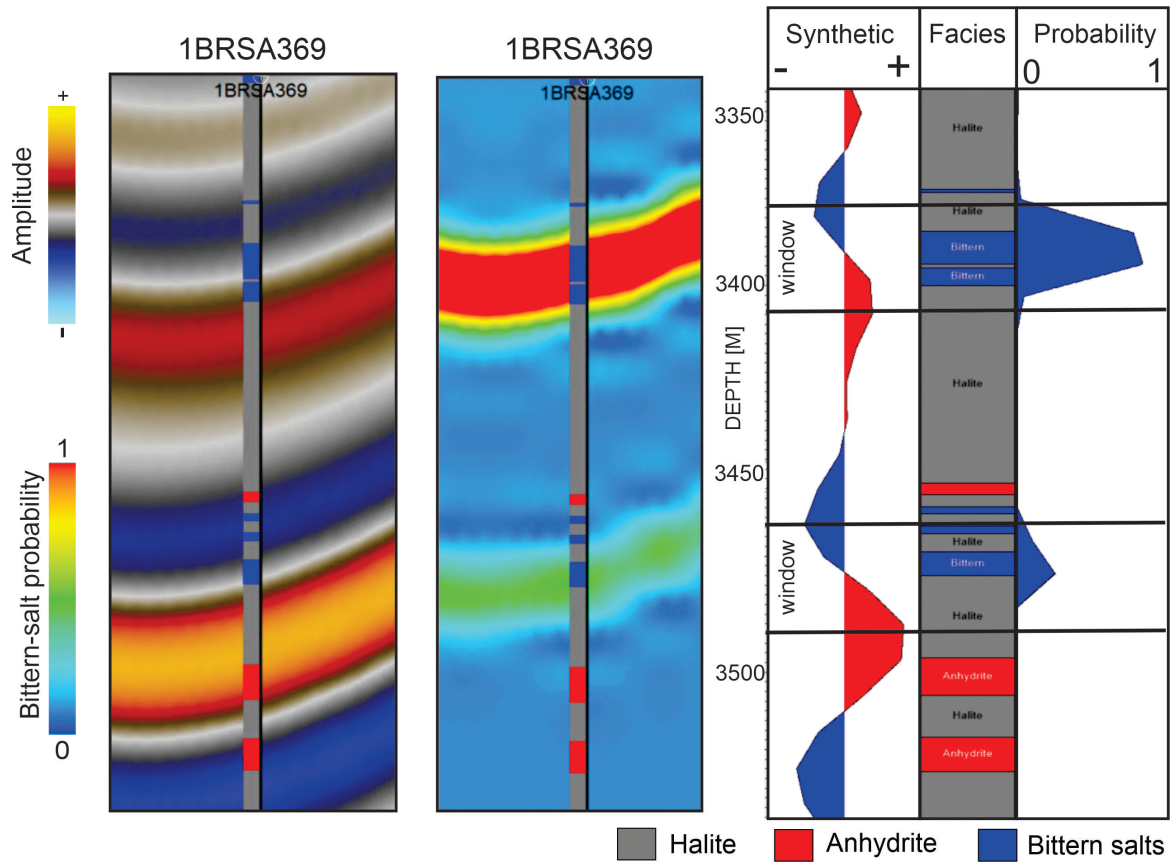

Figure 39: From left to right: seismic profile of seismic amplitude and bittern-salts probability zoomed in 1BRSA369; log extractions of seismic amplitude and bittern-salts probability along with the facies description in 1BRAS369. Seismic data supports the definition of the window on which the sum of probability and bittern-salts thickness are computed. The window is defined between the negative and positive amplitudes.

as a window between the negative and positive amplitudes that encapsulates the bittern-salts sequence (Figure 39).

Our dataset enables us to identify 24 intervals that display the large variability of bittern-salts layering patterns. For each interval, we calculate the sum of probability and the total thickness of the bittern-salts sequence. Posteriorly, the technique proceeds with the computation of the expectation, P10, P50, and P90 of the seismic-based thickness estimation (Table 13). Figure 40 depicts graphically the sum of probability and total thickness, as specified in Table 13. Additionally, it includes the uncertainty estimation of the forward modeled data quantified by Equations 4.3, 4.5 and 4.6. It is expected that 80% of points fall between P10 and P90 bounds. Most points lie between these bounds, thereby confirming that the noise-free synthetic experiment is in accordance with the model of uncertainty. The simulations effectively capture the variability of the salt layering patterns and provide the risk management of the evaluation of seismic-estimated thin-bed thicknesses even below seismic resolution.

Table 13: Sum of the probabilities and thicknesses of the bittern-salts layering. The thicknesses represent the total thicknesses of the bittern-salts layers enclosed in the window of investigation. Based on the joint distribution (Figure 34), the method computes the expectation, P10, P50 and P90 of thin-bed thickness estimation to assess the intrinsic seismic uncertainty below seismic resolution.

Seismic attribute	Well data	Seismic-based thickness estimation			
Sum of probability	Thickness	Expectation	P10	P50	P90
0.08	3.8	5.4	2.4	5.6	8.1
0.19	4.0	5.5	2.5	5.7	8.2
0.07	4.0	5.4	2.4	5.6	8.1
0.17	4.9	5.5	2.5	5.7	8.2
0.75	5.9	6.0	3.0	6.2	8.6
0.12	6.1	5.5	2.4	5.7	8.1
3.06	8.1	8.0	5.0	8.2	10.5
3.21	9.6	8.1	5.2	8.3	10.6
13.65	13.1	15.4	13.2	15.4	17.6
6.48	13.7	10.8	8.3	10.9	13.1
14.97	14.4	16.1	14	16.1	18.3
17.34	17.1	17.5	15.5	17.5	19.6
13.96	17.5	15.6	13.4	15.6	17.8
19.07	18.3	18.6	16.7	18.6	20.6
16.82	18.7	17.2	15.2	17.2	19.3
22.90	20.6	21.4	19.4	21.4	23.5
22.30	20.6	20.9	18.9	20.9	23.0
21.89	22.3	20.6	18.6	20.6	22.7
21.22	22.4	20.1	18.2	20.1	22.2
26.28	24.7	24.1	22.0	24.1	26.4
26.18	26.3	24.0	21.9	24	26.3
27.59	27.3	25.2	23.0	25.2	27.4

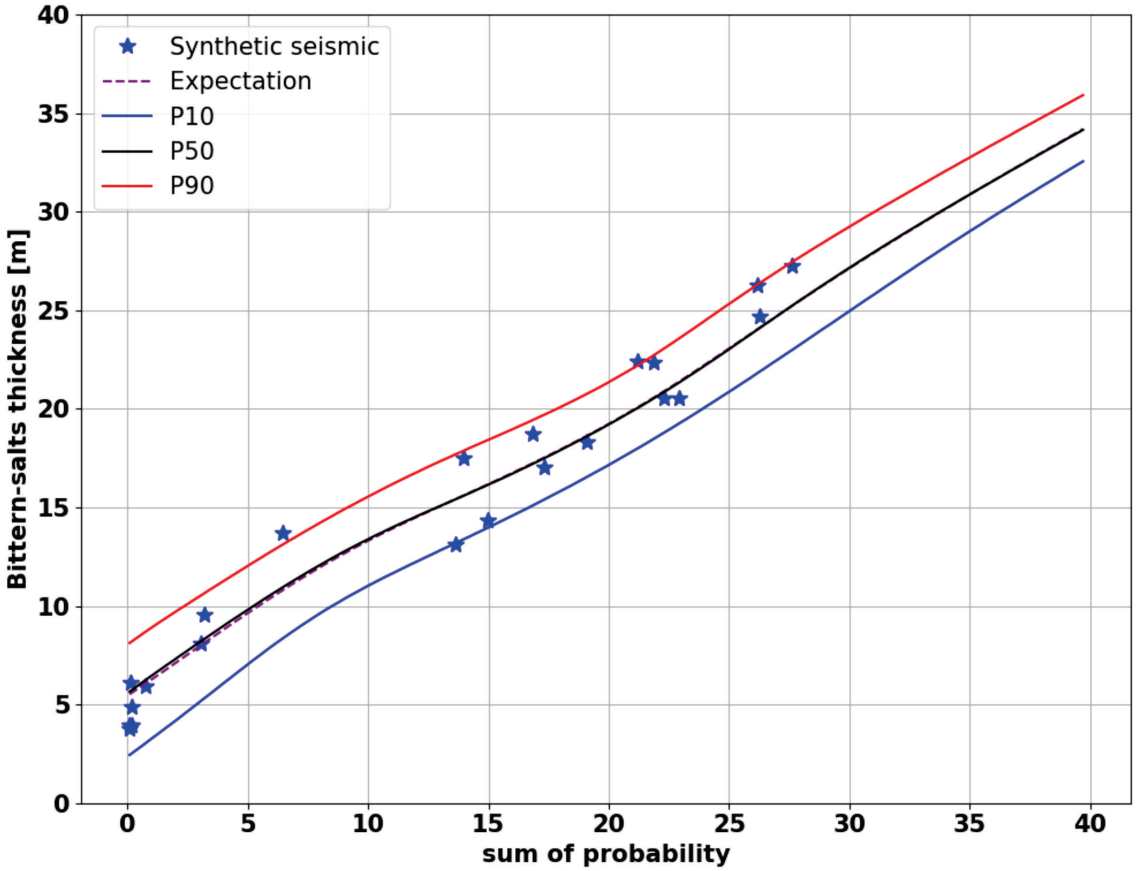

Figure 40: Expectation, P10, P50 and P90 of the seismic-based thin-bed thickness estimation. Each point stands for the total thicknesses of the bittern-salts layering enclosed in the window of investigation. They represent the bittern-salts layering patterns in well-log facies description. Expectation, P10, P50 and P90 curves are the same as in Figure 36, thereby being a product of the forward modeling. The seismic attribute was derived from the noise-free synthetic amplitude.

4.7 Application to field seismic data

The success of the application in synthetic data encouraged us to test the seismically thin-bed estimation in field data. The main drawback of dealing with field seismic is that incoherent and coherent noises reduce the quality of data. The process is quite challenging in salt sequences because the intense halokinesis poses structurally complex-shaped deformations to salt sequences, impairing the seismic imaging in and around these geological bodies (JONES; DAVISON, 2014; JARDIM et al., 2015; MAUL; SANTOS; SILVA, 2018a; ZAMBRINI et al., 2020). Despite the inherent issues, we expect that the estimation still holds.

The workflow of application to field seismic data adopts the similar methodology applied to synthetic data. The seismic inversion provides the acoustic impedance volume, which is later on

submitted to Bayesian classification to generate the bittern-salts probability. Figure 41 displays the outcomes.

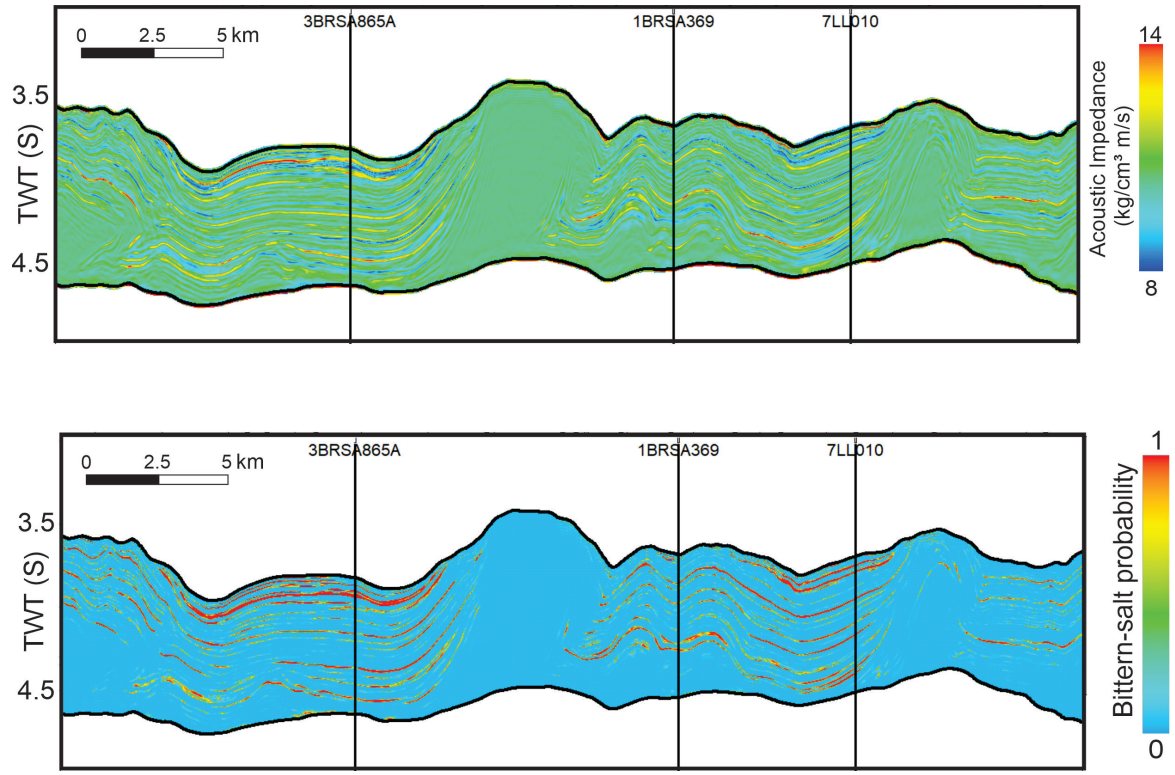

Figure 41: Impedance acoustic (above) and bittern-salts probability (below) of the salt succession in the Santos Basin derived from seismic inversion and Bayesian classification applied to field seismic data. Low acoustic impedance is related to high probability of bittern salts. Noise degenerates the event continuity when comparing to the noise-free synthetic data.

The halokinesis-associated deformations are noticeable throughout the seismic profile in the Sao Paulo Plateau in the Santos Basin (Figure 41). The seismic morphology of the events presents a significant variation. Towards NW from 7LL010, seismic events are highly reflective and near-parallel. 7LL010 drilled steeply high-reflective isoclinal events whereas moderately isoclinal anticlines prevail around 1BRSA369. Towards SE, 3BRSA865A drilled undeformed high-amplitude reflections. Towards the trend NW-SE, the intense salt flow created moderately-inclined-to-overfold anticlines.

The multilayered salt sequences, which form the vertical stack of low and high acoustic impedance, are the responses of the predominantly vertical succession of bittern salts, halite, and anhydrite. Boreholes 3BRSA865A, 1BRSA969, and 7LL010 confirm these depositional sequences of different salt types. Still, a careful inspection in Figure 41 discloses the effect of noise on bittern-salts probability. Despite the preservation of the salt morphology, noise deteriorates the event continuity. Noticeably, bittern-salts probability exhibits patchy discontinuities.

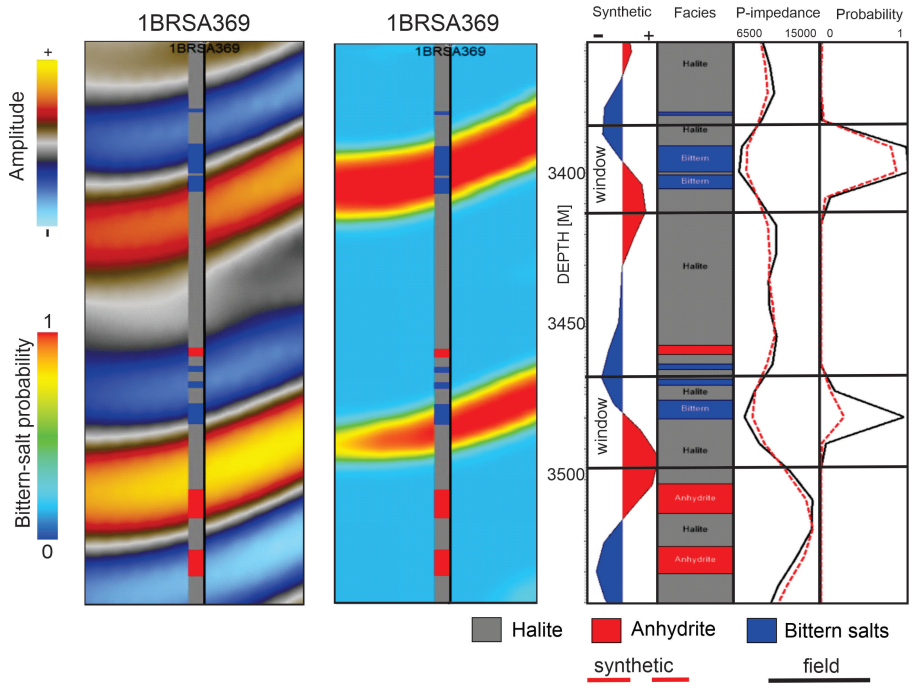

Figure 42: From left to right: seismic profile of seismic amplitude and bittern-salts probability zoomed in 1BRSA369; log extractions of seismic amplitude, acoustic impedance, and bittern-salts probability along with the facies description in well 1BRAS369. The amplitude log is the extraction of field seismic data in Figure 41. The dashed trace corresponds to the noise-free synthetic seismic data while the continuous black line stands for the field seismic data.

We extract the values of acoustic impedance and bittern-salts probability along the borehole to create a well log. Figure 42 displays the seismic profile around 1BRSA369 and the extracted logs. The dashed trace corresponds to the noise-free synthetic seismic data while the continuous black line stands for the field seismic data. The mismatch between the curve is the result of noise content. Therefore, we modify the algorithm to include the noise.

Quantitatively, we regard the relative error of the seismic-inverted and log-computed impedances as quantifiable variable of noise content (Err). The relative error is given as follows:

$$Err = \frac{AI_{seis} - AI_{log}}{AI_{log}}. \tag{4.7}$$

where AI_{log} is the well-log acoustic impedance and AI_{seis} is the seismic-inverted acoustic impedance.

Figure 43 outlines the distribution of the relative error for four wells. The relative error contains a representative sampling of the acoustic impedance misfit in the seismic inversion. Additionally, we include the simulation of the relative error modeled by a Normal distribution with

zero mean and 0.49 variance, N(0.00; 0.49).

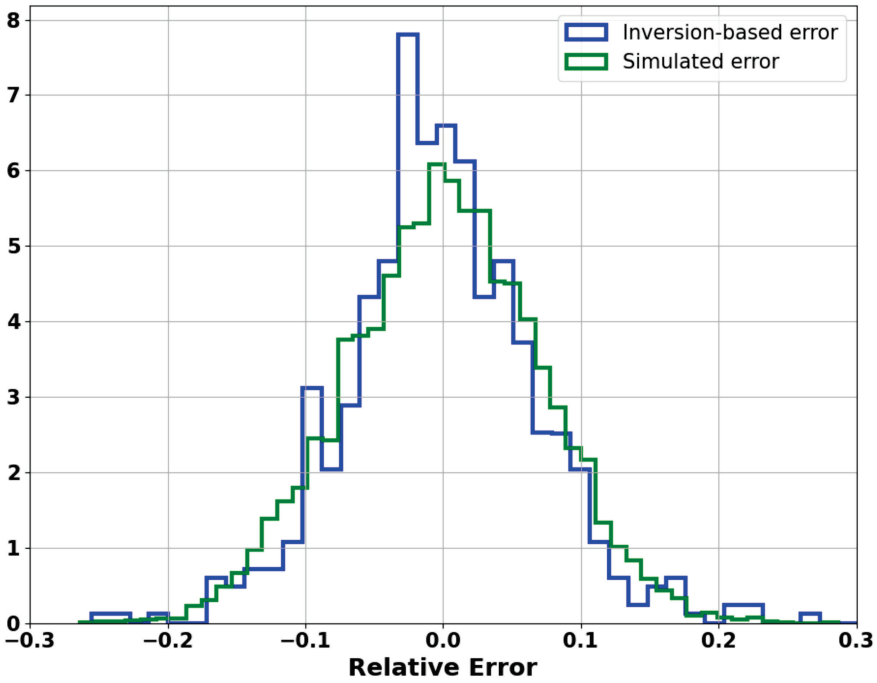

Figure 43: Relative error of the seismic-inverted and log-computed impedances (blue) and simulation of the relative error (green). We assume that the relative error is normally distributed with zero mean and 0.49 variance N(0.00; 0.49). The methodology brings the error simulation to bear the quantification of noise level in field data.

The inclusion of the noise content is a step that follows the simulation of acoustic impedance. First, we simulate the facies, and, then attribute to each of them appropriate values of elastic properties. At this stage, the algorithm randomly perturbs the acoustic impedance by introducing the simulated relative error to result in the noisy acoustic impedance. Later, Backus' average emulates the acoustic impedance at the seismic scale. The Bayesian classification is likewise applied to the noisy acoustic impedance to replicate the bittern-salts probability of the field seismic data. Figure 44 shows the outcomes of this approach.

To the application to the field data, we follow the similar approach performed to the synthetic data, however, at this point, we include the noise. The algorithm simulates 500 pseudowells by which we compute the sum of bittern-salts probability and the total thickness of the bittern salts with the presence of noise (Figure 44). The procedure continues with the estimation of a non-parametric joint distribution of these two variables by applying Gaussian KDE (similar to one presented in Figure 34). The joint distribution is illustrated in Figure 45 by the level curves, which encompasses the variability of the noisy field data.

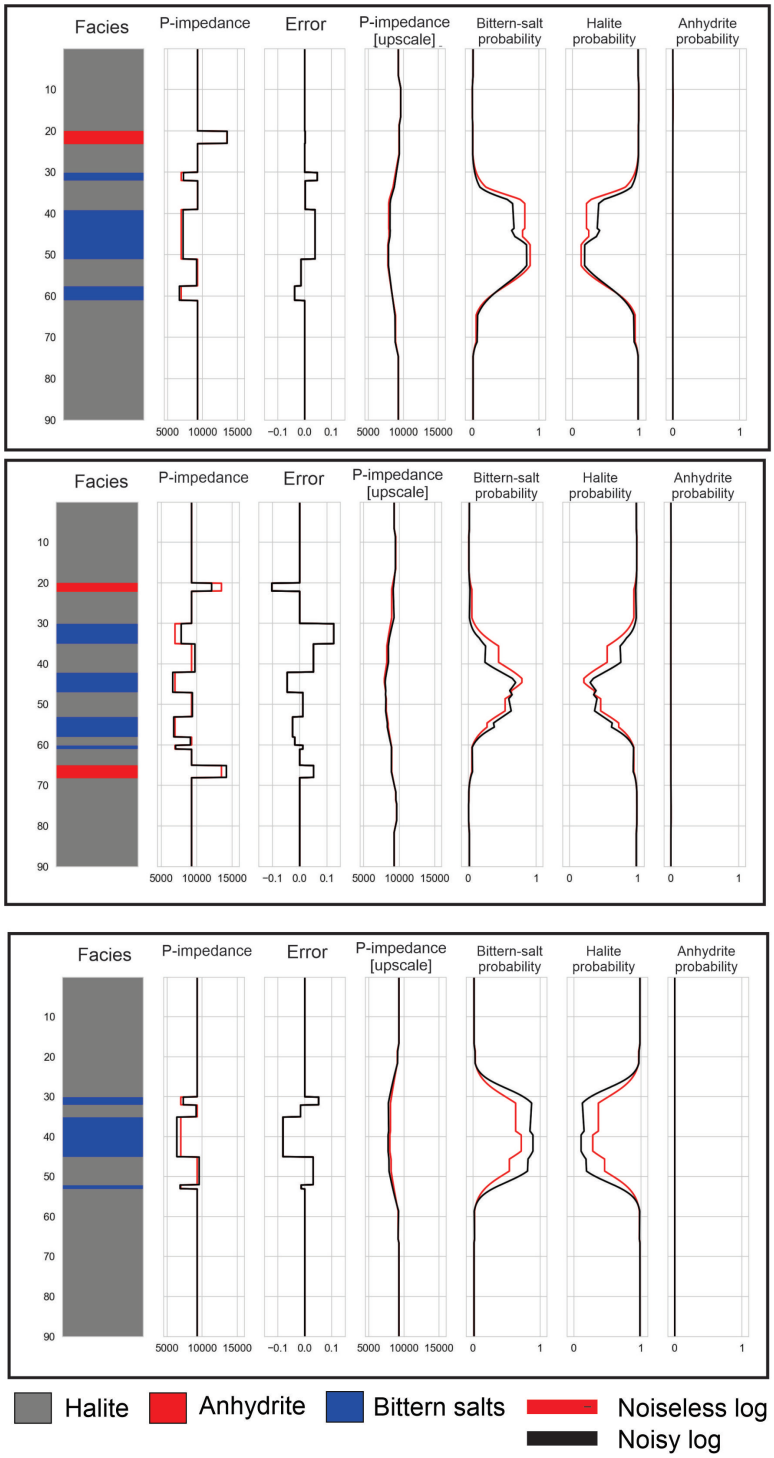

Figure 44: Three simulations out of 500 based on salt layering patterns. Facies simulations follow similar assumptions of Figure 32. The red line corresponds to the noise-free simulations and the black line relates the noise-included simulations. We assume that the error is normally distributed based on the relative error of the seismic-inverted and log-computed impedances. The error modifies the acoustic impedance, thereby creating noisy acoustic impedance to simulate the response of the seismic inversion of the field data. Bayesian classification is applied to noisy acoustic impedance to create the facies probability.

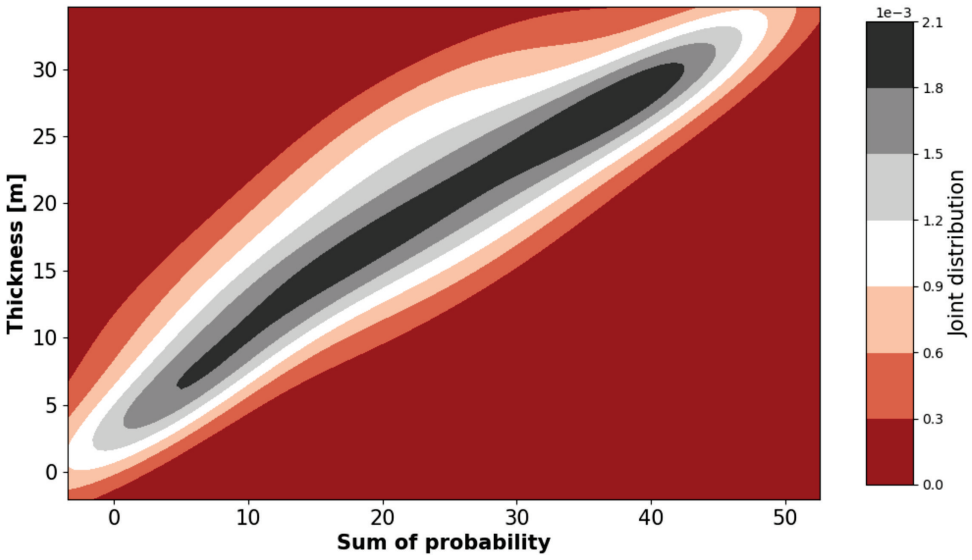

Figure 45: Contour maps of joint distribution (10^{-3}) of the the sum of probability and the total thickness of bittern-salts layering by the application of the Gaussian kernel density estimation. The noise-included simulation supports the Gaussian KDE to emulate the field seismic response.

Similar to the application to the field data, the algorithm simulates 500 pseudowells by which we compute the sum of bittern-salts probability and the total thickness of the bittern salts. The procedure continues with the estimation of a non-parametric joint distribution of these two variables by applying Gaussian KDE. The level curves of the joint distribution are illustrated in Figure 45.

Based on the field data, we calculate the sum of probability and the total thickness of the bittern-salts sequence for the 24 intervals with varying layering patterns of bittern-salts sequences. The positive and negative amplitudes define the window of investigation, reset to fit into the field seismic traces. Equations 4.3, 4.5, and 4.6 establish the assessment of the uncertainty. As result, Table 14 lists the sum of bittern-salts probability and the total thickness of bittern salt, along with the expectation, P10, P50, and P90 of the seismic estimation of thin-bed thickness. Figure 46 graphically illustrates expectation, P10, P50, and P90 curves with the points in Table 14.

Table 14: List of the sum of bittern-salts probability and the total thickness of the bittern-salts layering. The total thickness is enclosed in the window of investigation defined in the field data. Based on the joint distribution (Figure 45), the method computes the expectation, P10, P50, and P90 of thin-bed thickness estimation to assess the intrinsic seismic uncertainty below seismic resolution.

Seismic attribute	Well data	Seismic-based thickness estimation			
Sum of probability	Thickness	Expectation	P10	P50	P90
0.19	3.8	5.7	0.4	4.1	9.1
0.11	4	5.6	0.3	4	8.9
0.20	4.9	5.7	0.4	4.1	9.1
3.30	5.9	7.6	2.5	6.6	13
0.07	6.1	5.6	0.3	4.0	8.9
8.93	7.5	11.9	6.3	11.2	18.4
9.97	8.1	12.7	6.9	12.0	19.3
3.95	9.6	8.1	2.9	7.2	13.7
2.40	12.3	7.0	1.9	5.9	12
17.1	13.1	17.5	11.3	17	24.4
12.24	13.7	14.3	8.4	13.7	21.1
18.27	14.8	18.1	11.9	17.7	25.1
13.07	16.3	14.9	9.0	14.3	21.7
19.27	17.1	18.7	12.4	18.2	25.7
18.03	17.2	18.0	11.8	17.5	25
22.58	17.4	20.4	14.1	20.1	27.3
22.7	17.5	20.5	14.2	20.1	27.4
30.25	18.3	24.2	18.4	24	30.4
21.5	18.8	19.9	13.5	19.5	26.8
25.13	22.4	21.7	15.4	21.4	28.5
17.71	23.1	17.8	11.6	17.3	24.8
20.63	24.7	19.4	13.1	19	26.4
26.97	26.3	22.6	16.5	22.4	29.2
34.34	28.9	26.1	21.0	26.0	31.5

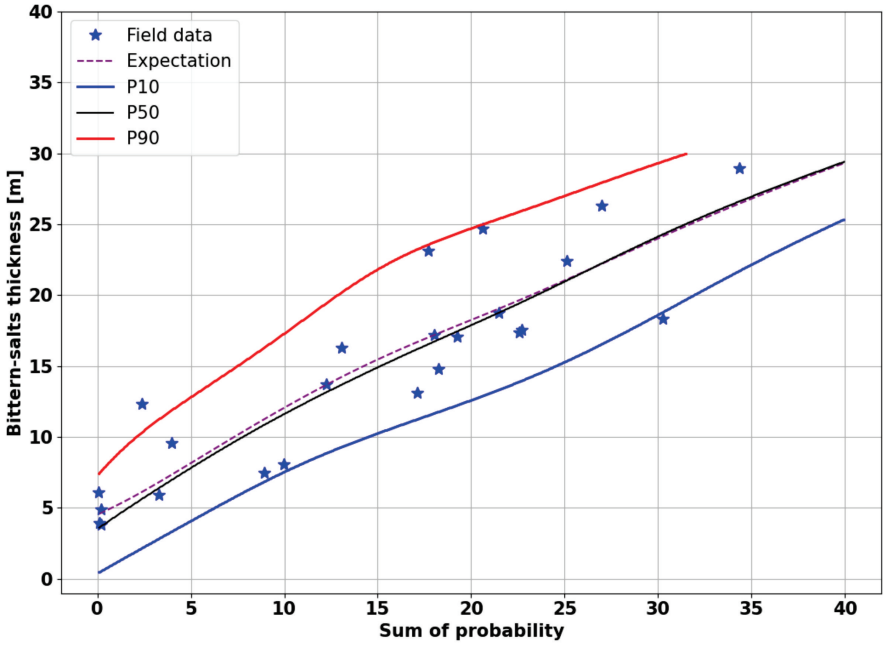

Figure 46: Expectation, P10, P50, and P90 of the seismic-based thin-bed thickness estimation. Each point stands for the total thickness of the bittern-salts layering enclosed in the window of investigation in the field seismic data. Expectation, P10, P50, and P90 curves are the product of the forward modeling of the noise-included simulations.

4.7.1 Blind-test

The blind test is a practical method to inspect the predictability of the seismic data. It consists of removing one well from the dataset, rerun the workflow and then compare the results with the actual data of that well (TRIPPETTA et al., 2021). The idea is to verify the forecast at a single well location. In the face of few boreholes, an alternative is to withdraw one well from the workflow and start over the entire procedure. Chiefly, the well is not included in the seismic inversion. Table 15 presents the uncertainty estimation of seismic-based thickness at borehole LL10, which is chosen as a blind test. Except for the 12.3-m thick bittern-salts layering, the estimations lie between P10 and P90 bounds.

4.8 Discussion

Seismic rock characterization relies on indirect measurements of rock properties that, to obtain optimal outcomes, combine data from different sources. Indirect evaluations and combinations of different data sources raise several uncertainties. Below seismic resolution, the geological bed

Table 15: Blind-test results with the exclusion of LL10. Table lists of the sum of bittern-salts probability and the total thickness of the bittern-salts layering, as well as, the expectation, P10, P50, and P90 of thickness estimation. The total thickness is enclosed in the window of investigation defined in the field data. Except for the 12.3-m-thick bittern-salts layering, the estimations lie between P10 and P90 bounds.

Seismic attribute	Well data	Seismic-based thickness estimation			
Sum of probability	Thickness	Expectation	P10	P50	P90
0.3	4.0	5.7	0.4	4.2	9.2
2.2	12.3	6.9	1.7	5.8	11.8
18.2	16.3	18.1	11.8	17.6	25.1
18.1	17.1	18.0	11.8	17.6	25
12.5	17.2	14.5	8.6	13.9	21.3
24.6	17.5	21.4	15.1	21.1	28.2
21.4	18.8	19.8	13.5	19.4	26.8
20.1	22.4	19.1	12.8	18.7	26.1
21.2	24.7	19.7	13.4	19.4	26.7

interpretation based on seismic amplitude delivers overestimated thin thickness appraisals (RAYLEIGH, 1945; WIDESS, 1973). Under this circumstance, the estimation of thin-bed thickness becomes complex and risky. Bearing that in mind, this paper specifically delves into the uncertainty estimation of seismically thin-bed thicknesses.

4.8.1 Deterministic appraisal vs advantages of simulations

Wedge models serve as a prototype to assess the limits of seismic resolution (BROWN, 2011). This two-layer model consists of wedge-shaped facies embedded in another type of thick facies. The thickness below the misfit between the seismic signal and the layer interface corresponds to the seismic resolution. In our dataset, the seismic resolution, regarding this procedure, is 25 m.

As expected, arrangements of different layering patterns significantly modify the seismic signal. Even in the case wherein the total thickness is fixed, distinct layering patterns alter the seismic amplitude. Figure 47 displays the noiseless seismic responses of 15-m-thick bittern salts. The total thickness is identical, seemingly are the peak and trough of the seismic signal; however, the amplitudes and acoustic impedances are unlike. The interpretation of peak and trough as the bed thickness gives rise to the overestimation of the layer. That is strong evidence of the intrinsic risk of seismic rock characterization.

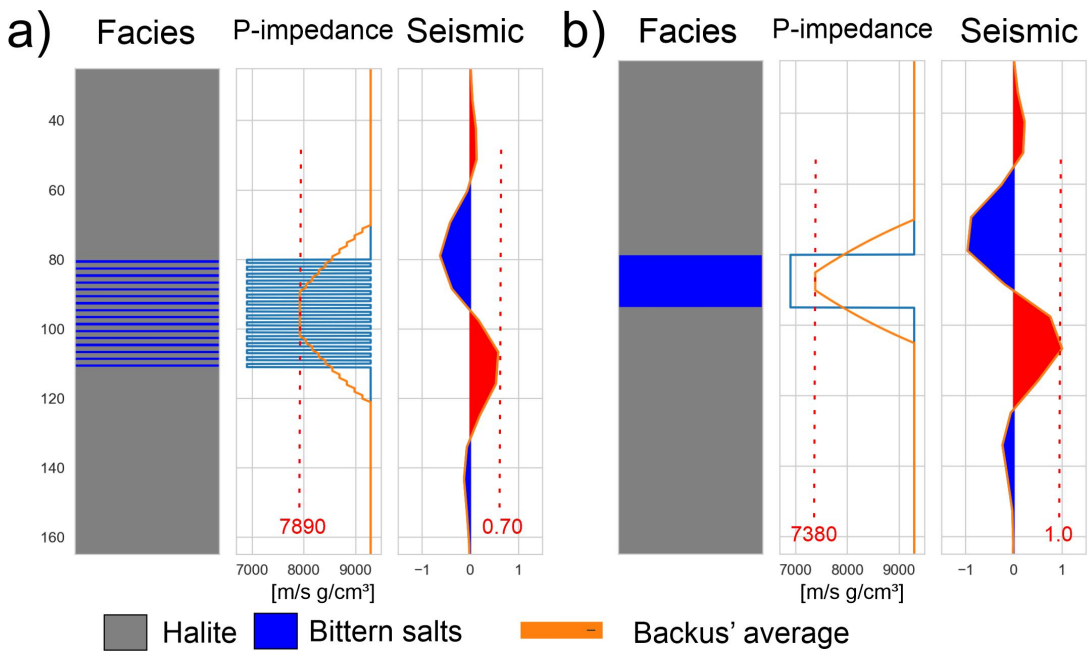

Figure 47: Seismic amplitude and acoustic impedance response of 15-m-thick bittern salts (blue in the facies track) embedded in a thick halite layer (grey in the facies track). The interpretation of the peak and trough as the layer thickness leads to the overestimation of the bed measurement (approximately 25 m). Despite the same thickness, the layering patterns alter the seismic amplitude and acoustic impedance, which, in turn, can be used to quantitatively evaluate the thickness.

All models are simplifications of reality. However, the wedge model has two serious limitations. First, it neglects layering patterns essentially because the model is blocky. For this model, only the facies configuration of Figure 47(a) is replicated. Second, the encasing facies is usually identical. It limits the model to a two-facies model. Facies description of the salt formation of the Santos Basin reports vast layering patterns and geological successions of anhydrite, halite, and bittern salts. Therefore, wedge models are unsuitable for these depositional settings.

Simulation is a powerful tool that overcomes two wedge-related oversimplifications of the subsurface. It permits the inclusion of layering configurations and several facies. The Monte Carlo simulation is a commonly stochastic technique that can be performed to generate geological scenarios (DVORKIN; GUTIERREZ; GRANA, 2016). However, the geological scenarios are site-specific. The bittern-salts sequences of the Santos Basin are embedded in thick halite layers. Also, thin anhydrite may occur at the top and the base of the sequence. The imposition of these constraints on simulation replicates the facies behavior and the correlation between seismic attribute and rock property (Figure 46). If the algorithm disregards the inclusion of the thin anhydrite, most of the points will not fall between P10 and P90 bounds. Therefore, the two-facies wedge model is a deficient description of salt

formations.

The computation of expectation, P10, P50, and P90 curves of thin-bed thickness is one procedure by which the uncertainty can be analyzed. These curves were derived from the non-parametric joint distribution between the seismic attribute and rock properties. As a statistically flexible tool, the algorithm can be adaptable to other predictions. For instance, we can tailor the methodology to sand/shale successions or computation of net-to-gross (NTG) by emulating the elastic response of these facies. Since the gross thickness of the evaporites is fixed in every simulation, the NTG is proportional to the facies-specific total thickness and, therefore, we expect a similar response. The readers find in Mukerji and Mavko (2008) an example for the uncertainty assessment of NTG in sand/shale sequences. The authors compute P10, P50, and P90 curves based on the simulation of seismic amplitude response.

4.8.2 The signal and the noise

The methodology sets out with the evaluation of uncertainty under different scenarios of geological sequence patterns. The forward modeling demonstrates that the facies-specific total thickness results in different values of the seismic attribute. For instance, 10-m-thick bittern salts admit approximately values from 3 to 7 of the sum of bittern-salts probability. This reflects the inherent uncertainty of seismic estimation under seismic resolution, which is quantitatively captured by the methodology. The synthetic data corroborates the forwarding modeling. However, the application to the field data reveals that the uncertainty is underestimated. The negligence of the noise in the forward modeling is the chief reason to explain the phenomena. Therefore, noise needs to be included to validate the prediction.

A collection of methodology to estimate the seismic-to-noise ratio is based on the ratio of the power spectrum of the signal and the noise (RUTTEN; VALETON; GRUNSVEN, 1972; WHITE, 1984). To objectively distinguish between signal and noise, the algorithms rely on correlations among adjacent traces, since they assume that geological layers are locally continuous (DASH; OBAIDULLAH, 1970; ZHAO; MAO; CHEN, 2019). These heuristic computations of seismic noise disregard well data in

their implementation and are quantitatively unsuitable for simulation.

The best practice of the inclusion of noise is still undefined in the literature. The books of Simm and Bacon (2014) and Dvorkin, Gutierrez and Grana (2016) hold valuable discussions about the estimation of uncertainty based on the simulation of pseudowells. The authors focus on the evaluation of uncertainty due to intrinsic seismic response, that is to say, on how the arrangements of the stacking patterns of geological sequences and the elastic properties therein affect the seismic signal. However, these books overlook the addition of noise in the simulation and, consequently, they do not evaluate the negative effect of noise content in seismic signatures.

To gauge the noise content in the simulation, we need to stipulate what is noise. Silver (2015) states that "the signal is the truth. The noise is what distracts us from the truth". The first step to model the noise is to establish the premises of what is the truth. This task is controversial in subsurface applications because all measurements are indirect. Notwithstanding the disagreements with which data is true, we define the nearest true response as well log. The choice is based on the fact that seismic signal is about the response of elastic properties and the well logs provide more reliable measurements thereof.

We regard the noise as the error between the seismic-inverted and well-log acoustic impedance at the seismic scale. This assumption permits a quantifiable estimation whose variables are normally distributed (Figure 43). Consequently, we include the data-specific normal curve to simulate the noise. As depicted in Figure 46, the inclusion of noise properly assesses the uncertainty of the field data. Most of the variables lie between P10 and P90 bounds.

Remarkably, the comparison of the assessment of uncertainty in synthetic and field data highlights the influence of noise on the quantitative seismic interpretation. While in a noiseless simulation a 10-m-thick bittern salts produce a range from 3 to 9 in the seismic attribute, in the noisy simulation they result in a range from 2 to 15. The opposite also confirms the negative influence of noise. For instance, the sum of probability about 10 yields approximately P10 = 11 m and P90 = 16 m in noiseless simulation. The inclusion of noise yields P10 = 7 m and P90 = 17 m.

4.8.3 The paradox of the null facies probability

Figures 36 and 46 graphically illustrate the uncertainty assessment of the total thickness of a bittern-salts sequence. They also induce us to a somewhat inconsistent understating. The extrapolation of P10 and P90 curves to the null sum of probability yields a non-null prediction of the total thickness of the bittern-salts sequence. As the probability is always positive, it signifies that even null facies probability leads to an estimation of non-null thickness. To exemplify, if a borehole drills a big halite dome with no occurrence of bittern salts, the sum of bittern-salts probability is expectedly null. Nevertheless, according to the simulations, this scenario can result in a non-null expectation, P10, P50, and P90 of the total thickness of bittern-salts sequences. This issue arises in synthetic and field data.

At first glance, the results contradict what is expected. However, the explanation lies in the construction of pseudowells. The rock sequence mirrors the evaporite formation of the Santos Basin. Above and below the bittern-salts sequence, there may be a occurrence of thin anhydrite layers. Anhydrite presents high acoustic impedance, while bittern salts exhibit low acoustic impedance. There are simulations of layering patterns that render a thin anhydrite layer right above or below a thin bittern-salts layer. At the seismic scale, the Backus' average reduces these contrasts to a near-constant acoustic impedance which corresponds to halite layers. Consequently, Bayesian classification gives rise to a high probability of halite and, in some scenarios, to a null probability of bittern salts. If the algorithm disregards the anhydrite, the limit of null probability will result in the null total thickness of bittern salts by the seismic estimation. However, the absence of the anhydrite layers is inconsistent with the geological settings of the salt formation of the Santos Basin.

4.8.4 Comparisons to other methodologies and advantages

Zeng and Marfurt (2015) discuss the recent development in the analysis of seismically thin beds chiefly based on signal processing of seismic amplitude. Advances in thin-bed attribute identifiers include spectral decomposition, wavelet transform, spectral inversion, and spectral balancing with bandwidth extension (PURYEAR; CASTAGNA, 2008; LEPPARD; ECKERSLEY; PURVES, 2010; MATOS et al., 2011). Other techniques bear on the enhancement of seismic resolution by the

application of inverse q-filter to recover high frequencies (WANG, 2008; LUPINACCI et al., 2017). Despite the success in increasing the seismic resolution, these works overlook the assessment of the inherent uncertainties.

Geostatistical inversion assesses the uncertainty of the seismic-driven rock properties by generating multiple realizations of elastic properties which are consistent with seismic amplitude and well data (DOYEN, 2007). The introduction of geostatistical techniques in the inversion process promotes the appraisal of high-resolution elastic properties that are compatible with the fine-scale of the 3D grid. Additionally, the inclusion of statistical rock-physics constraints delivers facies and the uncertainties thereof in fine scale, thereby mapping possible layering patterns (GONZÁLEZ; MUKERJI; MAVKO, 2008; GRANA, 2018; TALARICO et al., 2020). The effective performance of the geostatistical inversion requires the construction of structurally stratigraphic grids. In depositional settings subjected to intensive deformations, such as salt formations, the creation of a detailed stratigraphic grid is a struggling task, and, in some cases, unfeasible. Therefore, the geostatistical inversion may be an unrealistic procedure in these areas.

As a routine task for reservoir characterization, the seismic inversion can be affordably extended to the seals. Although the seismic-inverted elastic properties depend on the initial model, the construction thereof is simpler compared to the model required for geostatistical inversion (see details in Teixeira and Lupinacci (2019)). Therefore, the efforts are concentrated in the forwarding modeling to convert the sum of probability to thin-bed thickness.

4.8.5 Interpretation of facies probability

The interpretation of probability is still an open discussion in the academy and the debate has involved powerful intellects of the 20th century to set up the grounds for useful applications (SALSBURG, 2002). One interpretation is frequentist which relates the probability to the ratio of favorable events to the possible aleatory events (VENN, 1866; FISHER, 1951). Although this view provides a meaningful representation of the value of probability, it is an unfeasible description of facies probability.

The subjective probability proposes that probability is a degree of rational belief based on solid evidence. It entails that the calculation of probability is a mathematical solution to order the magnitude of the uncertainty (KEYNES, 1921). The Bayesian classification applies the Bayes' theorem to the seismic-inverted elastic properties to assess the order of magnitude of uncertainty of facies interpretation under this information. Therefore, the facies probability can be interpreted as a rationally measurable belief of facies occurrences in accordance with their respective response of elastic properties.

Within the window of investigation, the rise of the bittern-salts probability indicates an increase in the total thickness of these facies. One can use a similar evaluation to estimate facies proportion when performing the seismic reservoir characterization. Facies proportion is a ratio between the net facies and the gross rock sequence. Our simulation fixes the gross rock sequence and lets thickness vary; therefore, the variation of facies proportion is linearly dependent on thickness. It leads to the conclusion that the facies proportion can be estimated from facies probability properly. For instance, working on a clastic reservoir dataset, Teixeira et al. (2017a) suggest that formations at boreholes with higher sandstone proportions gauge a higher average of facies probability at the same window of computation. However, the authors overlook the forwarding modeling and miss the uncertainty assessments due to the limitation of the dataset restrained solely to three wells. Furthermore, we believe that the core of Bayesian classification intertwines the interpretation of facies proportion and facies probability because it permits the modification of the a priori probability based on consistently previous knowledge of local geology. González et al. (2016) apply this concept to create region-weighted probabilities and incorporate prior geological knowledge which constrains the locations of more-probable facies. Local inclusion of prior more-favorable facies subjectively implies the interpretation of more occurrences of the facies therein. For instance, if we assign region 1 to have more probable facies A than region 2, we geologically interpret that region 1 has more thickness or proportion of the facies A. Here, we go a step further to quantitatively prove the correspondence of the a posteriori facies probability and rock property.

4.9 Conclusion

This paper proposes a method to estimate thin-bed bittern salts in salt formations and the uncertainties inherent to this assessment. The topic of interest ensues from the fact this salt type is a key input to geomechanical models which calculate the wellbore creep behavior during the life of the well. The development of fields that underlie salt seals, such as the Brazilian presalt reservoirs, depends on the predictability of bittern salts to reduce the risks of incidents that largely impact the project devaluation.

The scarcity of wells hampers the uncertainty estimation based on seismic-driven rock property. We resort to the generation of the pseudowells to circumvent this issue. As a site-specific simulation, the pseudowells mirror a typical cyclicity of salt sequence in the Santos Basin. In our case, they emulate a bittern-salts sequence embedded in a thick halite layer. The simulations include random anhydrite at the top and the base of the sequence which is fundamental to the forward modeling. It indicates that the two-facies model improperly reproduces the salt successions. The generation of pseudowell proved to be a crucial step to efficiently unveil the variability of the thin-bed thickness assessment.

In this paper, we identify the interpretation of facies probability as a seismic attribute to estimate rock properties, specifically, the seismically thin-bed thickness of salt formation. To prove this statement, we perform forwarding modeling and multiple simulations of subsurface rock sequences and elastic properties, which mirror the depositional settings in the Santos Basin. The observation indicates a relation between the sum of probability and the total thickness. The higher the sum of probability, the thicker facies successions are.

The construction of the non-parametric joint probability density function (joint PDF) unlocked the uncertainty measurements of the estimation. By the joint PDF, we successfully estimate the P10, P50, and P90 and the expectation of the total thickness of thin-bed bittern salts based on the seismic-driven bittern-salts probability. Furthermore, this paper provides a quantitatively adaptable method to include the noise content of the field data. We argue that the noise estimation is assessed by the difference of log-measured and the seismic-inverted acoustic impedance. By premise, therefore,

it is a data-specific calibration. When we include the noise in the forward modeling, the simulations capture the variability of the field data.

The Bayesian seismic classification reveals the intrinsic uncertainty of the three-dimension elastic-property-based facies classification. The procedure renders the facies probability. The subjective interpretation of probability provides a comprehensive diagnosis for this volume. It establishes that probability is a measurement to order the magnitude of the uncertainty. In addition to this view, the forward modeling in this paper presents an alternative interpretation which indicates that the facies probability can be interpreted as a quantitative seismic attribute to derive the thin-bed thickness. The proposed methodology can be adapted for reservoir thin-bed prediction since it enables the simulation of carbonates and siliciclastic rocks.

5 Epilogue

I believe that henceforth an epilogue is more appropriate as an overall conclusion since each article has its own.

The giant pre-salt reservoir shifted the attention to the inner events of the intrasalt formation in the Santos Basin, Brazilian offshore. At the beginning of the 2010s, it was well established that the identification of the top and the base of salt bodies in this basin was insufficient to the properly technological developments of the newly discovered, ultra deep-water pre-salt reservoirs. Each segment in the E&P chains surveyed the benefits of enhancing the recognition of the evaporite to succeed in the full applicability of the related expertises. Nevertheless, it turned out to be that, despite the necessity to describe the rock properties in evaporite formations, the solution was not solidified and lacked a suitable formulation.

This thesis opens a door to reveal the salt types in the ancient evaporite deposits, the seal rock of most giant reservoirs. The characterization of these deposits with unrelated analogous in the present days relies extensively on the well and seismic data. Nevertheless, until the findings of this thesis, the interpretation of these basinwide sediments is underpinned by seismic amplitude. This amplitude-based analysis is the first approach to characterization; however, it does not exploit the full ability of the seismic data. In this sense, this thesis founds a milestone in the proposal and in the broad employment of the seismic-inverted data to explore the utter ability of seismic data to reveal the salt types and rock properties behind the wiggles.

The investigation started with the analysis of the elastic-property responses in the well data in a methodology often referred to as rock-physics analysis. Rock-physics analysis is the starting point and bedrock that underpin the quantitative seismic interpretation. It connects the elastic properties and the rock properties. In *Elastic properties estimation*, chapter 2, I extend the application of the empirical equations as a property predictor to the depositional environment of the evaporites. This fact was not properly documented in the literature. In *Quantitative seismic-stratigraphic interpretation*, chapter 3, rock-physics analysis takes forms in the estimation of facies-dependent distribution. This procedure primarily indicates that the acoustic impedance succeeds in distinguishing the salt types. I

insist that rock-physics is crucial before any examination of seismic-inverted elastic properties.

This manuscript also describes an experiment that proves that the acoustic impedance drastically reduces the uncertainties in the seismic interpretation of salt types in comparison to the standard use of seismic amplitude. I performed this experiment under noise-controlled data to avoid the interference of spurious contamination. This key step played such a critical role in the calibration of the seismic responses in the development of the second article (chapter 3) that this noiseless experiment was employed to calibrate the results of the third one (chapter 4). I argue that the test in synthetic data in lead-edging researches is a prime step to obtain reliable geological interpretation.

In the first article (chapter 2), the objective is very clear and aims at a problem of elastic properties. Rock physics indicated the high correlation of the elastic properties in these rocks and I took the advantage of this reality to explore the prediction of the seismic-inverted data. The experiment was supported by a blind test to study the seismic prediction of an undrilled area, where E&P chains place valuable prior information. Nevertheless, at this point, the research lacked, in my opinion, an in-depth evaluation of the reason for the outcomes. As I observed, rock physics linked the elastic properties of these deposits and the facies-dependent elastic-property behaviors. When the noiseless experiment demonstrated that seismic data can reproduce the expectation of rock-physics analysis, it broadened the application of seismic-inverted outcomes. Therefore, the first article brings the estimation of the elastic properties, the second one amplifies the application to Bayesian classification. The impact is that I was able to strengthen the use of seismic data to an unprecedented level by focusing on evaporite formations, providing an important leap from qualitative to a quantitative interpretation. Articles and books miss this formalism in the workflow of quantitative seismic interpretation in salt sequences. Among the developments described in Preface, I argue that quantitative characterization is the major contribution of this thesis.

The combination of the rock-physics analysis and acoustic impedance volume in the Bayesian framework reveals the salt types behind the wiggles and provides an uncertainty analysis of this process. In performing these steps, I engaged in the powerful development of the consequences, reinterpreting the salt cycles in the seismic data. At this moment, however, the seismic horizon represented the onset of a new cycle because the anhydrite was properly reconsigned in the facies volume. This interpretation

is not fully achieved in seismic amplitude which relates solely to the acoustic character of the formation. The connection between acoustic behavior and salt types is necessary. One may argue that seismic welltie can offer a way to perform this task without the seismic-inverted acoustic impedance. Yes, but partially, mainly because the interpretation is robust, in this case, around the well. If one needs to extend the interpretation in basinwide undrilled areas, the seismic amplitude is highly ambiguous and the well control is absent, leading to misinterpretations. The confidence in the interpretation of seismic amplitude due to its ambiguity is restricted around the wells. I raised this confidence.

I engaged in the further expansion of the subsequent use of quantitative outcome. In the possession of the seismic cyclostratigraphy performed in this thesis, I decided to analyze the distribution of the salt types spatially. To this end, I calculated the facies-dependent proportion maps for each cycle, an impossibility with the use of seismic amplitude solely. The maps revealed what I have observed in the well data: an increase in bittern-salts proportion in the upper cycle. This led me to state an assumption that the evaporite formation in the Santos Basin was undergoing high levels of aridity in C4. C4 is poorly determined in the well dataset of my study area. Nevertheless, it created the possibility to analogously explore the quantification performed in previous works. Remarkably the comparison of the seismic-driven quantification of my thesis and well-based quantification in literature converged, proving my intial assumption. This quantifiable convergence testifies to the robustness of the method not only by this thesis and my dataset but also by previous ones.

The third and final act was ignited by the necessity to identify the thin-bed bittern-salts thickness, an open debate to the simulation of geomechanical models. During the investigation of methodologies that could potentially support this task, I came across something unexpected. The assessment of the uncertainty in the estimation of thin-layer rocks is vaguely described in literature, despite the increasing concern about this measurement. The application in seismic data of the pseudowells to devise experiments that unveil the variability is very scarse. Therefore, to accomplish this job, I needed to examine the mathematical foundations of Statistics that can disclose the uncertainty in the seismic-based estimations.

The most time spent in *Probabilistic estimation of seismically thin-layer thicknesses*, chapter 4, was due to the implementation of the code in Python. This point requires a caveat about the time

of each article. Before initiating this Ph.D. program, I had previous experience in estimation of the elastic properties of siliciclastic and carbonate rocks. The development of *Elastic properties estimation* was the swiftest of the three. Nevertheless, it took time to learn about the academic discipline of writing a paper about the clarification of scientific evidence. In *Quantitative seismic-stratigraphic interpretation*, I needed to dive into the enigmatic evaporites with which I was not familiar and to explore the contribution of quantitative seismic interpretation in these formations. The third one challenged me to code a new algorithm in Python.

I coded the probabilist estimation of thin-bed thickness from the beginning essentially because there is no off-the-shelf implementation. This allowed me to adjust the code when the model could not explain the reality. I believe that I could not derive the outcome if this was not for this evolution.

The simulation of pseudowells was an appropriate choice because it unleashed the use of regularly applicable two-facies models or wedge models. It is not suitable for the highly heterogeneous rocks, which present a wide value of the elastic properties. In simulations I can include many facies as the depositional sequence requires. The turning point during the codification was the implementation of the Kernel Density Function (KDE). It saved time and permited the computation in a continuous space. The function related, of course, the sum of probability and thickness, two quantifiable variables. I am unaware of the employment of KDE to this proposal. Moreover, it came to my mind that it can be applied to any quantifiable variables. Despite being out of the scope of this thesis, I put down an experiment to fully understand the large execution of this procedure. I tested the use of the KDE in uncertainty estimation of effective porosity from acoustic impedance. It works! It is a powerful statistical tool. This thesis, therefore, provides comprehension for the uncertainty analysis of thin-bed thickness or any quantifiable well-to-seismic attributes. Additionally, it extends to reservoir rocks the original proposal in developing a tool for the uncertainty assessment.

Still, some limitations halt the maturation of further ideas that hover my mind while developing this thesis. The main reason behind this restriction is the limitation of dataset. John Warren warns about this: “very few oil companies wish to characterize what is an undeniable seal facies.” (WARREN, 2006). This lack of data is a persistent challenge to the characterization of evaporites. In rock-physic analysis, laboratory measurements are relevant to the interpretation of the results. This information is

absent in the Ariri Formation. The unavailability of side cores impairs a full comprehension of the connection between salt types and elastic properties. I have found some works that provide laboratory measurement in rock salt, nevertheless, they are restricted to halite-rich samples. Evidently, it is expected that the salt proportions alter the elastic-property response and, consequently, the seismic signal. In the absence of laboratory measurements in the Santos Basin, I regard the facies interpretation as a description without uncertainty. Strong assumption and under solid critiques as it is, I found no alternative, because any uncertainty attributed to this interpretation, in the absence of side cores, can comparatively face the same criticism.

The anhydrite caprock at the base and the top of the Ariri Formation bewilders me due to the continuous basinwide extension. I heard explanations about this phenomenon that make use of the anhydrite creep behavior in comparison to the other salts to explain the immobility of anhydrite at the top and the base of the formation. During this Ph.D. investigation, I encounter articles that provide another more plausible explanation. NaCl-undersaturated meteoric fluids enrich insoluble evaporites and dissolute the halite that forms anhydrite in a post-depositional salt flow, creating anhydrite seals in salt-bearing formations (JACKSON; LEWIS, 2012; GEORGE et al., 2017). This interpretation delivers more clarification to basinwide anhydrite caprock in the Santos Basin. Additionally, while analyzing the salt facies in the seismic section, I noted that, in parts of the basin, underlain and overlying strata encasing this anhydrite are eroded, nevertheless the anhydrite remains intact. Anhydrite displays less creep behavior than halite and bittern salts, however, the implication of immobility of anhydrite is refutable. An investigation in the salt mini-basin in the Santos Basin marks that anhydrite moves along with the other salts. In paraphrasing Stephen Stinger in the case of derivation of the Normal curve by Gauss, the argument of immobility to explain the anhydrite caprock is circular and *non sequitur*, It is the use of conclusion as an axiom. Probably, the NaCl-poor open-marine Albian sediments in contact with halite engendered the anhydritization. Based on similar reasoning, NaCl-undersaturated fluid migration after the salt deposition may lead to the formation of anhydrite at the top of the pre-salt reservoirs. I believe this topic needs in-depth investigations in the Santos Basin.

Evaporite: sediments, resources, and hydrocarbon of Warren (2006) is a masterpiece of our time. In Chapter 5 John Warren discusses the ancient evaporite deposits starting with a stunning

question: “Is the present the key to the past in evaporite studies?”. He continues: “What I am questioning is strict actualistic approach to the sedimental interpretation of evaporites diversity we see in our current icehouse climate mode and eustacy is sufficient to broad to explain the diversity of ancient evaporites. (...) An understanding of the shortcomings inherent in applying strict uniformitarian models is tied to current styles of continent-scale tectonics and icehouse eustacy.”. It is an open question if Uniformitarism applies to ancient widespread evaporites. How much can we explore the findings of current evaporite formations to these ancient basinwide deposits? Most understanding of these formations is supported by the principle of exclusion, that is, illogical assumptions need to be discarded to understand the mechanism that resulted in the observation. For instance, Harraz (2015) describes an inspection in which 1000-m-thick column of seawater results in 17 m of evaporite, among which 1 m of Mg-K-rich salts is precipitated. What does it tell us about the ancient basinwide deposits which record 30-m-thick Mg-k-rich salt? It informs that brine concentration at the present days is not comparable to the hypersaline seawater at the time of the precipitation of the Ariri Formation because the reverse reasoning that 30-km-thick seawater formed these salts is unplausible and illogical. It does not answer what we see, it excludes some hypotheses.

In his book John Warren still put down: “Widespread marine evaporites require particular tectonic and/or eustatic conditions to accumulate, conditions that are not present on the world’s modern surface. They will be in the future, and they have been many times in the past.”. Environments in which these accumulations are deposited are unsuitable for human life. When it will happen again, we will not be here anymore to infer about them. Disappointing as it is, this makes the ancient basinwide evaporite even more enigmatic and fascinating.

The history of the Normal curve started with De Moivre, however, it did not end with Laplace. By the 1920s, Jarl Linderber (1876 – 1932) and Paul Levy (1886 - 1971) demonstrated that there is more than one condition to obtain the Normal curve. They proved that the Central Limit Theorem assumes many forms (SALSBURG, 2002). This thesis applied the Normal curve to derive the facies probability in intrasalt formations and stochastic simulations to mirror evaporite depositions. Normal curve and stochastic simulations are products of the historical development of the Central Limit Theorem. None of these scientists who devised it would ever imagine its vast applicability. It is hard to

stipulate to where one research will lead because it depends on intricated unpredictable events. One thing is right: it is just the beginning of the quantitative seismic interpretation in evaporites formations.

Never at rest!

6 References

ABELHA, M.; PETERSOHN, E. The state of the art of the Brazilian pre-salt exploration. In: *AAPG Annual Convention and Exhibition*. [S.l.: s.n.], 2018.

ALVES, T. M. et al. An incomplete correlation between pre-salt topography, top reservoir erosion, and salt deformation in deep-water Santos Basin (SE brazil). *Marine and Petroleum Geology*, Elsevier BV, v. 79, p. 300–320, 2017.

AMARAL, P. J. et al. Estudo estatístico da velocidade dos sais na camada evaporítica. *International Congress of the Brazilian Geophysical Society*, 2015.

ARCHIBALD, R. C. Abraham De Moivre. Springer Science and Business Media LLC, v. 117, n. 2946, p. 551–551, 1926.

AVSETH, P.; MUKERJI, T.; MAVKO, G. *Quantitative Seismic Interpretation: Applying rock physics tools to reduce interpretation risk*. [S.l.]: Cambridge, 2005.

BABEL, M.; SCHREIBER, B. Geochemistry of evaporites and evolution of seawater. In: *Treatise on Geochemistry*. [S.l.]: Elsevier, 2014. p. 483–560.

BACKUS, G. E. Long-wave elastic anisotropy produced by horizontal layering. *Journal of Geophysical Research*, Wiley-Blackwell, v. 67, n. 11, p. 4427–4440, 1962.

BAI, G.; XU, Y. Gaint fields retain dominance in reserve growth. *Oil and Gas Journal*, v. 112, n. 2, p. 44–51, 2014.

BANIK, N.; KOESOEMADINATA, A.; ELKASEEH, K. G. Young's modulus from point-receiver surface seismic data. *SEG Technical Program Expanded Abstracts*, p. 2794–2798, 2010.

BAYES, T. Essay towards solving a problem in the doctrine of chances. *Philosophical Transaction of the Royal Society*, Royal Society, v. 53, p. 370–418, 1763.

BECKER, F.; BECHSTADT, T. Sequence stratigraphy of a carbonate-evaporite succession (Zechstein 1, Hessian Basin, Germany). *Sedimentology*, Wiley, v. 53, n. 5, p. 1083–1120, 2006.

BERTONI, C.; CARTWRIGHT, J. A. Major erosion at the end of the Messinian salinity crisis: evidence from the Levant Basin, Eastern Mediterranean. *Basin Research*, Wiley, v. 19, n. 1, p. 1–18, jan. 2007.

BISHOP, C. *Pattern Recognition and Machine Learning*. [S.l.]: Springer, 2006.

BRANDÃO, A.; VIDIGAL-SOUZA, P.; HOLZ, M. Evaporite occurrence and salt tectonics in the Cretaceous Camamu-Almada Basin, northeastern Brazil. *Journal of South American Earth Sciences*, Elsevier BV, v. 97, p. 102421, 2020.

BROWN, A. et al. Tuning effects, lithological effects and depositional effects in the seismic response of gas reservoirs. *Geophysical Prospecting*, Wiley, v. 34, n. 5, p. 623–647, 1986.

BROWN, A. R. *Interpretation of Three-Dimensional Seismic Data*. [S.l.]: Society of Exploration Geophysicists and American Association of Petroleum Geologists, 2011.

BRUHN, C. H. et al. Campos Basin: Reservoir characterization and management - historical overview and future challenges. In: *Offshore Technology Conference*. [S.l.]: Offshore Technology Conference, 2003.

BRUN, J.-P.; MAUDUIT, T. P.-O. Rollovers in salt tectonics: The inadequacy of the listric fault model. *Tectonophysics*, Elsevier BV, v. 457, n. 1-2, p. 1–11, 2008.

CARCIONE, J. M.; HELLE, H. B.; GANGI, A. F. Theory of borehole stability when drilling through salt formations. *Geophysics*, Society of Exploration Geophysicists, v. 71, n. 3, p. F31–F47, may 2006.

CARMINATTI, M.; WOLFF, B.; GAMBOA, L. New exploratory frontiers in Brazil. *19th World Petroleum Congress*, 2008.

CARTWRIGHT, J. et al. Strain partitioning in gravity-driven shortening of a thick, multilayered evaporite sequence. *Geological Society, London, Special Publications*, Geological Society of London, v. 363, n. 1, p. 449–470, 2012.

CASTAGNA, J. P.; BATZLE, M. L.; EASTWOOD, R. L. Relationships between compressional-wave and shear-wave velocities in clastic silicate rocks. *Geophysics*, Society of Exploration Geophysicists, v. 50, n. 4, p. 571–581, apr 1985.

CASTAGNA, J. P.; BATZLE, M. L.; KAN, T. K. Rock physics - the link between rock properties and avo response. In: *Offset-Dependent Reflectivity—Theory and Practice of AVO Analysis*. [S.l.]: Society of Exploration Geophysicists, 1993. p. 113–172.

CHITALE, V. et al. Learning from deployment of a variety of modern petrophysical formation evaluation technologies and techniques for characterization of a pre-salt carbonate reservoir: Case study from Campos Basin, Brazil. *55th Annual Logging Symposium,*, 2014.

COBBOLD, P. R. et al. Seismic and Experimental Evidence for Thin-Skinned Horizontal Shortening by Convergent Radial Gliding on Evaporites, Deep-Water Santos Basin, Brazil. In: *Salt Tectonics: A Global Perspective*. [S.l.]: American Association of Petroleum Geologists, 1995. ISBN 9781629810867.

CONNOLLY, P. A simple, robust algorithm for seismic net pay estimation. *The Leading Edge*, Society of Exploration Geophysicists, v. 26, n. 10, p. 1278–1282, 2007.

CONTRERAS, J. et al. Seismic stratigraphy and subsidence analysis of the southern Brazilian margin (Campos, Santos and Pelotas Basins). *Marine and Petroleum Geology*, Elsevier BV, v. 27, n. 9, p. 1952–1980, 2010.

CORNELIUS, S.; CASTAGNA, J. P. Variation in salt-body interval velocities in the deepwater Gulf of Mexico: Keathley Canyon and Walker Ridge areas. *Interpretation*, Society of Exploration Geophysicists, v. 6, n. 1, p. T15–T27, 2018.

COSTA, A. M. et al. Geomechanics applied to the well design through salt layers in Brazil:a history of success. *44th U.S. Rock Mechanics Symposium and 5th U.S. Canada Rock Mechanics Symposium*, 2010.

COSTA, A. M. et al. Geomechanics applied to the well design through salt layers in Brazil: A history of success. In: *Multiscale and Multiphysics Processes in Geomechanics*. [S.l.]: Springer Berlin Heidelberg, 2011. p. 165–168.

DALE, A. I. Bayes or Laplace? An examination of the origin and early applications of Bayes' theorem. *Archive for History of Exact Sciences*, Springer, v. 27, n. 1, p. 23–47, 1982.

DASH, B. P.; OBAIDULLAH, K. A. Determination of signal and noise statistics using correlation theory. *Geophysics*, SEG, v. 35, n. 1, p. 24–32, 1970.

DAVISON, I. Geology and tectonics of the South Atlantic Brazilian salt basins. *Geological Society, London, Special Publications*, Geological Society of London, v. 272, n. 1, p. 345–359, 2007.

DAVISON, I.; ANDERSON, L.; NUTTALL, P. Salt deposition, loading and gravity drainage in the Campos and Santos salt basins. *Geological Society, London, Special Publications*, Geological Society of London, v. 363, n. 1, p. 159–174, 2012.

DEBEYE, H. W. J.; RIEL, P. Lp-norm deconvolution. *Geophysical Prospecting*, Wiley, v. 38, n. 4, p. 381–403, 1990.

DEKKING, F. M. et al. *A Modern Introduction to Probability and Statistics*. [S.l.]: Springer London, 2005.

DEMERCIAN, S.; SZATMARI, P.; COBBOLD, P. Style and pattern of salt diapirs due to thin-skinned gravitational gliding, Campos and Santos Basins, offshore Brazil. *Tectonophysics*, Elsevier BV, v. 228, n. 3-4, p. 393–433, 1993.

DIAS, R. et al. Salt stratification and least square migration to improve pre-salt reservoir images: Santos Basin, Brazilian offshore example. In: *Second EAGE/PESGB Workshop on Velocities*. [S.l.]: EAGE Publications BV, 2019.

DOOLEY, T. P. et al. Enigmatic structures within salt walls of the Santos Basin—part 2: Mechanical explanation from physical modelling. *Journal of Structural Geology*, Elsevier BV, v. 75, p. 163–187, 2015.

DOYEN, P. *Seismic Reservoir Characterization: An Earth Modelling Perspective*. [S.l.]: EAGE, 2007.

DUDA, R. O.; HART, P. E.; STORK, D. G. *Pattern Classifications*. [S.l.]: John Wylie & Sons, 2000.

DUSSEAULT, M.; MAURY, V.; SANFILIPPO, F. Drilling through salt: Constitutive behavior and drilling strategies. *6th North America Rock Mechanics Symposium*, 2004.

DVORKIN, J.; GUTIERREZ, M.; GRANA, D. *Seismic reflections of rock properties*. [S.l.]: Cambridge, 2016.

DVORKIN, J.; WOLLNER, U. Rock-physics transforms and scale of investigation. *Geophysics*, Society of Exploration Geophysicists, v. 82, n. 3, p. MR75–MR88, 2017.

EFRON, B. Bayes' theorem in the 21st century. *Science*, American Association for the Advancement of Science (AAAS), v. 340, n. 6137, p. 1177–1178, 2013.

FALCÃO, L. *O sal estratificado e sua importância na modelagem de velocidade para fins de migração sísmica*. Dissertation (MSc) — Universidade Federal Fluminense, 2017.

FARIA, D. L.; REIS, A. T. dos; SOUZA, O. G. de. Three-dimensional stratigraphic-sedimentological forward modeling of an aptian carbonate reservoir deposited during the sag stage in the Santos Basin, brazil. *Marine and Petroleum Geology*, Elsevier BV, v. 88, p. 676–695, dec 2017.

FARIAS, F. et al. Evaporitic carbonates in the pre-salt of Santos Basin – genesis and tectonic implications. *Marine and Petroleum Geology*, Elsevier BV, v. 105, p. 251–272, jul 2019.

FARMER, P. et al. Exploring the subsalt. *Oilfield Review*, Wiley, v. 8, n. 1, p. 50–54, 1996.

FENG, Y. E.; STEINBERG, J.; RESHEF, M. Intra-salt deformation: Implications for the evolution of the Messinian evaporites in the Levant Basin, eastern mediterranean. *Marine and Petroleum Geology*, Elsevier BV, v. 88, p. 251–267, 2017.

FERREIRA, D. J. A.; LUPINACCI, W. M. An approach for three-dimensional quantitative carbonate reservoir characterization in the Pampo field, Campos Basin, offshore Brazil. *AAPG Bulletin*, American Association of Petroleum Geologists AAPG/Datapages, v. 102, n. 11, p. 2267–2282, 2018.

FIDUK, J. C.; ROWAN, M. G. Analysis of folding and deformation within layered evaporites in blocks BM-s-8 &-9, Santos Basin, Brazil. *Geological Society, London, Special Publications*, Geological Society of London, v. 363, n. 1, p. 471–487, 2012.

FISHER, R. *The design of experiments*. [S.l.]: Oliver and Byod, 1951.

FONSECA, J. et al. Combination of the salt stratifications and the least-square migration to evaluate their improvements for the pre-salt reservoir images in the Santos Basin, Brazilian offshore. In: *Proceedings of the 16th International Congress of the Brazilian Geophysical Society&Expogef*. [S.l.]: Brazilian Geophysical Society, 2019.

FONSECA, J. S. et al. Dealing with evaporitic salts section in Santos Basin during geological seismic velocity construction. *15th International Congress of the Brazilian Geophysical Society & EXPOGEF*, Brazilian Geophysical Society, 2017.

FORMIGLI, J. Pre-salt reservoirs offshore Brazil: Perspectives and challenges. In: *Bank of America Energy Conference*. [S.l.: s.n.], 2007.

FORNARI, M.; RISACHER, F.; FÉRAUD, G. Dating of paleolakes in the central altiplano of Bolivia. *Palaeogeography, Palaeoclimatology, Palaeoecology*, Elsevier BV, v. 172, n. 3-4, p. 269–282, aug 2001.

FREITAS, J. R. *Ciclos deposicionais evaporíticos da bacia de Santos: uma análise cicloestratigráfica a partir de dados de 2 poços e traços de sísmica*. Dissertation (MSc) — Universidade Federal do Rio Grande do Sul, 2006.

GALTON, F. *Hereditary Genius*. [S.l.]: Macmillan, 1869.

GALTON, F. *Natural Inheritance*. [S.l.]: Macmillan, 1889.

GAMBOA, L. et al. Geotectonic controls on CO2 formation and distribution processes in the Brazilian pre-salt basins. *Geosciences*, MDPI AG, v. 9, n. 6, p. 252, 2019.

GAMBOA, L. P. et al. Evaporitos estratificados no Atlantico Sul: interpretação sísmica e controle tectono-estratigráfico na Bacia de Santos. In: *Sal: Geologia e Tectônica, Exemplos nas Bacias Brasileiras*. [S.l.]: Editora Beca, 2009. p. 342–361.

GARCIA, S. F. M. et al. Structural modeling based on sequential restoration of gravitational salt deformation in the Santos Basin (Brazil). *Marine and Petroleum Geology*, Elsevier BV, v. 35, n. 1, p. 337–353, aug 2012.

GARDNER, G. H. F.; GARDNER, L. W.; GREGORY, A. R. Formation velocity and density: the diagnostic basics for stratigraphy traps. *Geophysics*, Society of Exploration Geophysicists, v. 39, n. 6, p. 770–780, dec 1974.

GASSMANN, F. ?ber die elastizit?t por?ser medien. *Vier Natur Gesellschaft*, 1951.

GENT, H. V.; URAI, J. L.; KEIJZER, M. de. The internal geometry of salt structures – a first look using 3d seismic data from the Zechstein of the Netherlands. *Journal of Structural Geology*, Elsevier BV, v. 33, n. 3, p. 292–311, 2011.

GEORGE, M. et al. Seismic interpretation and characterization of anhydrite caprocks in the Tromsø Basin, SW Barents Sea. *Marine Geology*, Elsevier, v. 390, p. 36–50, 2017.

GILLISPIE, C. C. *Pierre-Simon Laplace, 1749-1827: A Life in Exact Science*. [S.l.]: Princeton University Press, 2000.

GOBATTO, F. et al. Refining velocity model within the salt section in Santos Basin: An innovative workflow to include the existing stratification and its considerations. *SEG Technical Program Expanded Abstracts*, Society of Exploration Geophysicists, 2016.

GONZÁLEZ, E. F.; MUKERJI, T.; MAVKO, G. Seismic inversion combining rock physics and multiple-point geostatistics. *Geophysics*, Society of Exploration Geophysicists, v. 73, n. 1, p. R11–R21, 2008.

GONZÁLEZ, M. et al. Proposed workflow to incorporate stratification within salt section using velocity and seismic attributes. In: *Third EAGE/SBGf Workshop 2016*. [S.l.]: EAGE Publications BV, 2016.

GRANA, D. Joint facies and reservoir properties inversion. *Geophysic*, Society of Exploration Geophysicists, v. 83, n. 3, p. M15–M24, 2018.

GREENBERG, M. L.; CASTAGNA, J. P. Shear-wave velocity estimation in porous rocks: theoretical formulation, preliminary verification and application. *Geophysical Prospecting*, Wiley-Blackwell, v. 40, n. 2, p. 195–209, 1992.

GRIFFITHS, M.; HEMBD, J.; PRIGENT, H. Applications of interbed multiple attenuation. *The Leading Edge*, Society of Exploration Geophysicists, v. 30, n. 8, p. 906–912, 2011.

GUARDADO, L. R.; GAMBOA, L. A. P.; LUCCHESI, C. F. Petroleum Geology of the Campos Basin Brazil, a Model for a Producing Atlantic Type Basin. In: *Divergent/Passive Margin Basins*. [S.l.]: American Association of Petroleum Geologists, 1989. ISBN 9781629811307.

GUERRA, M. C. M.; UNDERHILL, J. R. Role of halokinesis in controlling structural styles and sediment dispersal in the Santos Basin, offshore Brazil. *Geological Society, London, Special Publications*, Geological Society of London, v. 363, n. 1, p. 175–206, 2012.

GüNEŞ, P.; AKSU, A.; HALL, J. Internal seismic stratigraphy of the Messinian evaporites across the northern sector of the eastern Mediterranean Sea. *Marine and Petroleum Geology*, Elsevier BV, v. 91, p. 297–320, mar. 2018.

HACKING, I. *The Emergence of Probability: A Philosophical Study of Early Ideas About Probability, Induction and Statistical Inference*. [S.l.]: Cambridge University Press, 2013.

HAMMOND, A. L. Bright spot: Better seismological indicators of gas and oil. *Science*, American Association for the Advancement of Science (AAAS), v. 185, n. 4150, p. 515–517, 1974.

HAN, D.-h. *Effects of porosity and clay content on acoustic properties of sandstones and unconsolidated sediments*. Thesis (PhD) — Stanford University, 1986.

HARDIE, L. A. Evaporites - marine or non-marine? *American Journal of Science*, American Journal of Science (AJS), v. 284, n. 3, p. 193–240, 1984.

HARRAZ, H. Z. *EVAPORITE SALT DEPOSITS*. [S.l.]: Unpublished Presentation, 2015.

HEUMANN, C.; SCHOMAKER, M.; SHALABH. *Introduction to Statistics and Data Analysis*. [S.l.]: Springer, 2016.

HILL, S. J. Inversion-based thickness determination. *The Leading Edge*, SEG, v. 24, n. 5, p. 477–480, 2005.

HILTERMAN, F. J. *Seismic Amplitude Interpretation*. [S.l.]: Society of Exploration Geophysicists and European Association of Geoscientists and Engineers, 2001.

HOMRIGHAUSEN, S. et al. New age and geochemical data from the Walvis Ridge: The temporal and spatial diversity of South Atlantic intraplate volcanism and its possible origin. *Geochimica et Cosmochimica Acta*, Elsevier BV, v. 245, p. 16–34, 2019.

INFANTE, E.; CHENEVERT, M. Stability of boreholes drilled through salt formations displaying plastic behavior. *SPE Drilling Engineering*, Society of Petroleum Engineers (SPE), v. 4, n. 01, p. 57–65, mar 1989.

JACKSON, C. A.-L. et al. Salt thickness and composition influence rift structural style, northern North Sea, offshore Norway. *Basin Research*, Wiley, v. 31, n. 3, p. 514–538, 2019.

JACKSON, C. A.-L. et al. Enigmatic structures within salt walls of the Santos Basin—part 1: Geometry and kinematics from 3d seismic reflection and well data. *Journal of Structural Geology*, Elsevier BV, v. 75, p. 135–162, jun 2015.

JACKSON, C. A.-L.; LEWIS, M. M. Origin of an anhydrite sheath encircling a salt diapir and implications for the seismic imaging of steep-sided salt structures, egersund basin, northern north sea. *Journal of the Geological Society*, Geological Society of London, v. 169, n. 5, p. 593–599, 2012.

JACKSON, C. A.-L. et al. Geological and geophysical expression of a primary salt weld: An example from the Santos Basin, Brazil. *Interpretation*, Society of Exploration Geophysicists, v. 2, n. 4, p. SM77–SM89, 2014.

JACKSON, M.; CRAMEZ, C.; FONCK, J.-M. Role of subaerial volcanic rocks and mantle plumes in creation of South Atlantic margins: implications for salt tectonics and source rocks. *Marine and Petroleum Geology*, Elsevier BV, v. 17, n. 4, p. 477–498, 2000.

JACKSON, M. P. A.; HUDEC, M. R. *Salt Tectonics*. [S.l.]: Cambridge University Press, 2017.

JARDIM, F. et al. Estimating amplitude uncertainties through illumination studies for a pre-salt reservoir. *14th International Congress of the Brazilian Geophysical Society & EXPOGEF,*, Brazilian Geophysical Society, aug 2015.

JI, S. et al. Dirty salt velocity inversion: The road to a clearer subsalt image. *Geophysics*, Society of Exploration Geophysicists, v. 76, n. 5, p. WB169–WB174, sep 2011.

JONES, I. F.; DAVISON, I. Seismic imaging in and around salt bodies. *Interpretation*, v. 2, n. 4, p. SL1–SL20, 2014.

JUSTEN, J. C. R. *Análise das propriedades elásticas de rochas e minerais evaporíticos*. Dissertation (MSc) — Pontíficia Universidade Católica do Rio de Janeiro, 2014.

JUSTEN, J. C. R.; JR., E. A. V.; SOUZA, I. A. e Ailton L. S. de. Análise das propriedades elásticas de rochas e minerais evaporíticos. *13th International Congress of the Brazilian Geophysical Society & EXPOGEF*, Society of Exploration Geophysicists and Brazilian Geophysical Society, 2013.

KALLWEIT, R. S.; WOOD, L. C. The limits of resolution of zero-phase wavelets. *Geophysics*, Society of Exploration Geophysicists, v. 47, n. 7, p. 1035–1046, 1982.

KARNER, G. D.; GAMBÔA, L. A. P. Timing and origin of the atlantic pre-salt sag basins and their capping evaporites. *Geological Society, London, Special Publications*, Geological Society of London, v. 285, n. 1, p. 15–35, 2007.

KEMPER, M. Rock physics driven inversion: the importance of workflow. *First Break*, EAGE Publications, v. 28, n. 10, 2010.

KEYNES, J. M. *A treatise on probability*. [S.l.]: Dover Phoenix, 1921.

KRIEF, M. et al. A petrophysical interpretation using the velocities of p and s waves. *The Log Analyst*, v. 31, n. 6, p. 355–369, 1990.

KUKLA, P. A.; STROZYK, F.; MOHRIAK, W. U. South Atlantic salt basins – witnesses of complex passive margin evolution. *Gondwana Research*, Elsevier BV, v. 53, p. 41–57, 2018.

LATIMER, B. R.; DAVISON, R.; RIEL, P. v. An interpreter's guide to understanding and working with seismic-derived acoustic impedance data. *The Leading Edge*, v. 19, p. 242–256, 2000.

LATIMER, R. B. Inversion and interpretation of impedance data. In: *Interpretation of Three-Dimensional Seismic Data*. [S.l.]: Society of Exploration Geophysicists and American Association of Petroleum Geologists, 2011. p. 309–350.

LEPPARD, C.; ECKERSLEY, A.; PURVES, S. Quantifying the temporal and spatial extent of depositional and structural elements in 3D seismic data using spectral decomposition and multiattribute RGB blending. In: *Seismic imaging of depositional and geomorphic systems: 30th Annual GCSSEPM Foundation Bob F. Perkins Research Conference*. [S.l.]: GCSSEPM, 2010. p. 1–10.

LI, S. et al. Numerical modelling of the displacement and deformation of embedded rock bodies during salt tectonics: A case study from the South Oman salt basin. *Geological Society, London, Special Publications*, Geological Society of London, v. 363, n. 1, p. 503–520, 2012.

LOFI, J. et al. Refining our knowledge of the Messinian salinity crisis records in the offshore domain through multi-site seismic analysis. *Bulletin de la Societe Geologique de France*, EDP Sciences, v. 182, n. 2, p. 163–180, 2011.

LUPINACCI, W. M. et al. A combined time-frequency filtering strategy for q-factor compensation of poststack seismic data. *Geophysics*, Society of Exploration Geophysicists, v. 82, n. 1, p. V1–V6, 2017.

LUPINACCI, W. M. et al. Impact of halokynesis in seismic interpretation and generation of the top salt surface in a distal portion of the Santos Basin. *Brazilian Journal of Geophysics*, Sociedade Brasileira de Geofisica, v. 37, n. 2, 2019.

MANN, J.; RIGG, J. New geological insights into the Santos Basin. *GeoExPro*, v. 9, n. 1, 2012.

MARKETOS, G.; GOVERS, R.; SPIERS, C. Ground motions induced by a producing hydrocarbon reservoir that is overlain by a viscoelastic rocksalt layer: a numerical model. *Geophysical Journal International*, Oxford University Press (OUP), v. 203, n. 1, p. 198–212, aug 2015.

MATOS, M. C. de et al. Detecting stratigraphic discontinuities using time-frequency seismic phase residues. *Geophysics*, Society of Exploration Geophysicists, v. 76, n. 2, p. P1–P10, 2011.

MAUL, A. *Caracterização sísmica das estratificações da seção evaporítica salina e suas aplicações nos projetos de exploração, desenvolvimento e produção de hidrocarbonetos*. Thesis (PhD in Geophysics and Geology) — Universidade Federal Fluminense, 2020.

MAUL, A. et al. Benefits of inserting salt stratification to detail velocity model prior to least-squares reverse-time migration. *Journal of Applied Geophysics*, Elsevier BV, v. 195, p. 104469, 2021.

MAUL, A. et al. The impact of heterogeneous salt velocity models on the gross rock volume estimation: an example from the Santos Basin pre-salt, Brazil. *Petroleum Geoscience*, Geological Society of London, v. 27, n. 4, p. 2020–105, 2021.

MAUL, A. et al. Observing amplitude uncertainties for a pre-salt reservoirs using illumination study (hit-maps). *77th EAGE Conference and Exhibition*, EAGE Publications BV, 2015.

MAUL, A.; SANTOS, M. A. C.; SILVA, C. G. Few considerations, warnings and benefits for the E&P industry when incorporating stratifications inside salt sections. *Brazilian Journal of Geophysics*, Brazilian Journal of Geophysics, v. 36, n. 4, p. 1, 2018.

MAUL, A.; SANTOS, M. C.; SILVA, C. Evaporitic section characterization and its impact over the pre-salt reservoirs, example in the Santos Basin. *Rio Oil & Gas Expo and Conference*, 2018.

MAUL, A. R. et al. Improving pre-salt reservoir seismic images when considering the stratifies evaporite insersion in the inital model for the velocity updating processes prior to the seismic migration. *Brazilian Journal of Geophysics*, Sociedade Brasileira de Geofisica, v. 37, n. 3, p. 235, 2019.

MAVKO, G.; MUKERJI, T.; DVORKIN, J. *The Rock Physics Handbook - Tools for Seismic Analysis of Porous Media*. [S.l.]: Cambridge, 2009.

MECKEL, L. D.; NATH, A. K. Geologic considerations for stratigraphic modeling and interpretation. In: *Seismic Stratigraphy — Applications to Hydrocarbon Exploration*. [S.l.]: American Association of Petroleum Geologists, 1977.

MODICA, C. J.; BRUSH, E. R. Postrift sequence stratigraphy, paleogeography, and fill history of the deep-water Santos Basin, offshore southeast Brazil. *AAPG Bulletin*, American Association of Petroleum Geologists AAPG/Datapages, v. 88, n. 7, p. 923–945, 2004.

MOHRIAK, W.; HOBBS, R.; DEWEY, J. Basin-forming processes and the deep structure of the Campos Basin, offshore brazil. *Marine and Petroleum Geology*, Elsevier BV, v. 7, n. 2, p. 94–122, 1990.

MOHRIAK, W.; NEMČOK, M.; ENCISO, G. South atlantic divergent margin evolution: rift-border uplift and salt tectonics in the basins of SE Brazil. *Geological Society, London, Special Publications*, Geological Society of London, v. 294, n. 1, p. 365–398, 2008.

MOHRIAK, W. et al. Salt tectonics and structural styles in the deep-water province of the Cabo Frio region, Rio de Janeiro, brazil. *AAPG*, v. 65, p. 273–304, 1995.

MOHRIAK, W. U. et al. Petroleum geology of the Campos Basin, offshore brazil. *Geological Society, London, Special Publications*, Geological Society of London, v. 50, n. 1, p. 119–141, 1990.

MOHRIAK, W. U.; SZATMARI, P.; ANJOS, S. Salt: geology and tectonics of selected Brazilian basins in their global context. *Geological Society, London, Special Publications*, Geological Society of London, v. 363, n. 1, p. 131–158, 2012.

MOREIRA, J. L. P. et al. Bacia de Santos. *Boletim de Geociência da Petrobras*, v. 15, n. 2, p. 531–549, 2007.

MUKERJI, T. et al. Mapping lithofacies and pore-fluid probabilities in a North Sea reservoir: Seismic inversions and statistical rock physics. *Geophysics*, SEG, v. 66, n. 4, p. 988–1001, 2001.

MUKERJI, T.; MAVKO, G. The flaw of averages and the pitfalls of ignoring variablity in attribute interpretations. *The Leading Edge*, SEG, v. 27, n. 3, p. 382–384, 2008.

NEFF, D. B. Estimated pay mapping using three-dimensional seismic data and incremental pay thickness modeling. *Geophysics*, Society of Exploration Geophysicists, v. 55, n. 5, p. 567–575, 1990.

NEFF, D. B. Amplitude map analysis using forward modeling in sandstone and carbonate reservoirs. *Geophysics*, Society of Exploration Geophysicists, v. 58, n. 10, p. 1428–1441, 1993.

OLIVEIRA, L. et al. Geological velocity approach in order to obtain a detailed velocity model for the evaporitic section - Santos Basin. *International Congress of the Brazilian Geophysical Society*, 2015.

OSTRANDER, W. J. Plane-wave reflection coefficients for gas sands at nonnormal angles of incidence. *Geophysics*, Society of Exploration Geophysicists, v. 49, n. 10, p. 1637–1648, 1984.

PARZEN, E. On estimation of a probability density function and mode. *The Annals of Mathematical Statistics*, Institute of Mathematical Statistics, v. 33, n. 3, p. 1065–1076, 1962.

PEARSON, K. Contributions to the mathematical theory of evolution. *Philosophical Transactions of the Royal Society of London. A*, The Royal Society, v. 185, p. 71–110, 1894. ISSN 02643820.

PEARSON, K. VII. Mathematical contributions to the theory of evolution.—III. regression, heredity, and panmixia. The Royal Society, v. 187, p. 253–318, 1896.

PEARSON, K. Historical note on the origin of the normal curve of errors. *Biometrika*, Oxford Press, v. 16, n. 3, p. 402, 1924.

PENNA, R.; LUPINACCI, W. M. 3d modelling of flow units and petrophysical properties in Brazilian presalt carbonate. *Marine and Petroleum Geology*, Elsevier BV, v. 124, p. 104829, 2021.

PEREIRA, M. J.; FEIJó, F. J. Bacia de Santos. *Boletim de Geociências da Petrobras*, v. 8, n. 1, p. 219–234, 1994.

PETERSON, R. A.; FILLIPPONE, W. R.; COKER, F. B. The synthesis of seismograms from well logdata. *Geophysics*, Society of Exploration Geophysicists, v. 20, n. 3, p. 516–538, 1955.

PICHEL, L. M. et al. Base-salt relief controls salt-tectonic structural style, são paulo plateau, santos basin, brazil. *Basin Research*, Wiley, 2019.

PICHEL, L. M. et al. Geometry and kinematics of salt-detached ramp syncline basins. *Journal of Structural Geology*, Elsevier BV, v. 115, p. 208–230, 2018.

PICKETT, G. Acoustic character logs and their applications in formation evaluation. *Journal of Petroleum Technology*, Society of Petroleum Engineers (SPE), v. 15, n. 06, p. 659–667, 1963.

PLACKETT, R. L. Studies in the history of probability and statistics. XXIX: The discovery of the method of least squares. JSTOR, v. 59, n. 2, p. 239, 1972.

POIATE, E.; MAIA, A.; FALCAO, J. L. Well design for drilling through thick evaporite layers. In: *IADC/SPE Drilling Conference*. [S.l.]: Society of Petroleum Engineers, 2006.

PONTES, R. *Seismic characterization of internal salt cycles: a case study in Santos Basin, Brazil*. Dissertation (MSc) — Universidade Federal Fluminense, 2019.

PONTES, R. B.; MAUL, A.; SILVA, C. G. Seismic characterization of internal salt cycles: A case study in the Santos Basin, Brazil. *Brazilian Journal of Geophysics*, v. 39, n. 2, p. 5–11, 2021.

PURYEAR, C. I.; CASTAGNA, J. P. Layer-thickness determination and stratigraphic interpretation using spectral inversion: Theory and application. *Geophysics*, Society of Exploration Geophysicists, v. 73, n. 2, p. R37–R48, 2008.

QUIRK, D. G. et al. Salt tectonics on passive margins: examples from Santos, Campos and Kwanza Basins. *Geological Society, London, Special Publications*, Geological Society of London, v. 363, n. 1, p. 207–244, 2012.

RAITH, A. F. et al. Evolution of rheologically heterogeneous salt structures: a case study from the NE Netherlands. *Solid Earth*, Copernicus GmbH, v. 7, n. 1, p. 67–82, 2016.

RAITH, A. F.; URAI, J. L.; VISSER, J. Structural and microstructural analysis of k–mg salt layers in the Zechstein 3 of the Veendam Pillow, NE Netherlands: development of a tectonic mélange during salt flow. *Netherlands Journal of Geosciences*, Cambridge University Press (CUP), v. 96, n. 4, p. 331–351, 2017.

RANGEL, H. D.; GUIMARÃES, P. d. T. M.; SPADINI, A. R. Barracuda and Roncador Giant Oil Fields, Deep-water Campos Basin, Brazil. In: *Giant Oil and Gas Fields of the Decade 1990-1999*. [S.l.]: American Association of Petroleum Geologists, 2003. ISBN 9781629810539.

RAYLEIGH, J. W. *The theory of sound*. [S.l.]: Dover Publushing, 1945.

RODRIGUEZ, C. et al. Dual tectonic-climatic controls on salt giant deposition in the Santos Basin, offshore Brazil. *Geosphere*, Geological Society of America, v. 14, n. 1, p. 215–242, jan 2018.

RODRIGUEZ, C. R. et al. Deep-water reservoir distribution on a salt-influenced slope, Santos Basin, offshore brazil. Center for Open Science, 2019.

ROSA, A. L. R. *The Seismic Signal and Its Meaning*. [S.l.]: Society of Exploration Geophysicists, 2018.

RUTTEN, K.; VALETON, M.; GRUNSVEN, T. van. Measurement of the signal to noise ratio in seismic profiling. *Marine Geophysical Researches*, Springer Science and Business Media LLC, v. 1, n. 4, p. 445–450, 1972.

SALSBURG, D. *Lady tasting tea: how statistics revolutionized science in the twentieth century*. [S.l.]: Holt McDougal, 2002.

SARG, J. The sequence stratigraphy, sedimentology, and economic importance of evaporite–carbonate transitions: a review. *Sedimentary Geology*, Elsevier BV, v. 140, n. 1-2, p. 9–34, apr 2001.

SCHRAMM, M. W.; DEDMAN, E. V.; LINDSEY, J. P. Practical stratigraphic modeling and interpretation. In: *Seismic Stratigraphy — Applications to Hydrocarbon Exploration*. [S.l.]: American Association of Petroleum Geologists, 1977.

SCHREIBER, B. C.; TABAKH, M. E. Deposition and early alteration of evaporites. *Sedimentology*, Wiley, v. 47, p. 215–238, 2000.

SERRA, O. *Element Mineral Rock Catalog*. [S.l.]: Schlumberger, 1990.

SHEYNIN, O. B. Newton and the classical theory of probability. *Archive for History of Exact Sciences*, Springer, v. 7, n. 3, p. 217–243, 1971. ISSN 00039519, 14320657.

SILVER, N. *The Signal and the Noise: why so many predictions fail–but some don't*. [S.l.]: Penguin Books, 2015.

SILVERMAN, B. W. *Density estimation for statistic and data analysis*. [S.l.]: Chapman & Hall, 1986.

SIMM, R. Simple net pay estimation from seismic: a modelling study. *First Break*, EAGE Publications, v. 27, n. 9, 2009.

SIMM, R.; BACON, M. *Seismic Amplitude: An Interpreter's Handbook*. [S.l.]: Cambrigde Press, 2014.

STIGLER, S. *The history of Statistics: the measurement of uncertainty before 1900*. [S.l.]: Belknap Harvad, 1986.

STROZYK, F. The internal structure of the Zechstein Salt and related drilling risks in the Northern Netherlands. In: *Permo-Triassic Salt Provinces of Europe, North Africa and the Atlantic Margins*. [S.l.]: Elsevier, 2017. p. 115–128.

STROZYK, F. et al. 3d seismic study of complex intra-salt deformation: An example from the Upper Permian Zechstein 3 stringer, western Dutch offshore. *Geological Society, London, Special Publications*, Geological Society of London, v. 363, n. 1, p. 489–501, 2012.

STROZYK, F. et al. Regional variations in the structure of the permian zechstein 3 intrasalt stringer in the northern netherlands: 3d seismic interpretation and implications for salt tectonic evolution. *Interpretation*, Society of Exploration Geophysicists, v. 2, n. 4, p. SM101–SM117, nov. 2014.

TALARICO, E. C. S. et al. Uncertainty quantification in seismic facies inversion. *Geophysics*, Society of Exploration Geophysicists, v. 85, n. 4, p. M43–M56, 2020.

TEDESCHI, L. R. et al. New age constraints on aptian evaporites and carbonates from the South Atlantic: Implications for oceanic anoxic event 1a. *Geology*, Geological Society of America, v. 45, n. 6, p. 543–546, 2017.

TEIXEIRA, L. et al. Quantitative seismic interpretation integrated with well-test analysis in turbidite and presalt reservoirs. *The Leading Edge*, Society of Exploration Geophysicists, v. 36, n. 11, p. 931–937, 2017.

TEIXEIRA, L. et al. Rock physics and seismic inversion to identify stratification within salt section supporting velocity, facies modeling and geomechanical analysis. *15th International Congress of the Brazilian Geophysical Society & EXPOGEF*, Brazilian Geophysical Society, 2017.

TEIXEIRA, L.; LUPINACCI, W. M. Elastic properties of rock salt in the Santos Basin: Relations and spatial predictions. *Journal of Petroleum Science and Engineering*, Elsevier BV, v. 180, p. 215–230, 2019.

TEIXEIRA, L.; LUPINACCI, W. M.; MAUL, A. Quantitative seismic-stratigraphic interpretation of the evaporite sequence in the Santos Basin. *Marine and Petroleum Geology*, Elsevier BV, v. 122, p. 104690, 2020.

TEIXEIRA, L. et al. Seismic-based salt characterisation for geomechanical modelling of a presalt reservoir. *80th EAGE Conference and Exhibition*, 2018.

TORIBIO, T. et al. Characterizing evaporitic section and geomechanical properties using seismic inversion, a case study for Santos Basin. *15th International Congress of the Brazilian Geophysical Society & EXPOGEF,*, Brazilian Geophysical Society, 2017.

TRIPPETTA, F. et al. A multidisciplinary study of a natural example of a CO2 geological reservoir in Central Italy. *International Journal of Greenhouse Gas Control*, Elsevier BV, v. 12, p. 72–83, 2013.

TRIPPETTA, F. et al. Laboratory measurements of the physical properties of Triassic evaporites from Central Italy and correlation with geophysical data. *Tectonophysics*, Elsevier BV, v. 492, n. 1-4, p. 121–132, 2010.

TRIPPETTA, F. et al. Carbonate-ramp reservoirs modelling best solutions: Insights from a dense shallow well database in Central Italy. *Marine and Petroleum Geology*, Elsevier BV, v. 126, p. 104931, 2021.

TRUDGILL, B. D. Evolution of salt structures in the northern paradox basin: controls on evaporite deposition, salt wall growth and supra-salt stratigraphic architecture. *Basin Research*, Wiley, v. 23, n. 2, p. 208–238, jul. 2010.

TUCKER, M. Sequence stratigraphy of carbonate-evaporite basins: models and application to the Upper Permian (Zechstein) of northeast England and adjoining North Sea. *Journal of the Geological Society*, Geological Society of London, v. 148, n. 6, p. 1019–1036, 1991.

VENN, J. *The logic of chances*. [S.l.]: Dover Publicationsl, 1866.

VERNIK, L. *Seismic Petrophysics in Quantitative Interpretation*. [S.l.]: Society of Exploration Geophysicists, 2016.

VERNIK, L.; FISHER, D.; BAHRET, S. Estimation of net-to-gross from p- and s-impedance in deepwater turbidites. *The Leading Edge*, Society of Exploration Geophysicists, v. 21, n. 4, p. 380–387, 2002.

VIRIEUX, J.; OPERTO, S. An overview of full-waveform inversion in exploration geophysics. *Geophysics*, Society of Exploration Geophysicists, v. 74, n. 6, p. WCC1–WCC26, nov 2009.

WANG, H.; SAMUEL, R. 3d geomechanical modeling of salt-creep behavior on wellbore casing for presalt reservoirs. *SPE Drilling & Completion*, Society of Petroleum Engineers (SPE), v. 31, n. 04, p. 261–272, dec 2016.

WANG, P.; HUANG, S.; WANG, M. Improved subsalt images with least-squares reverse time migration. *Interpretation*, Society of Exploration Geophysicists, v. 5, n. 3, p. SN25–SN32, 2017.

WANG, Y. *Seismic Inverse Q Filtering*. [S.l.]: Blackwell, 2008.

WARREN, J. *Evaporites: Sediments, Resources and Hydrocarbons*. [S.l.]: Springer, 2006.

WARREN, J. Evaporites. In: *Encyclopedia of Earth Sciences Series*. [S.l.]: Springer International Publishing, 2016. p. 1–8.

WARREN, J. K. Evaporites through time: Tectonic, climatic and eustatic controls in marine and nonmarine deposits. *Earth-Science Reviews*, Elsevier BV, v. 98, n. 3-4, p. 217–268, 2010.

WEIJERMARS, R.; JACKSON, M. P. Predicting the depth of viscous stress peaks in moving salt sheets: Conceptual framework and implications for drilling. *AAPG Bulletin*, American Association of Petroleum Geologists AAPG/Datapages, v. 98, n. 5, p. 911–945, 2014.

WESTERN, P. G.; BALL, G. J. 3D prestack depth migration in the Gulf of Suez: A case history. *Geophysical Prospecting*, Wiley, v. 40, n. 4, p. 379–402, 1992.

WHITE, R. Signal and noise estimation from seismic reflection data using spectral coherence methods. *Proceedings of the IEEE*, Institute of Electrical and Electronics Engineers (IEEE), v. 72, n. 10, p. 1340–1356, 1984.

WIDESS, M. B. How thin is a thin bed? *Geophysics*, SEG, v. 38, n. 6, p. 1176–1180, 1973.

WRIGHT, V. P.; BARNETT, A. J. An abiotic model for the development of textures in some South Atlantic Early Cretaceous lacustrine carbonates. *Geological Society, London, Special Publications*, Geological Society of London, v. 418, n. 1, p. 209–219, 2015.

YAN, F. et al. Seismic velocities of halite salt: Anisotropy, heterogeneity, dispersion, temperature, and pressure effects. *Geophysics*, v. 81, n. 4, p. D293–D301, 2016.

YANG, D. et al. Image registration guided wavefield tomography for shear-wave velocity model building. *Geophysics*, Society of Exploration Geophysicists, v. 80, n. 3, p. U35–U46, may 2015.

ZAMBRINI, J. et al. The impact of the complex evaporites features' on the seismic illumination of the underlying rocks: A case study in the Brazilian presalt. *Journal of Petroleum Science and Engineering*, Elsevier BV, v. 191, p. 107177, 2020.

ZENG, H.; MARFURT, K. J. Recent progress in analysis of seismically thin beds. *Interpretation*, Society of Exploration Geophysicists, v. 3, n. 3, p. SS15–SS22, 2015.

ZHAO, Y.; MAO, N.-B.; CHEN, X. Calculation method of the signal-to-noise ratio attribute of seismic data based on structural orientation. *Applied Geophysics*, Springer Science and Business Media LLC, v. 16, n. 4, p. 455–462, 2019.

ZONG, J. et al. Elastic properties of rock salt: Laboratory measurements and Gulf of Mexico well-log analysis. *Geophysics*, Society of Exploration Geophysicists, v. 82, n. 5, p. D303–D317, 2017.